



National Library
of Canada

Canadian Theses Service

Ottawa, Canada
K1A 0N4

Bibliothèque nationale
du Canada

Services des thèses canadiennes

CANADIAN THESES

THÈSES CANADIENNES

NOTICE

The quality of this microfiche is heavily dependent upon the quality of the original thesis submitted for microfilming. Every effort has been made to ensure the highest quality of reproduction possible.

If pages are missing, contact the university which granted the degree.

Some pages may have indistinct print especially if the original pages were typed with a poor typewriter ribbon or if the university sent us an inferior photocopy.

Previously copyrighted materials (journal articles, published tests, etc.) are not filmed.

Reproduction in full or in part of this film is governed by the Canadian Copyright Act, R.S.C. 1970, c. C-30.

AVIS

La qualité de cette microfiche dépend grandement de la qualité de la thèse soumise au microfilmage. Nous avons tout fait pour assurer une qualité supérieure de reproduction.

S'il manque des pages, veuillez communiquer avec l'université qui a conféré le grade.

La qualité d'impression de certaines pages peut laisser à désirer, surtout si les pages originales ont été dactylographiées à l'aide d'un ruban usé ou si l'université nous a fait parvenir une photocopie de qualité inférieure.

Les documents qui font déjà l'objet d'un droit d'auteur (articles de revue, examens publiés, etc.) ne sont pas microfilmés.

La reproduction, même partielle, de ce microfilm est soumise à la Loi canadienne sur le droit d'auteur, SRC 1970, c. C-30.

THIS DISSERTATION
HAS BEEN MICROFILMED
EXACTLY AS RECEIVED

LA THÈSE A ÉTÉ
MICROFILMÉE TELLE QUE
NOUS L'AVONS REÇUE

THE UNIVERSITY OF ALBERTA

STRUCTURAL CHARACTERIZATION OF ALBERTA GAS OILS

by

FARHAD KHOORASHEH

A THESIS

SUBMITTED TO THE FACULTY OF GRADUATE STUDIES AND RESEARCH
IN PARTIAL FULFILMENT OF THE REQUIREMENTS FOR THE DEGREE
OF MASTER OF SCIENCE

DEPARTMENT OF CHEMICAL ENGINEERING

EDMONTON, ALBERTA

SPRING 1986

Permission has been granted
to the National Library of
Canada to microfilm this
thesis and to lend or sell
copies of the film.

The author (copyright owner)
has reserved other
publication rights, and
neither the thesis nor
extensive extracts from it
may be printed or otherwise
reproduced without his/her
written permission.

L'autorisation a été accordée
à la Bibliothèque nationale
du Canada de microfilmer
cette thèse et de prêter ou
de vendre des exemplaires du
film.

L'auteur (titulaire du droit
d'auteur) se réserve les
autres droits de publication;
ni la thèse ni de longs
extraits de celle-ci, ne
doivent être imprimés ou
autrement reproduits sans son
autorisation écrite.

ISBN 0-315-30285-2

THE UNIVERSITY OF ALBERTA

RELEASE FORM

NAME OF AUTHOR FARHAD KHOASHEH

TITLE OF THESIS STRUCTURAL CHARACTERIZATION OF ALBERTA
GAS OILS

DEGREE FOR WHICH THESIS WAS PRESENTED MASTER OF SCIENCE

YEAR THIS DEGREE GRANTED SPRING 1986

Permission is hereby granted to THE UNIVERSITY OF ALBERTA LIBRARY to reproduce single copies of this thesis and to lend or sell such copies for private, scholarly or scientific research purposes only.

The author reserves other publication rights, and neither the thesis nor extensive extracts from it may be printed or otherwise reproduced without the author's written permission.

(SIGNED) *f.khorasheh.....*

PERMANENT ADDRESS:

.... 26.. Niknam.. Street..
.... Naft.. Ave.....
.... Tehran.. Iran.....

DATED ...January 15....19 86

THE UNIVERSITY OF ALBERTA,
FACULTY OF GRADUATE STUDIES AND RESEARCH

The undersigned certify that they have read, and recommend to the Faculty of Graduate Studies and Research, for acceptance, a thesis entitled STRUCTURAL CHARACTERIZATION OF ALBERTA GAS OILS submitted by FARHAD KHORASHEH in partial fulfilment of the requirements for the degree of MASTER OF SCIENCE.

Supervisor

Date Jan. 15, 1986

Abstract

A method of Functional Group Analysis (FGA) was developed for structural characterization of Alberta gas oils. The aim of FGA was to characterize the chemical composition of gas oils in terms of the concentration of a selected set of functional groups using data from Nuclear Magnetic Resonance (NMR), elemental analysis (EA), and Infra-red spectroscopy (IR).

As a first step in the analysis, gas oils were separated into class fractions enriched in selected functional groups. Asphaltenes were removed by precipitation from an n-pentane/benzene solution of oil. The deasphaltened oil was then subjected to class separation by column chromatography to give saturates, aromatics, Polar I, Polar II, and Polar III fractions. The polar fractions were distinguished by the increasing polarity of their constituent groups.

For each fraction, data from EA, $^1\text{H-NMR}$, and IR were used to obtain linear constraints relating the unknown concentration of functional groups to the analytical data. The less accurate data from $^{13}\text{C-NMR}$ were used to formulate an objective function which was minimized subject to the linear constraints. A quadratic programming algorithm was used in the minimization procedure to obtain the functional group concentrations.

FGA was applied to a number of synthetic mixtures with known group concentrations. The predicted concentrations of

some hydrocarbon functional groups such as gamma methyl, beta methyl, hydroaromatic ring, naphthenic methylene, total alkyl substituents, and mono + diaromatics were fairly accurate with an estimated error of \pm 15 %. Concentrations of chain methylene, methyne, and naphthenic methyl were less accurate with an error of \pm 40 %.

The structural profiles of various class fractions of Syncrude-Coker Gas Oil (SCGO) revealed some of the strengths and weaknesses of FGA. For each fraction, typical structural features such as aromaticity, degree of aromatic ring condensation, degree of substitution on aromatic rings, etc., were easily determined from the profiles. The profiles also provided the concentration of various heteroatom groups, in particular the distribution of sulphur in aliphatic and aromatic structures. On the other hand, discrimination between mono and diaromatics, and various polyaromatics was not possible.

Structural profiles of gas oils from different geographic locations indicated that feedstocks with relatively similar physical properties had appreciable differences in chemical composition. For example, Cold Lake Gas Oil (CLGO) and Lloydminster Vacuum Gas Oil (LVGO) had very similar elemental composition, specific gravity, and boiling range (within 6 °C). However, CLGO had 18% more heteroaromatics, 50% more polyaromatics, and 52% more hydroaromatic rings than LVGO. The distribution of sulphur between aromatic and aliphatic structures was also different

with 61% of sulphur as thiophenoaromatics in LVGO compared with 43% in CLGO. Such differences in chemical characteristics could result in different reactivity for the above feedstocks under processing conditions.

Comparison of the profiles of hydroprocessed SCGO with those of the original sample revealed significant changes in the concentration of various functional groups. For example, concentration of phenanthrene was reduced by 25%, and aromaticity decreased from 36% to 28% indicating the hydrogenation of aromatics. Desulphurization of thiophenoaromatics, deoxygenation of dibenzofurans, and partial hydrogenation of condensed aromatics were responsible for the increase in benzene concentration from 0.082 to 0.188 moles/100 grams of sample. Such changes indicated that FGA would be a promising tool in kinetic modelling for hydroprocessing of gas oils.

Acknowledgements

I would like to take this opportunity to express my sincere appreciation to all those who made this work enjoyable and a rewarding experience. In particular, I would like to thank:

Dr. I.G. Dalla Lana and Dr. M.R. Gray for their valuable advice, guidance, and constant encouragement;

Mr. J. Zou for developing the analytical method for the class separation procedure;

Dr. J. Thiel for his expert analysis of the NMR spectra and many fruitful discussions;

Dr. J. Jacobson for completing the IR analysis;

Dr. P.A. Barrow and Mr. R. Pack for developing the software for the digitizer program;

Dr. H.A. Rangwala for providing the reactor data and products;

Alberta Oil Sands Technology and Research Authority for providing the financial support for this work; and finally, I am gratefully indebted to my wife, Mahnaz, for her patience and understanding.

Table of Contents

Chapter	Page
1. Introduction	1
2. Literature Survey	7
2.1 Application of FGA for Structural Analysis	7
2.2 Chemical Structures in Bitumen and Heavy Oils	8
3. Analytical Methods for FGA	17
3.1 Class Separation by Column Chromatography	17
3.2 Elemental Analysis	18
3.3 $^1\text{H-NMR}$	18
3.4 $^{13}\text{C-NMR}$	19
3.5 IR Spectroscopy	21
4. Mathematical Formulation of FGA for Characterization of Gas Oils	28
4.1 Development of Mathematical Procedure	28
4.2 Additional Constraints	31
4.3 Optimization Procedure	33
4.4 Restrictions on Group Selections	36
4.5 Summary	38
5. Application of FGA to Known Mixtures	42
5.1 Sample Preparation and Analytical Methods	42
5.2 Peak Assignment for $^{13}\text{C-NMR}$ Spectra	43
5.3 Discussion of Results	44
5.3.1 $^1\text{H-NMR}$ Data	44
5.3.2 $^{13}\text{C-NMR}$ Data	45
5.3.3 FGA Results	51
5.4 Summary	54
6. Application of FGA to Syncrude Coker Gas Oil (SCGO) .	79

6.1 Analytical Data For SCGO	79
6.2 Structural Characterization of SCGO by FGA	80
6.2.1 Saturates	80
6.2.2 Aromatics	81
6.2.3 Polar I	82
6.2.4 Polar II	83
6.2.5 Polar III	84
6.3 Effect of ^{13}C -NMR Data on the Structural Profiles	87
6.4 Treatment of Resins	90
6.5 Summary	91
7. Structural Characterization of Alberta Gas Oils	107
7.1 Description of Gas Oils	107
7.2 Analytical Data	108
7.3 FGA Results	110
7.4 Summary	116
8. Structural Characterization of Hydroprocessed Syncrude Coker Gas Oil	129
8.1 Comparison of Structural Profiles of SC-101 with SCGOF2	130
8.2 Summary	134
9. Conclusions and Recommendations	138
9.1 Conclusions	138
9.2 Recommendations	140
List of References.....	142
Appendix A : Modifications to the Quadratic programming Algorithm.....	148
A.1 Description of the Algorithm	148
A.2 Modifications to the Algorithm	150

A.3 Correction of Sign Violations	152
Appendix B : Program Listing and Documentation	154
B.1 Program OPTIMA	158
B.2 Subroutine MAINP	170
B.3 Marquardt Algorithm	204

List of Tables

Table	Page
II.1 Results for Functional Group Concentrations of Cold Lake Tar Sands (Allen et al., 1985).....	13
II.2 Functional Groups for Gas Oils.....	14
III.1 ^1H -NMR Band Assignment for Gas Oils.....	23
III.2 ^{13}C -NMR Band Assignment for Gas Oils.....	24
IV.1 Constraint Matrix Coefficients.....	39
IV.2 Objective Function Coefficients.....	40
V.1 Composition of Synthetic Mixtures.....	57
V.2 Carbon-13 Peak and Band Assignment for S1.....	58
V.3 Carbon-13 Peak and Band Assignment for MA1.....	59
V.4 Carbon-13 Peak and Band Assignment for PA1.....	61
V.5 Carbon-13 Peak and Band Assignment for TS2.....	63
V.6 References for ^{13}C Peak Assignments.....	65
V.7 Analytical Data and FGA Results for S1.....	66
V.8 Analytical Data and FGA Results for S2.....	67
V.9 Analytical Data and FGA Results for MA1.....	68
V.10 Analytical Data and FGA Results for MA2.....	69
V.11 Analytical Data and FGA Results for PA1.....	70
V.12 Analytical Data and FGA Results for TS1.....	71
V.13 Analytical Data and FGA Results for TS2.....	72
V.14 Analytical Data and FGA Results for TS3.....	73
V.15 % Error in ^1H -NMR Band Intensities.....	74
V.16 % Error in ^{13}C -NMR Band Intensities.....	75
V.17 % Error in Predicted Group Concentrations.....	76

V.18	Effect of Weighting Factors on TS2 Profiles.....	77
VI.1	Properties of SCGO.....	94
VI.2	Class Separation Results for SCGO.....	95
VI.3	Elemental Analyses (Wt %) of SCGO Fractions.....	96
VI.4	¹ H-NMR data for SCGO Fractions.....	97
VI.5	¹³ C-NMR data for SCGO Fractions.....	98
VI.6	Structural Profiles of SCGO Fractions.....	99
VI.7	Structural profiles of SCGO.....	100
VI.8	Analytical Data for SCGO (whole oil analysis)....	101
VI.9	Comparison of ¹³ C-NMR data with FGA Results for SCGO.....	102
VI.10	¹³ C-NMR Data for SCGO Fractions (data from the spectrum integration curve).....	104
VI.11	Structural Profiles of SCGO Fraction (¹³ C-NMR data from spectrum integration curve)...	105
VI.12	Structural Profiles of SCGO Resin Fraction.....	106
VII.1	Properties of Gas Oils.....	118
VII.2	Class Separation Results (Wt. % of whole oil)....	119
VII.3	Elemental Analyses of Gas Oils.....	120
VII.4	¹ H-NMR Data for Gas Oils (% of total hydrogen)...	121
VII.5	¹³ C-NMR Data for Gas Oils (% of total carbon)...	122
VII.6	Concentration of Polar III Groups from IR,.....	123
VII.7	Structural Profiles of SCGOF2 Fractions.....	124
VII.8	Structural Profiles of CLGO Fractions.....	125
VII.9	Structural Profiles of LVGO Fractions.....	126
VII.10	Structural Profiles of EMRGO Fractions.....	127
VII.11	Summary of the Important Structural Features	

of Gas Oils.....	128
VIII.1 Analytical Data for SC-101.....	135
VIII.2 Structural Profiles of SC-101 Fractions.....	136
VIII.3 Structural Profiles for SC-101 and SCGOF2.....	137

List of Figures

Figure	Page
I.1 Representation of a Complex molecule by Functional Groups.....	6
III.1 Class Separation Scheme.....	22
III.2 ^1H -NMR Spectrum of SCGO Polar I.....	25
III.3 ^{13}C -NMR Spectrum of LVGO Aromatics.....	26
III.4 IR Spectrum of SCGO Polar III.....	27
IV.1 Constraints and Objective Function for a Mixture..	41
V.1 Extent of Overlap in ^{13}C Bands of LVGO Aromatics.....	78
VI.1 ^{13}C -NMR Spectrum of SCGO Polar I.....	103

Nomenclature

- A constraint matrix
- b right hand side vector of constraints representing elemental analysis and $^1\text{H-NMR}$ data
- C $n \times n$ matrix defining the quadratic part of the objective function in Wolfe's algorithm
- C13 right hand side vector for the objective function equations representing carbon analysis and $^{13}\text{C-NMR}$ data
- C0 objective function matrix
- d sum of column entries in the tableau for simplex method
- F objective function
- I identity matrix
- J Jacobian of the objective function
- m number of constraints
- n number of functional groups
- P $1 \times n$ matrix defining the linear part of the objective function in Wolfe's algorithm
- r iteration number in Marquardt algorithm
- s number of bands observed in $^{13}\text{C-NMR}$ spectra
- t number of independent variables
- U m component vector in Wolfe's algorithm
- V n component vector in Wolfe's algorithm
- W m component vector of artificial variables in Wolfe's algorithm
- WF weighting factors
- X functional groups concentration, moles/100 grams

- \underline{z}^1 m component vector of artificial variables in Wolfe's algorithm
- \underline{z}^2 m component vector of artificial variables in Wolfe's algorithm
- δ hydrogen or carbon chemical shift, ppm
- δ radius of increment vector in Marquardt algorithm
- λ Marquardt parameter
- μ parameter defining the linear part of the objective function which is maximized to 1.0 in phase III of Wolfe's algorithm
- ϕ objective function equations with dependent variables expressed as linear combinations of independent variables

Superscripts

- t transpose of a matrix
- -1 inverse of a matrix
- $+$ adjusted objective function coefficients with dependent variables expressed as linear combinations of independent variables

Subscripts

- i counter for rows of the constraint matrix
- j counter for columns of the constraint and the objective function matrices corresponding to functional groups
- k counter for rows of the objective function matrix

1. Introduction

In order to predict the kinetic behavior of processes such as upgrading of a heavy oil, one requires a chemical description of the oil. In studies where kinetic models are based on boiling range or class fraction, one can obtain an adequate representation of the oil behavior for a specific composition over the range of process conditions studied. There are extensive published studies on hydroprocessing of heavy oils. In the case of hydrodesulphurization for example, the rate of sulphur removal is generally correlated with total sulphur concentration. Chung (1982) obtained a pseudo first order rate expression in liquid phase sulphur concentration (mol mL^{-1}) for hydrodesulphurization of Lloydminster Vacuum Gas Oil which provided a good fit for the rate data. Beuther and Schmid (1963) studied the catalytic hydrodesulphurization of Middle Eastern crudes and obtained a rate expression second order in weight percent of sulphur. Metzger et al. (1971) showed that the desulphurization of Kuwait Virgin distillates was adequately represented by a rate expression with order of 1.7 in weight percent of sulphur. Schuit and Gates (1973) concluded that desulphurization of many reactants over a wide range of conditions was first order in reactant concentration and in hydrogen partial pressure. They recognized that petroleum feedstocks should be considered as a mixture of sulphur containing compounds each of which reacts at a rate proportional to its concentration. Due to a wide range of

reactivities for various sulphur compounds, the sulphur removal rate can be first to second order in the total feed sulphur content depending on the feedstock and operating conditions.

A major limitation of such modelling methods is that they do not provide any information about reaction pathways involving different structures each with different reactivity. Since heavy oils contain many complex structures, any single lumped parameter would be inadequate to describe the chemical changes in the oil. For conventional modelling methods, the predictive ability is limited by the imprecise relationship between reactivity and bulk properties of the oil.

Before any kinetic modelling study is undertaken for processes involving complex hydrocarbon mixtures, one requires a technique for characterizing the chemical composition of the mixture. Heavy oils, coal-derived liquids, and other organic fuels contain very complex structures and no single analytical technique can identify and quantify all the structures that are present. Many characterization studies are available, but to be useful for modelling purposes, the resulting classification must be easy to implement, should describe the major reactive structures adequately, and yet retain flexibility to incorporate various sources of analytical information.

A common approach for structural characterization of hydrocarbon mixtures is to obtain a set of average

structural parameters based on nuclear magnetic resonance (NMR) data (Brown and Ladner, 1960). These parameters characterize the mixture in terms of aromaticity, average chain length, degree of aromatic ring condensation, and degree of substitution on aromatic rings as well as other structural features. Average molecule construction (Oka et al., 1977) is another technique which uses the structural parameters obtained from NMR data together with average molecular weight data to construct an average molecule to represent the mixture. Both of these approaches provide information on average structural features and not the actual structures present.

In 1983, Allen proposed the Functional Group Analysis (FGA) approach for structural characterization of complex hydrocarbon mixtures. FGA takes the approach that a representative set of functional groups account for the majority of the important structures that are present. As shown in Figure I.1, a large complex molecule is viewed as a combination of simple functional groups. The purpose of FGA is to quantify the chemical character of a feedstock or product in terms of the concentration of an appropriate set of selected functional groups.

The choice of functional groups to represent a sample depends on the information available on the structures present in that sample. The qualitative interpretation of analytical data from such sources as $^1\text{H-NMR}$, $^{13}\text{C-NMR}$, and infra-red (IR) spectroscopy can also provide information on

the presence of particular functional groups. Once a set of functional groups has been chosen, their concentrations are determined so as to satisfy the analytical data from such sources as elemental analysis, $^1\text{H-NMR}$, $^{13}\text{C-NMR}$, IR, and mass spectroscopy.

The purpose of this study is to develop a method of Functional Group Analysis for structural characterization of gas oils obtained from Alberta bitumen. Class separation of gas oils by column chromatography is used to obtain fractions which are enriched in selected functional groups. This separation is a necessary first step towards the characterization of gas oils, which facilitates the appropriate choice of functional groups to represent the separated fractions. Quantitative information from elemental analysis, $^1\text{H-NMR}$, $^{13}\text{C-NMR}$, and semi-quantitative data from IR spectroscopy are used to obtain the structural profiles of various fractions.

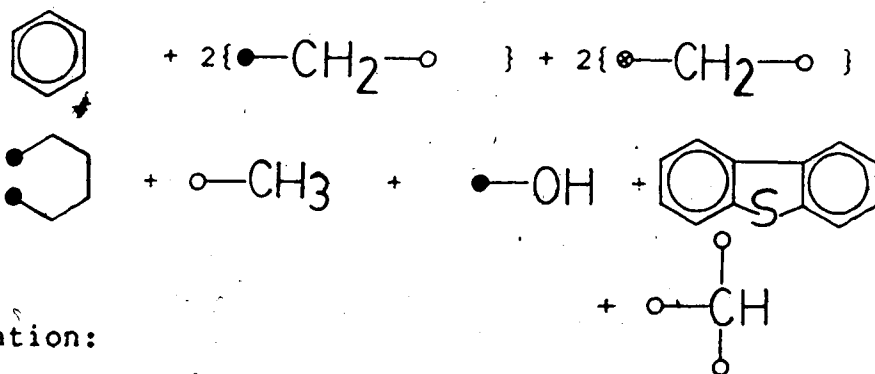
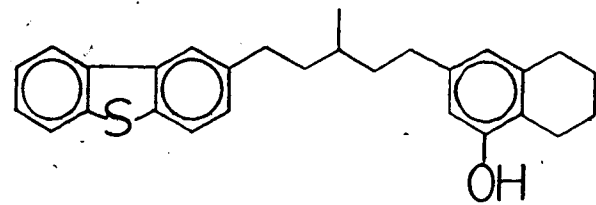
The concentration of the functional groups can serve as a first step in kinetic modelling studies. Development of a mathematical model which would predict the changes in the concentration of functional groups is difficult and beyond the scope of this study.

In chapter 2, recent applications of FGA by other workers for structural characterization of organic fuels, in particular for coal derived liquids, will be briefly reviewed. The work of other researchers in identifying the chemical structures in Alberta bitumen will be used to

obtain a set of functional groups for gas oils. The analytical methods used in this study are briefly discussed in chapter 3 and the mathematical formulation of FGA utilizing the data from these sources is presented in chapter 4.

In chapter 5, FGA is applied to a number of synthetic mixtures prepared from laboratory organic compounds to develop an estimate of the accuracy of the analysis. The structural profiles of various fractions of a Syncrude Coker Gas Oil (SCGO) are presented and discussed in chapter 6 to reveal the strengths and weaknesses of FGA.

A comparison of the structural profiles of gas oils obtained from various geographic locations is presented in chapter 7. In chapter 8, the structural profiles of the liquid product obtained from hydroprocessing of SCGO are presented to examine the changes in the functional group concentrations resulting from hydrotreatment. The conclusions of this study are summarized in chapter 9.



Notation:

- Bound to aromatic carbon
 - Bound to carbon alpha from aromatic ring
 - Bound to carbon beta or further from aromatic ring

Figure I.1 Representation of a Complex Molecule by Functional Groups

2. Literature Survey

2.1 Application of FGA for Structural Analysis

FGA has been used for structural characterization of several fossil fuels, in particular for coal-derived liquids (Allen, 1983; Petrakis et al., 1983). The dominant structures in a coal derived oil are various aromatic and hydroaromatic structures. Allen (1983) used information from elemental analysis, $^1\text{H-NMR}$, and carbon aromaticity from $^{13}\text{C-NMR}$ to obtain structural profiles for aromatics and various resin fractions obtained from hydroliquified coal samples.

FGA is also flexible in that various sources of data can be integrated to obtain the structural profiles of complex hydrocarbon mixtures. Allen et al. (1985), used information from class separation yields, $^1\text{H-NMR}$, elemental analysis, mass spectroscopy, and limited data from $^{13}\text{C-NMR}$ to characterize heavier fractions of shale oils, heavy crudes, and tarsands. For heavy oils, the set of functional groups representing the sample should include aliphatic groups such as methyl, methylene, and methyne groups to account for the presence of alkyl chains and branches in addition to various aromatic and hydroaromatic structures. Quantitative interpretation of mass spectra was difficult and involved some assumptions since the relationship between peak intensities and concentration is not always known. The assumptions involved in applying mass spectra information in FGA are outlined by Le (1985).

Allen (1983) obtained the structural profiles for a series of hydrodesulphurized coal liquids using elemental analysis, $^1\text{H-NMR}$, and high resolution mass spectroscopy. Examination of the profiles revealed some trends with increasing residence time. A decrease in the concentration of large aromatic clusters and an increase in the concentration of hydroaromatic and small aromatic clusters indicated partial hydrogenation of aromatic rings. The concentration of short aliphatic chains, however, remained relatively unchanged.

Allen et al. (1984) applied FGA to wood tars using data from elemental analysis, $^1\text{H-NMR}$, and $^{13}\text{C-NMR}$. The components of tar were rich in oxygen, containing between 34 and 43 % oxygen by weight. Consequently, the appropriate set of functional groups was dominated by oxygenated species. The structural profiles of the tars were used to obtain thermodynamic properties using group contribution methods, which demonstrated another application of FGA.

2.2 Chemical Structures in Bitumen and Heavy Oils

There is a lack of information on the application of FGA for structural characterization of gas oils derived from bitumen, which contain larger amounts of saturated structures than coal liquids. In a recent paper (Allen et al., 1985) FGA was applied to a sample of atmospheric tower bottoms from a Cold Lake heavy oil. The results, shown in Table II.1, indicate that most of the aromatic ring systems were heteroatomic, in particular dibenzothiophene. Elemental

analysis on the saturated fraction of heavy oil samples has shown the presence of considerable amounts of sulphur, likely in the form of naphthenic sulfides, which indicate that not all the sulphur is in the heteroatomic aromatic structures. Clearly the choice of dibenzothiophene as the only sulphur bearing group distorted the results of the analysis. The high concentration of heteroaromatics has resulted in a small concentration of benzene and naphthalene groups in the results. A better description of the oil can also be achieved if more information is extracted from ^{13}C -NMR spectra, in particular for the aromatic carbons. The aromatic carbon band (δ range 100-160 ppm) can be divided into three bands containing protonated aromatic carbon, non-protonated aromatic carbon bound to carbon, and non-protonated aromatic carbon bound to heteroatoms. This division would allow a better estimate of the concentration of heteroaromatic structures.

The choice of an appropriate set of functional groups for gas oils in this study was based on the work of other researchers to identify the chemical structures in Alberta bitumen and heavy oils.

Payzant et al. (1980) analyzed the saturated hydrocarbon fraction of the Cold Lake oil sand bitumen. Mass spectrometry was used to identify the mass series of hydrocarbon ring systems from acyclic and monocyclics to hexacyclics. The mono-, di-, and tricyclic saturated hydrocarbons were mainly alkyl substituted cyclohexanes,

decalins, and perhydrophenanthrenes, respectively. Steranes and hopanes constituted the tetra and pentacyclics respectively. Strausz et al. (1982) analyzed the aromatic hydrocarbon fraction of the Cold Lake bitumen, which was about 19 weight percent of the total bitumen. The results indicated the presence of mono, di, and trinuclear alkyl substituted aromatic structures, alkyl substituted di, tri, and tetrานuclear hydroaromatics, and thiaphenoaromatics such as alkyl benzothiophenes and dibenzothiophenes.

Selucky et al. (1978) carried out a detailed analysis of the deasphaltened Cold Lake bitumen using chromatographic separation followed by IR, UV, NMR, and GC/MS studies to determine the chemical composition. Based on mass spectra analysis, they identified various aromatic and hydroaromatic structures. The monoaromatics mainly contained alkyl benzenes, naphthalenebenzenes, dinaphthalenebenzenes, and benzothiophenes. Naphthalenes, dibenzofurans, and dibenzothiophenes mainly contributed to diaromatics while the triaromatics contained alkyl phenanthrenes and naphthenephenanthrenes.

Research has also been carried out in identifying various heteroatom functions and polar groups in the resin fraction of Alberta bitumen. Payzant et al. (1983) identified the presence of naphthenic sulfides and sulfoxides in Athabasca bitumen. Strausz (1984) identified the presence of carboxylic acids and cyclic and acyclic alcohols in Athabasca and Cold Lake bitumen. Bunger et al.

(1979) analyzed the separated fractions of Athabasca bitumen by IR spectroscopy and determined the concentration of functional groups such as phenols, carbazoles, esters, carboxylic acids, ketones, amides, and sulfoxides. Amines, ethers, furans, and quinoline are other structures which appear in coal liquids and may be present in some oils.

Table II.2 contains a list of 50 functional groups. Some of the groups account for the observed structures in Alberta bitumen. The table also includes structures for coal liquids and other possible structures for gas oils that have not been reported or discussed. Some of the groups represent structural isomers. For example, groups 17 and 19, and groups 18 and 21 represent different methylene and methyne groups respectively; however, they cannot be distinguished based on NMR data. Heteroatom groups such as alcohols, amines, ethers, thioethers, carbonyls, etc. could be adjacent to methyne, methylene, or methyl groups. However, only methylene groups alpha to such functionalities are allowed. Moreover, in the case of amines and amides, only primary structures are considered. From Table II.2, an appropriate set of groups can be selected to represent various fractions of the gas oils. For the saturates fraction for example, groups 23 and 24 account for cyclic structures while groups 19, 21, and 22 represent linear structures. The heteroatom content of saturates could be represented by the least polar groups such as ether and aliphatic thioether for oxygen and sulphur respectively.

Data from elemental analysis, $^1\text{H-NMR}$, $^{13}\text{C-NMR}$, and IR spectroscopy were used to obtain the concentration of the selected functional groups. These analytical methods are discussed in chapter 3.

Table II.1 Results for Functional Group Concentrations
of Cold Lake Tar Sands (Allen et al., 1985)

Concentrations in moles of functional groups/100 g of sample

Group	Structure	Concentration
Dibenzothiophene		0.15
Carbazole		0.03
Ether bridge		0.03
Ketone		0.001
Phenol		0.09
Carboxylic acid		0.02
Quinoline		0.001
Benzene		0.002
Naphthalene		0.001
Aniline		0.002
Hydroaromatic ring		0.07
Alpha methyl		0.009
Alpha methylene		0.23
Alpha methyne		0.24
Beta and Beta(+) methyl		1.01
Beta and Beta(+) methylene		2.03
Beta and Beta(+) methyne		0.97

Table II.2 Functional Groups for Gas Oils
 Group # Group name Structure

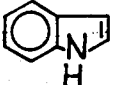
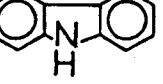
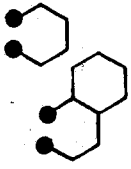
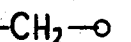
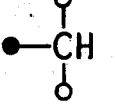
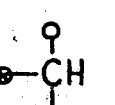
1	Benzene	
2	Naphthalene	
3	Phenanthrene	
4	Pyrene	
5	Benzothiophene	
6	Dibenzothiophene	
7	Dibenzofuran	
8	Indole	
9	Carbazole	
10	Quinoline	
11	Hydroaromatic ring	
12	Double hydroaromatic	
13	Alpha methylene	
14	Alpha methyl	
15	Alpha methyne	
16	Beta methyl	
17	Beta methylene	
18	Beta methyne	

Table II.2 (continued)

Group #	Group name	Structure
19	Chain methylene	$\text{O}-\text{CH}_2-\text{O}$
20	Naphthenic methyne	$\text{O}-\text{CH}=\text{O}$
21	Aliphatic methyne	$\text{O}-\text{CH}=\text{O}$
22	Gamma methyl	$\text{O}-\text{CH}_3$
23	Naphthenic methyl	$\text{O}-\text{CH}_3$
24	Naphthenic methylene	$\text{O}-\text{CH}_2-\text{O}$
25	Ketone bridge	$\text{O}=\text{C}-\text{O}$
26	Biphenyl bridge	$\text{O}-\text{C}_6\text{H}_4-\text{C}_6\text{H}_4-\text{O}$
27	Methylene bridge	$\text{O}-\text{C}_2\text{H}_4-\text{O}$
28	Double methylene bridge	$\text{O}-\text{C}_2\text{H}_2-\text{C}_2\text{H}_2-\text{O}$
29	Double hydroaromatic bridge	$\text{O}-\text{C}_6\text{H}_4-\text{C}_6\text{H}_4-\text{O}$
30	Aromatic olefin	$\text{O}-\text{CH}=\text{CH}-\text{O}$
31	Terminal olefin	$\text{O}-\text{CH}=\text{CH}_2$
32	Aromatic sulfoxide	$\text{O}-\text{S}-\text{CH}_2-\text{O}$
33	Aliphatic thioether	$\text{O}-\text{CH}_2-\text{S}-\text{CH}_2-\text{O}$
34	Aliphatic sulfoxide	$\text{O}-\text{CH}_2-\text{S}-\text{CH}_2-\text{O}$
35	Aliphatic amine	$\text{O}-\text{CH}_2-\text{NH}_2$
36	Aniline	$\text{O}-\text{NH}_2$

Table II.2 (continued)

Group #	Group name	Structure
37	Indoline	
38	Aromatic amide	
39	Aliphatic amide	
40	Aromatic ketone	
41	Carboxylic acid	
42	Aromatic ether bridge	
43	Phenol	
44	Cyclic alcohol	
45	Acyclic alcohol	
46	Naphthenic chain methyne	
47	Naphthenic chain methylene	
48	Benzofuran	
49	Thioether bridge	
50	Aliphatic ether	

Notation

- Bound to aromatic carbon
- Bound to naphthenic carbon
- ◐ Bound to carbon alpha from aromatic ring
- Bound to carbon beta or further from aromatic ring

3. Analytical Methods for FGA

3.1 Class Separation by Column Chromatography

Class separation by column chromatography was used to obtain fractions which were enriched in selected functional groups. The method was based on the work of Selucky and Strausz (Selucky, 1976; Selucky et al., 1977) to separate saturates and aromatics from the resins. The procedure was modified to recycle the solvents back into the chromatographic column. This recycle allowed the separation of relatively large quantities of oil for further analysis without the excessive consumption of the solvents. The recycle apparatus was based on Syncrude Analytical Method 5.1. The overall recovery from the separation procedure was generally in excess of 95 weight percent. The separation scheme indicating the various fractions is illustrated in Figure III.1. The three polar fractions were distinguished by the increasing polarity of their constituent groups. The silica gel column had an inside diameter of 2.4 cm and 48 cm of packing. The column was saturated with about 100 mL of solvent and after addition of approximately ten grams of oil, about 270 mL of solvent was added to the top of the column. About 150 mL of solvent was placed in a flask at the bottom of the column for recycle. The alumina/silica gel column was 3.0 cm in diameter with 45 cm of silica gel and 3.0 cm of alumina at the top. For this column, about 280 mL of solvent was used without recycle.

The class separation procedure was also modified to deal with lighter oils with relatively low initial boiling points. For lighter oils, some of the volatile components were evaporated with the solvents during the separation procedure and resulted in poor recovery; 83 to 85 % of the original sample. The volatile components were removed by distillation prior to the class separation. Distillation at 160 °C for four hours was sufficient to remove the more volatile components and give a 95 % balance on the fractions from class separation. The volatile components could be characterized by other analytical techniques such as gas chromatography.

3.2 Elemental Analysis

Elemental analysis was performed by the University of Alberta Microanalytical Laboratory using Perkin-Elmer model 240 and 240B analyzers for C, H, N, and O, and titration with Ba(ClO₄)₂ for sulphur analysis. The analyses were normalized.

3.3 ¹H-NMR

¹H-NMR provides information on the molecular environment of hydrogen atoms in the mixture. One can differentiate, for example, between hydrogen bonded to an aromatic ring, adjacent to a ring, or well removed from a ring. The spectrum is divided into seven bands each corresponding to a specific bonding environment and the intensity of each band is proportional to the amount of hydrogen in that particular bonding environment. The

relative amount of hydrogen in each band was obtained from the spectrum integration curve.

The ^1H -NMR spectra were recorded on a 60 MHz VARIAN A-56/60-A spectrometer using the constant wave technique. Hydrogen chemical shifts, δ , of individual fractions were measured using 30-50 % (by volume) solutions in CDCl_3 , with tetramethylsilane (TMS) as an internal standard.

The ^1H -NMR spectrum of the Polar I fraction of SCGO is illustrated in Figure III.2. The small smeared signal centered at $\delta=8.3$ ppm was due to the presence of phenanthrenes which have been identified in similar samples by mass spectroscopy (Selucky et al., 1977). The resonances that appear in this range are due to protons with steric hindrance such as the 4,5-protons of substituted (or alkyl-bridged) phenanthrenes (Chamberlain, 1974). The band assignment for ^1H -NMR is presented in Table III.1. There were some overlaps in the tail ends of adjacent bands. For the purpose of quantitative interpretation, the dividing point between two bands was taken at the point of intersection.

3.4 ^{13}C -NMR

^{13}C -NMR gives data on the molecular environment of carbon atoms in the mixture and one can differentiate between various types of aromatic and aliphatic carbon. The band assignment for ^{13}C -NMR is presented in Table III.2 and is based on a survey by Snape et al. (1979) on ^{13}C chemical shifts in aromatic hydrocarbons. The intensity of each band

is proportional to the amount of carbon in that particular bonding environment. In many cases, the behavior of the integration curve was poor and a digitizer was used to obtain the peak areas and hence a measure of the relative amounts of carbon in each band.

There was some uncertainty in the band intensities obtained from ^{13}C -NMR spectra, particularly in the chemical shift range between 22.5 and 37.5 ppm where the signals for various methylene groups appear. The change in the chemical shift of a particular group due to neighbouring substituents may cause some overlap between bands. Furthermore, the long relaxation times for non-protonated aromatic carbons result in signals with lower intensities (Abraham and Loftus, 1978).

The ^{13}C -NMR spectra were obtained on a 15.08 MHz Bruker WP-60 spectrometer equipped with a Nicolet NIC-80 computer system using the Fourier transform pulsed technique. The ^{13}C chemical shifts were measured at ambient temperature in CDCl_3 , with TMS as an internal reference. Concentrations were within the range of 20 - 40% (by volume) and chromium tris-acetyl acetone was used as the relaxation reagent. The recording conditions were as follows:

Pulse width (30°) - $3\mu\text{sec}$.

Acquisition time - 1.0 sec.

Spectral width - 3750 Hz

Number of pulses - 13,000 to 70,000

The ^{13}C -NMR spectrum for the aromatics fraction of Lloydminster Vacuum Gas Oil (LVGO) is illustrated in Figure III.3.

3.5 IR Spectroscopy

The IR spectrum of the Polar III fraction of SCGO is presented in Figure III.4. The strong band at 3300 cm^{-1} indicated the presence of hydroxyl groups, and a variety of carbonyl groups gave bands between 1750 and 1635 cm^{-1} . The ratio of the hydroxyl groups to carbonyls or the concentration of these groups can be obtained from the adsorption of each band measured by planimetry, and the adsorption coefficients for each band (Bunger, 1976).

Analytical data from the above methods were used to obtain the structural profiles of individual fractions of various gas oils. The methodology is discussed in chapter 4.

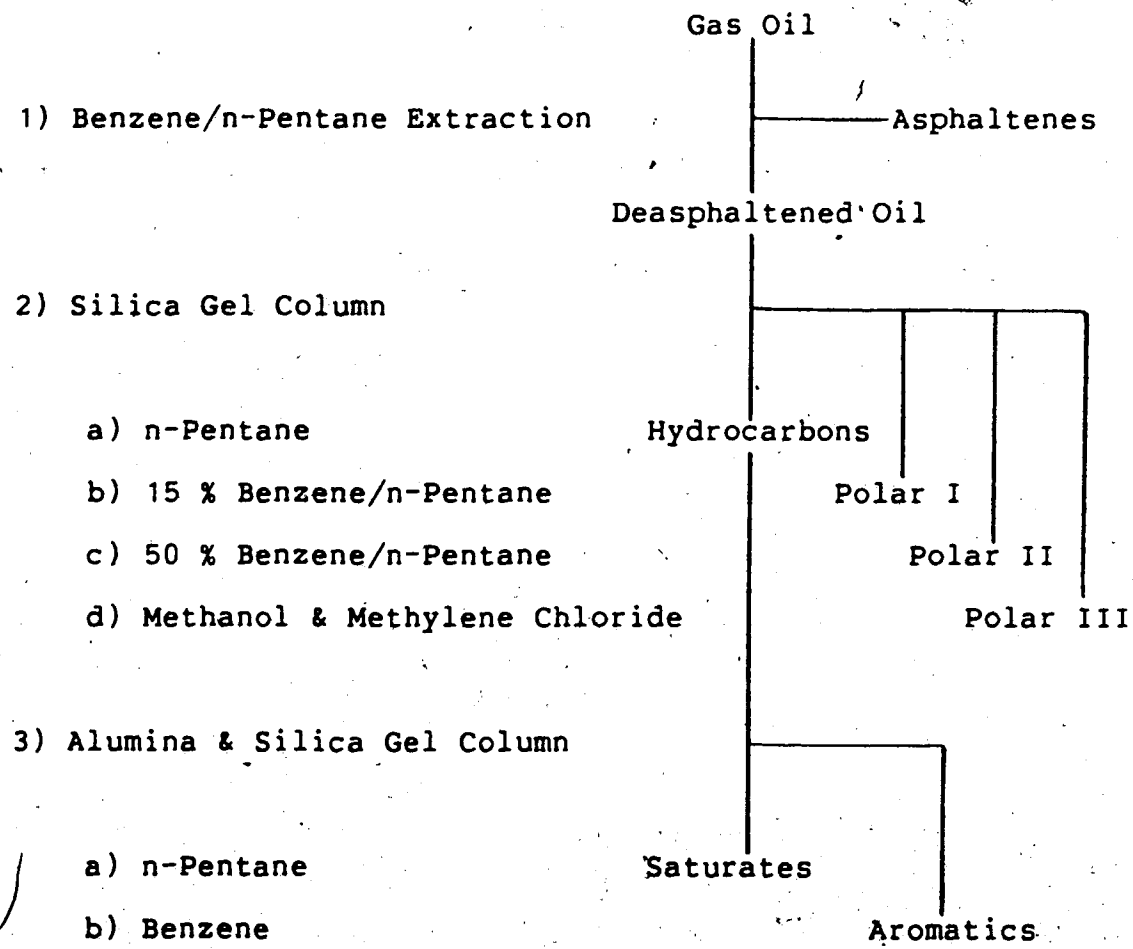


Figure III.1 Class Separation Scheme

Table III.1 $^1\text{H-NMR}$ Band Assignments for Gas Oils

Band #	Range, ppm.	Hydrogen Type
1	0.5 - 1.0	γ -methyl
2	1.0 - 2.0	β , naphthenic, alkyl-OH
3	2.0 - 4.5	α , amine, methylene α to sulfoxides, amides, amines, alkyl-OH
4	4.5 - 6.3	olefins
5	6.3 - 8.3	aromatic, amide, phenol
6	8.3 - 9.0	phenanthrene hindered H
7	9.0 - 11.0	aldehyde

Table III.2 ^{13}C -NMR Band Assignments for Gas Oils

Band #	Range, ppm.	Carbon Type
1	11. - 15	γ -methyl
2	15 - 18	β -methyl
3	18 - 20.5	α -methyl
4	20.5 - 22.5	naphthenic methyl, β -methylene in hydroaromatic rings
5	22.5 - 27.5	naphthenic methylene, β -methylene
6	27.5 - 37	α -methylene, γ -methylene, β -methylene in hydroaromatics, bridge methylene, methylene α to O and S
7	37 - 60.	naphthenic chain methylene; α , β , γ , and naphthenic methyne, methylene α to N
8	60 - 85	chloroform-d solvent
9	100 - 129.5	aromatic carbon bonded to hydrogen, olefins
10	129.5 - 140	aromatic carbon bonded to carbon
11	140 - 160	aromatic carbon bonded to O, N, S
12	160 - 185	carbonyl carbon in amides and acids
13	185 - 210	ketones

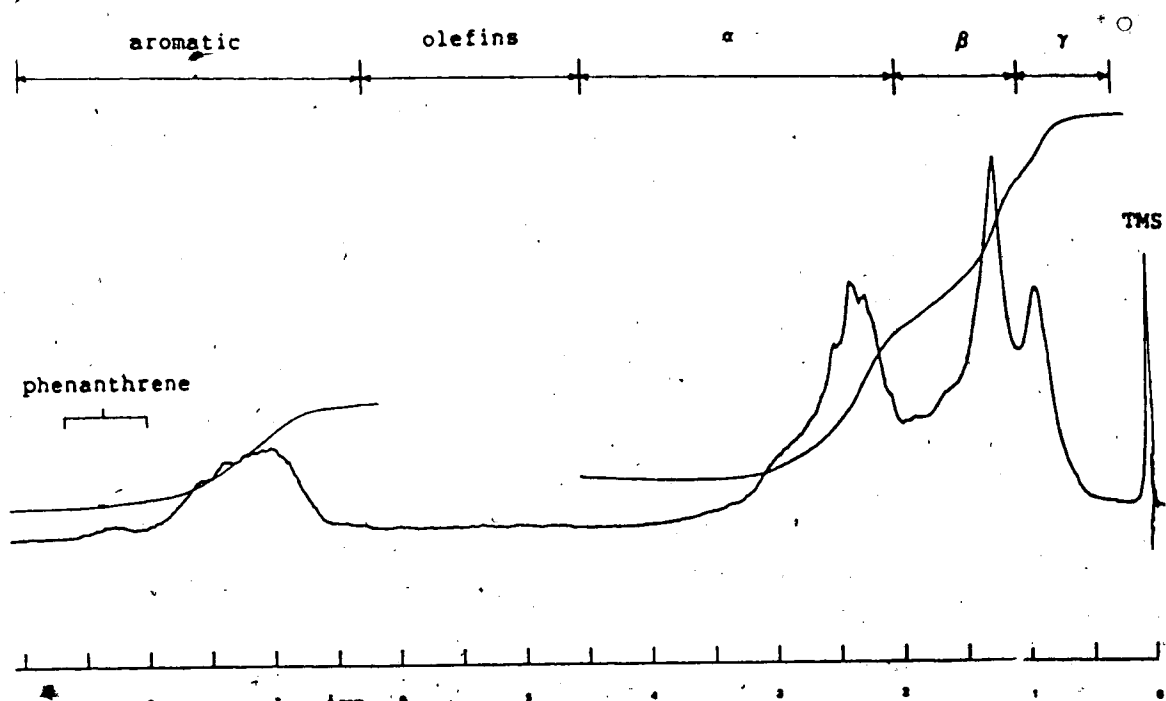


Figure III.2 $^1\text{H-NMR}$ Spectrum of SCGO Polar I

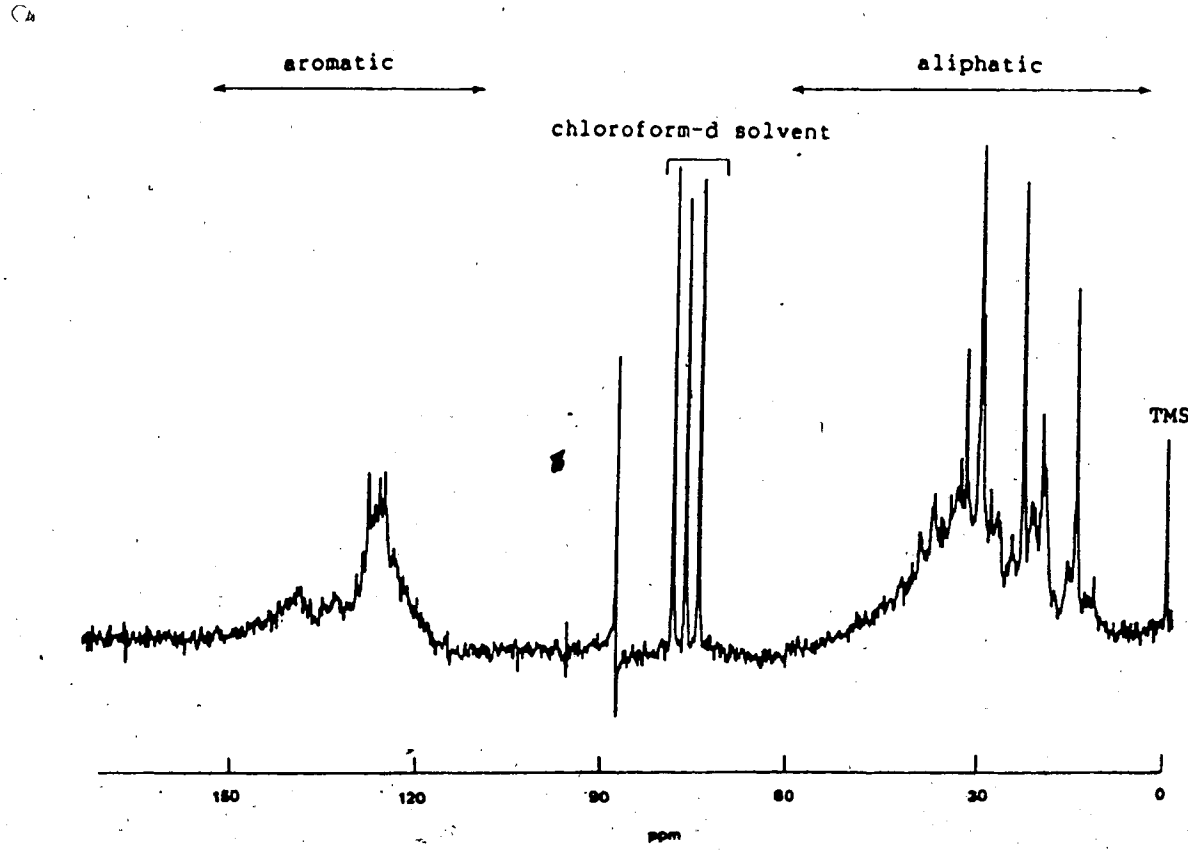


Figure III.3 ^{13}C -NMR Spectrum of LVGO Aromatics

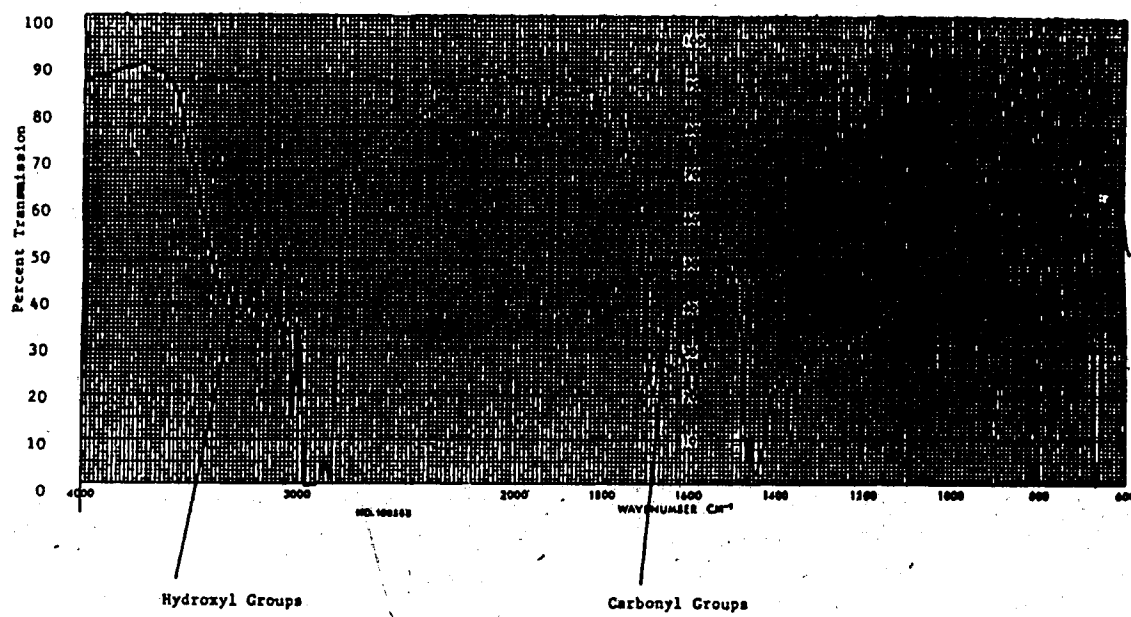


Figure III.4 IR spectrum of SCGO Polar III

4. Mathematical Formulation of FGA for Characterization of Gas Oils

4.1 Development of Mathematical Procedure

In the analysis of gas oils, quantitative data from elemental analysis, $^1\text{H-NMR}$, and $^{13}\text{C-NMR}$ for individual fractions were utilized to obtain structural profiles for each fraction. The analytical data from $^{13}\text{C-NMR}$ were less reliable than those obtained from elemental analysis and $^1\text{H-NMR}$. Consequently, in the mathematical formulation, more emphasis was placed on elemental analysis and $^1\text{H-NMR}$.

The concentration of a set of functional groups were related to the analytical data through a set of balance equations. For each band in the $^1\text{H-NMR}$ spectra containing a particular type of hydrogen, and for each element N, O, S, and C, a balance equation was written. For example, the total concentration of β -hydrogen as obtained from elemental analysis and $^1\text{H-NMR}$ data, should equal the total concentration of each functional group times the stoichiometric number of β -hydrogen in that group, summed over all groups. Hence, one could obtain a set of linear constraints given by equation (1):

$$\sum_{j=1}^n A_{ij} X_j = b_i \quad (1)$$

$(i = 1, \dots, m)$

where X_j are the unknown functional group concentrations (n groups in total); b_i are quantities obtained from elemental analysis and $^1\text{H-NMR}$ (m pieces of analytical information); and A_{ij} are stoichiometric coefficients which were uniquely

assigned to each functional group based on chemical composition and type of hydrogen. The constraint coefficients for functional groups in gas oils are presented in Table IV.1.

Non-negativity constraints were applied to individual functional groups to assure that the solution was physically reasonable, i.e. that all concentrations were greater than or equal to zero. These constraints were inequalities given by equation (2):

$$X_j \geq 0 \quad (2)$$

The concentration of functional groups could also be related to the analytical data obtained from $^{13}\text{C-NMR}$. The spectral scan was divided into 13 bands, each containing a particular type of carbon. A set of linear equations similar to equation (1) could be obtained for each band:

$$\sum_{j=1}^n C_{0kj} X_j = C_{13k} \quad (3)$$

$$(k = 1, \dots, 13)$$

where X_j are the unknown functional group concentrations, C_{13k} are experimental quantities of carbon in each band of the $^{13}\text{C-NMR}$ spectrum, and C_{0kj} are stoichiometric coefficients which were uniquely assigned to each group based on the type of carbon present in that group.

In applying FGA, one seeks to incorporate as much analytical information as possible in obtaining the concentration of a set of selected functional groups. The methodology to obtain the concentrations depends on the amount of analytical information available. For an

overdetermined system where the number of balance equations exceeds the number of unknown functional groups, the concentrations could be obtained by a least square procedure. In many cases, however, the number of equations is smaller than the unknown concentrations of functional groups. In such a case, the equations either have no solutions, which would suggest that the choice of functional groups is inappropriate, or that there exists a space of infinite solutions. For the latter, one can characterize the sample by applying an optimization technique to obtain a solution which minimizes an objective function. Detailed discussion of the methodology for above cases is given by Petrakis et al. (1983) and Allen et al. (1984).

Allen (1983) suggested that for underdetermined systems, the most accurate and reliable sources of data be used in constructing linear balance equations while the less accurate data be used in constructing the objective function. Consequently, in the characterization of gas oils, elemental analysis and ¹H-NMR data were used to obtain linear constraints given by equation (1). The objective function was formulated using analytical data from the ¹³C-NMR spectra. The objective function, F, takes the quadratic form given by equation (4):

$$F = \sum_{k=1}^{13} \{ C_{13k} - \sum_{j=1}^n CO_{kj} X_j \}^2 \quad (4)$$

The objective function coefficients, CO_{kj} , for the functional groups in gas oils are presented in Table IV.2.

The contribution of each band in the ^{13}C -NMR spectra was weighted to improve accuracy. Bands which uniquely specified a group were weighted more than the rest so the concentrations of groups representing these bands approximate the expected values. With the weighting factors, the objective function used in the computation scheme was of the form given by equation (5):

$$F = \sum_{k=1}^{13} \{WF_k (C13_k - \sum_{j=1}^n CO_{kj} X_j)\}^2 \quad (5)$$

where WF_k are weighting factors assigned to each band in the ^{13}C -NMR spectra. For bands specifying a single group, a weighting factor of 5 ensures a satisfactory agreement between calculated and expected values. Other bands which represent several functional groups were assigned weighting factors of 1.

4.2 Additional Constraints

The number of functional groups containing heteroatoms such as N, O, and S to account for the presence of such elements is limited because of insufficient quantitative data for heteroatoms. For each fraction recovered in the class separation procedure, the choice of heteroatomic functional groups is limited to one or two groups for each element representing the most likely structures in that fraction. In the case of the Polar III fraction for example, IR analysis indicated that phenol (group 43) and carbonyl attached to aromatic ring (group 40) were the most likely oxygen groups. The ratio of the concentration of phenols to carbonyls or their absolute concentrations could be obtained

from the adsorption of their respective bands in the IR spectra, measured by planimetry, and the adsorption coefficients for phenols and carbonyls (Bunger, 1976). This ratio or the absolute concentrations were introduced in the computation scheme as additional equality constraints.

Secondary constraints were introduced to ensure that the solution to equation (5) was physically reasonable. Two such constraints were utilized:

1. total concentration of chain terminating groups should be less than or equal to groups contributing to chains.
2. total concentration of aromatic substituents should be less than or equal to the total concentration of aromatic sites.

If phenolic or alcoholic hydrogens are present in a sample, their signals in the $^1\text{H-NMR}$ spectrum would be smeared among other bands and no unique band could be assigned to such hydrogens. The signals for phenolic hydrogens appear within band 5 while the chemical shift range for alcoholic hydrogens includes bands 2 and 3. If phenols and/or alcohols are present in a sample, to allow for the overlaps, the constraints for band 5 and/or bands 2 and 3 in equation (1) are converted to inequalities (left hand side of the above constraints would be less than or equal to the right hand sides). Additional inequality constraints would be introduced for phenols and/or alcohols so that their concentrations would be less than or equal to the concentration of hydrogen in band 5 and/or bands 2 and

3. If the absolute concentrations of phenols and/or alcohols are known, then the constraints for band 5 and/or bands 2 and 3 remain as equalities but the right hand sides of these constraints are reduced by amounts proportional to the known concentrations of phenols and/or alcohols respectively. In the case of alcohols, it is assumed that they are distributed equally between bands 2 and 3.

Once the linear constraints and the objective function were formulated, any one of a number of optimization techniques could be applied to obtain an optimal solution to equation (5) subject to constraints (1), (2), and other additional constraints.

4.3 Optimization Procedure

The optimization procedure used to obtain the structural profiles was the long form of Wolfe's algorithm for quadratic programming (Wolfe, 1959; Kunzi et al., 1968). The algorithm is suitable for optimization problems involving a quadratic objective function, subject to equality and inequality as well as non-negativity constraints. Computationally, the algorithm is very efficient and convergence to a global optimum is achieved in a limited number of iterations.

Another optimization procedure that has been applied in FGA (Allen, 1983; Le, 1985) is the direct search method of Luus and Jaackola (1973). This is an iterative method in which the solution for the next iteration is obtained by evaluating the objective function for a large number of

points chosen randomly and moving to the point which provides the most improvement on the objective function. Convergence to an optimum is achieved after a specified number of iterations by systematic reduction of the search region. The advantage of this method is that it requires very little programming; however, the algorithm is fairly slow and requires a considerable number of function evaluations.

The direct search method can be used independently to obtain the optimal solution to equation (5) subject to constraints mentioned previously. For this purpose one requires an initial feasible solution which could be obtained using the simplex method for linear programming (Dantzig, 1963). In this study, however, the direct search method was used as a further check for results obtained from the quadratic programming algorithm. The initial solution for the direct search method was that obtained from Wolfe's algorithm. The results were further checked by the Newton-Marquardt method (Marquardt, 1963) which is a least square parameter estimation method in which the direction of search is determined by the Jacobian of the objective function and λ , the Marquardt parameter. Neither method provided any improvement indicating that a global optimum was reached.

One difficulty that was encountered in using the Marquardt algorithm was that the algorithm was not suitable for optimization problems in which all variables should

satisfy the non-negativity constraint. To skirt this problem, whenever a non-negativity constraint was violated, the value of the objective function was set to a large value and hence the solution was rejected.

A computer program written in FORTRAN was developed for the optimization procedure. Because the constraint and the objective function coefficients were uniquely assigned to each group, it was possible to generalize the program to set up appropriate matrices representing the constraints and the objective function. The constraint matrix consists of rows representing linear constraints with the columns representing the functional groups. The column entries for a group correspond to the constraint coefficients for that group as specified in Table IV.1. Inequality constraints are converted to equality constraints by introducing appropriate slack variables, as is normal practice in linear programming. The objective function matrix consists of rows corresponding to each band in the $^{13}\text{C-NMR}$ spectrum while the columns represent the functional groups. The column entries for a group correspond to the objective function coefficients for that group as specified in Table IV.2. For illustration, the group coefficients in Tables IV.1 and IV.2 were used to obtain the constraints and objective function for an arbitrary mixture. These are presented in Figure IV.1.

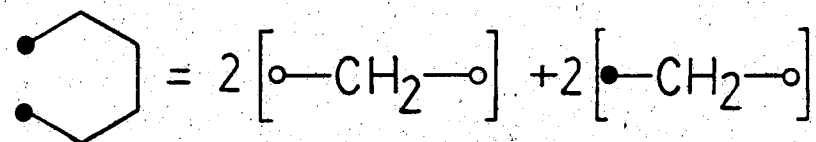
It should be noted that in applying Wolfe's algorithm to obtain the optimal solution, some modifications were made

in the selection rules involved in the simplex method to ensure that the optimal solution was obtained. These modifications resulted in some non-negativity constraints being violated during the course of the algorithm; however, when the solution was obtained, such violations were not observed. A detailed discussion of the modifications is presented in Appendix A. The listing of the program and documentation is included in Appendix B.

4.4 Restrictions on Group Selections

One may choose a large set of groups to represent gas oils obtained from bitumen; however, the appropriate number of groups is limited by the amount of quantitative information available as well as by the ability of the mathematical procedure to generate an exact solution for the structural profile.

In the selection of a set of functional groups, one should be wary of groups that are linear combinations of other groups. For example, the hydroaromatic ring, group 11, can be considered as a combination of alpha and chain methylene, groups 13 and 19 respectively, in the constraint matrix:



The hydroaromatic ring can be included in the analysis when the other two groups are present because its carbons on the β position are distinguished independently in the $^{13}\text{C-NMR}$ spectrum. By the same argument, one cannot distinguish

between naphthenic methyne in structures such as decalin, and methyne in a linear structure because their coefficients for the constraint and the objective function matrices are the same. Consequently, saturated cyclic structures identified by Payzant et al. (1980) must be represented by naphthenic methylene (group 24) rather than by explicit ring structures.

A limited number of aromatic structures and alkyl groups directly attached to aromatic rings can be chosen to represent a sample. If too many of these groups are included, an infinite number of solutions give the same minimum for the objective function. Such would be a case when a group with zero concentration appears in the solution. This could be identified by varying the order of groups in the quadratic programming algorithm, i.e. interchange of columns corresponding to the functional groups in the constraint and objective function matrices. If the solution is not unique, another solution would be obtained with a different group having zero concentration with no change in the value of the objective function; hence, one could obtain an infinite number of solutions between the two extremes. By selecting only the most significant groups, and by trial and error, zero concentrations could be eliminated thereby avoiding non-uniqueness for the solution. If a group remained zero despite the reordering of the coefficient matrix, the solution was accepted. This procedure provided a direct

check for the uniqueness.

4.5 Summary

In the computation scheme for FGA, data from four well established analytical methods; elemental analysis, $^1\text{H-NMR}$, IR, and $^{13}\text{C-NMR}$ were utilized. The more reliable information from elemental analysis and $^1\text{H-NMR}$ were used in constructing balance equations relating the concentration of functional groups to the analytical data. When applicable, secondary constraints were added using quantitative information from IR. An objective function was formulated using the analytical data from $^{13}\text{C-NMR}$. The optimization procedure was based on the long form of Wolfe's algorithm for quadratic programming. The computation scheme was fairly straightforward and was easily programmed for a computer. In the next chapter, the methodology outlined in this chapter will be applied to a number of synthetic mixtures prepared from common laboratory organic compounds with similar functional groups as those for gas oils. Comparison of the concentration of various groups predicted from FGA with known group concentrations would provide an estimate of the accuracy of FGA as well as the expected error in the analytical methods.

Table IV.1 Constraint Matrix Coefficients

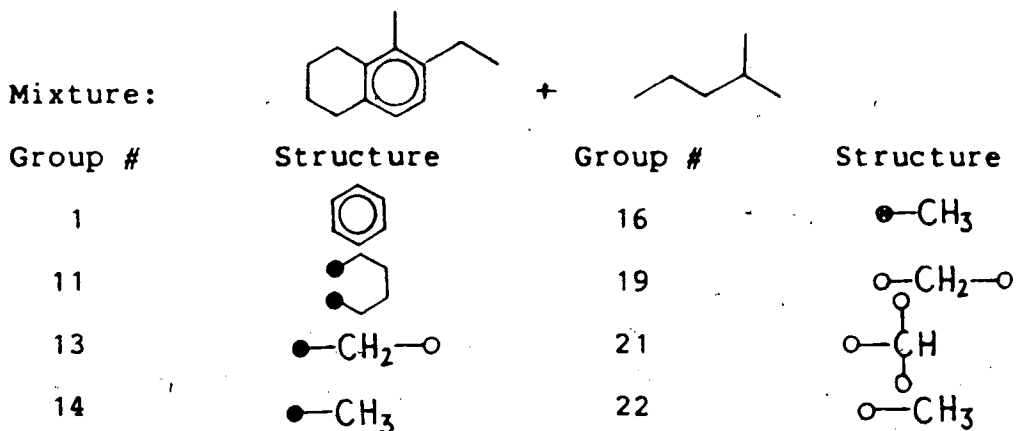
Group #	Elements and Various Types of Hydrogen												
	C	5	6	7	1	2	3	Ph-H	Al-H	4	0	S	N
1	6.0	6.0	0.0	0.0	0.0	0.0	0.0	0.0	0.0	0.0	0.0	0.0	0.0
2	10.0	8.0	0.0	0.0	0.0	0.0	0.0	0.0	0.0	0.0	0.0	0.0	0.0
3	14.0	8.0	2.0	0.0	0.0	0.0	0.0	0.0	0.0	0.0	0.0	0.0	0.0
4	16.0	10.0	0.0	0.0	0.0	0.0	0.0	0.0	0.0	0.0	0.0	0.0	0.0
5	8.0	6.0	0.0	0.0	0.0	0.0	0.0	0.0	0.0	0.0	0.0	1.0	0.0
6	12.0	8.0	0.0	0.0	0.0	0.0	0.0	0.0	0.0	0.0	0.0	1.0	0.0
7	12.0	8.0	0.0	0.0	0.0	0.0	0.0	0.0	0.0	0.0	1.0	0.0	0.0
8	8.0	6.0	0.0	0.0	0.0	0.0	1.0	0.0	0.0	0.0	0.0	0.0	1.0
9	12.0	8.0	0.0	0.0	0.0	0.0	1.0	0.0	0.0	0.0	0.0	0.0	1.0
10	3.0	1.0	0.0	0.0	0.0	0.0	0.0	0.0	0.0	0.0	0.0	0.0	1.0
11	4.0	-2.0	0.0	0.0	0.0	4.0	4.0	0.0	0.0	0.0	0.0	0.0	0.0
12	8.0	-2.0	0.0	0.0	0.0	11.0	3.0	0.0	0.0	0.0	0.0	0.0	0.0
13	1.0	-1.0	0.0	0.0	0.0	0.0	2.0	0.0	0.0	0.0	0.0	0.0	0.0
14	1.0	-1.0	0.0	0.0	0.0	0.0	3.0	0.0	0.0	0.0	0.0	0.0	0.0
15	1.0	-1.0	0.0	0.0	0.0	0.0	1.0	0.0	0.0	0.0	0.0	0.0	0.0
16	1.0	0.0	0.0	0.0	0.0	3.0	0.0	0.0	0.0	0.0	0.0	0.0	0.0
17	1.0	0.0	0.0	0.0	0.0	2.0	0.0	0.0	0.0	0.0	0.0	0.0	0.0
18	1.0	0.0	0.0	0.0	0.0	1.0	0.0	0.0	0.0	0.0	0.0	0.0	0.0
19	1.0	0.0	0.0	0.0	0.0	2.0	0.0	0.0	0.0	0.0	0.0	0.0	0.0
20	1.0	0.0	0.0	0.0	0.0	1.0	0.0	0.0	0.0	0.0	0.0	0.0	0.0
21	1.0	0.0	0.0	0.0	0.0	1.0	0.0	0.0	0.0	0.0	0.0	0.0	0.0
22	1.0	0.0	0.0	0.0	3.0	0.0	0.0	0.0	0.0	0.0	0.0	0.0	0.0
23	1.0	0.0	0.0	0.0	3.0	-1.0	0.0	0.0	0.0	0.0	0.0	0.0	0.0
24	1.0	0.0	0.0	0.0	0.0	2.0	0.0	0.0	0.0	0.0	0.0	0.0	0.0
25	1.0	-2.0	0.0	0.0	0.0	0.0	0.0	0.0	0.0	0.0	1.0	0.0	0.0
26	0.0	-2.0	0.0	0.0	0.0	0.0	0.0	0.0	0.0	0.0	0.0	0.0	0.0
27	1.0	-2.0	0.0	0.0	0.0	0.0	2.0	0.0	0.0	0.0	0.0	0.0	0.0
28	2.0	-2.0	0.0	0.0	0.0	0.0	4.0	0.0	0.0	0.0	0.0	0.0	0.0
29	6.0	-4.0	0.0	0.0	0.0	4.0	6.0	0.0	0.0	0.0	2.0	0.0	0.0
30	2.0	-1.0	0.0	0.0	0.0	0.0	0.0	0.0	0.0	0.0	0.0	0.0	0.0
31	2.0	0.0	0.0	0.0	0.0	0.0	0.0	0.0	0.0	3.0	0.0	0.0	0.0
32	1.0	-1.0	0.0	0.0	0.0	0.0	2.0	0.0	0.0	0.0	1.0	1.0	0.0
33	2.0	0.0	0.0	0.0	0.0	0.0	4.0	0.0	0.0	0.0	1.0	1.0	0.0
34	2.0	0.0	0.0	0.0	0.0	0.0	4.0	0.0	0.0	0.0	0.0	0.0	1.0
35	1.0	0.0	0.0	0.0	0.0	0.0	4.0	0.0	0.0	0.0	0.0	0.0	1.0
36	0.0	-1.0	0.0	0.0	0.0	0.0	2.0	0.0	0.0	0.0	0.0	0.0	1.0
37	2.0	-2.0	0.0	0.0	0.0	0.0	5.0	0.0	0.0	0.0	0.0	0.0	0.0
38	1.0	1.0	0.0	0.0	0.0	0.0	0.0	0.0	0.0	0.0	1.0	0.0	1.0
39	3.0	2.0	0.0	0.0	0.0	0.0	2.0	0.0	0.0	0.0	1.0	0.0	0.0
40	2.0	-1.0	0.0	0.0	0.0	2.0	0.0	0.0	0.0	0.0	1.0	0.0	0.0
41	1.0	-1.0	0.0	1.0	0.0	0.0	0.0	0.0	0.0	0.0	2.0	0.0	0.0
42	0.0	-2.0	0.0	0.0	0.0	0.0	0.0	0.0	0.0	0.0	1.0	0.0	0.0
43	0.0	-1.0	0.0	0.0	0.0	0.0	0.0	0.0	1.0	0.0	1.0	0.0	0.0
44	0.0	0.0	0.0	0.0	0.0	-1.0	0.0	0.0	1.0	0.0	1.0	0.0	0.0
45	1.0	0.0	0.0	0.0	0.0	0.0	2.0	0.0	1.0	0.0	1.0	0.0	0.0
46	1.0	0.0	0.0	0.0	0.0	1.0	0.0	0.0	0.0	0.0	0.0	0.0	0.0
47	1.0	0.0	0.0	0.0	0.0	2.0	0.0	0.0	0.0	0.0	1.0	0.0	0.0
48	8.0	6.0	0.0	0.0	0.0	0.0	0.0	0.0	0.0	0.0	0.0	1.0	0.0
49	0.0	-2.0	0.0	0.0	0.0	0.0	0.0	0.0	0.0	0.0	0.0	1.0	0.0
50	2.0	0.0	0.0	0.0	0.0	0.0	4.0	0.0	0.0	0.0	1.0	0.0	0.0

Ph-H; Phenolic Hydrogen Al-H; Alcoholic Hydrogen
 Column numbers refer to hydrogen type (see Table III.1)

Table IV.2 Objective function coefficients

Group #	Band #												
	1	2	3	4	5	6	7	8	9	10	11	12	13
1	0.0	0.0	0.0	0.0	0.0	0.0	0.0	0.0	6.0	0.0	0.0	0.0	0.0
2	0.0	0.0	0.0	0.0	0.0	0.0	0.0	0.0	8.0	2.0	0.0	0.0	0.0
3	0.0	0.0	0.0	0.0	0.0	0.0	0.0	0.0	10.0	4.0	0.0	0.0	0.0
4	0.0	0.0	0.0	0.0	0.0	0.0	0.0	0.0	10.0	6.0	0.0	0.0	0.0
5	0.0	0.0	0.0	0.0	0.0	0.0	0.0	0.0	5.0	1.0	2.0	0.0	0.0
6	0.0	0.0	0.0	0.0	0.0	0.0	0.0	0.0	8.0	2.0	2.0	0.0	0.0
7	0.0	0.0	0.0	0.0	0.0	0.0	0.0	0.0	8.0	2.0	2.0	0.0	0.0
8	0.0	0.0	0.0	0.0	0.0	0.0	0.0	0.0	5.0	2.0	1.0	0.0	0.0
9	0.0	0.0	0.0	0.0	0.0	0.0	0.0	0.0	8.0	2.0	2.0	0.0	0.0
10	0.0	0.0	0.0	0.0	0.0	0.0	0.0	0.0	0.0	1.0	2.0	0.0	0.0
11	0.0	0.0	0.0	2.0	0.0	2.0	0.0	0.0	-2.0	2.0	0.0	0.0	0.0
12	0.0	0.0	0.0	1.0	5.0	1.0	1.0	0.0	-2.0	2.0	0.0	0.0	0.0
13	0.0	0.0	0.0	0.0	0.0	1.0	0.0	0.0	-1.0	1.0	0.0	0.0	0.0
14	0.0	0.0	1.0	0.0	0.0	0.0	0.0	0.0	-1.0	1.0	0.0	0.0	0.0
15	0.0	0.0	0.0	0.0	0.0	0.0	1.0	0.0	-1.0	1.0	0.0	0.0	0.0
16	0.0	1.0	0.0	0.0	0.0	0.0	0.0	0.0	0.0	0.0	0.0	0.0	0.0
17	0.0	0.0	0.0	0.0	1.0	0.0	0.0	0.0	0.0	0.0	0.0	0.0	0.0
18	0.0	0.0	0.0	0.0	0.0	0.0	1.0	0.0	0.0	0.0	0.0	0.0	0.0
19	0.0	0.0	0.0	0.0	0.0	1.0	0.0	0.0	0.0	0.0	0.0	0.0	0.0
20	0.0	0.0	0.0	0.0	0.0	0.0	1.0	0.0	0.0	0.0	0.0	0.0	0.0
21	0.0	0.0	0.0	0.0	0.0	0.0	1.0	0.0	0.0	0.0	0.0	0.0	0.0
22	1.0	0.0	0.0	0.0	0.0	0.0	0.0	0.0	0.0	0.0	0.0	0.0	0.0
23	0.0	0.0	0.0	1.0	0.0	0.0	0.0	0.0	0.0	0.0	0.0	0.0	0.0
24	0.0	0.0	0.0	0.0	1.0	0.0	0.0	0.0	0.0	0.0	0.0	0.0	0.0
25	0.0	0.0	0.0	0.0	0.0	0.0	0.0	0.0	-2.0	2.0	0.0	0.0	1.0
26	0.0	0.0	0.0	0.0	0.0	0.0	0.0	0.0	-2.0	2.0	0.0	0.0	0.0
27	0.0	0.0	0.0	0.0	0.0	1.0	0.0	0.0	-2.0	2.0	0.0	0.0	0.0
28	0.0	0.0	0.0	0.0	0.0	2.0	0.0	0.0	-2.0	2.0	0.0	0.0	0.0
29	0.0	0.0	0.0	2.0	2.0	0.0	2.0	0.0	-4.0	4.0	0.0	0.0	0.0
30	0.0	0.0	0.0	0.0	0.0	0.0	0.0	0.0	1.0	1.0	0.0	0.0	0.0
31	0.0	0.0	0.0	0.0	0.0	0.0	0.0	0.0	-1.0	1.0	0.0	0.0	0.0
32	0.0	0.0	0.0	0.0	0.0	1.0	0.0	0.0	-1.0	0.0	1.0	0.0	0.0
33	0.0	0.0	0.0	0.0	0.0	2.0	0.0	0.0	0.0	0.0	0.0	0.0	0.0
34	0.0	0.0	0.0	0.0	0.0	2.0	0.0	0.0	0.0	0.0	0.0	0.0	0.0
35	0.0	0.0	0.0	0.0	0.0	0.0	1.0	0.0	0.0	0.0	0.0	0.0	0.0
36	0.0	0.0	0.0	0.0	0.0	0.0	0.0	0.0	-1.0	0.0	1.0	0.0	0.0
37	0.0	0.0	0.0	0.0	1.0	0.0	1.0	0.0	-2.0	1.0	1.0	0.0	0.0
38	0.0	0.0	0.0	0.0	0.0	0.0	0.0	0.0	-1.0	1.0	0.0	1.0	0.0
39	0.0	0.0	0.0	0.0	0.0	1.0	0.0	0.0	0.0	0.0	0.0	1.0	0.0
40	0.0	0.0	0.0	0.0	0.0	0.0	1.0	0.0	0.0	-1.0	1.0	0.0	1.0
41	0.0	0.0	0.0	0.0	0.0	0.0	0.0	0.0	-1.0	1.0	0.0	1.0	0.0
42	0.0	0.0	0.0	0.0	0.0	0.0	0.0	0.0	-2.0	0.0	2.0	0.0	0.0
43	0.0	0.0	0.0	0.0	0.0	0.0	0.0	0.0	-1.0	0.0	1.0	0.0	0.0
44	0.0	0.0	0.0	0.0	-1.0	1.0	0.0	0.0	0.0	0.0	0.0	0.0	0.0
45	0.0	0.0	0.0	0.0	0.0	1.0	0.0	0.0	0.0	0.0	0.0	0.0	0.0
46	0.0	0.0	0.0	0.0	0.0	0.0	1.0	0.0	0.0	0.0	0.0	0.0	0.0
47	0.0	0.0	0.0	0.0	1.0	0.0	0.0	0.0	0.0	0.0	0.0	0.0	0.0
48	0.0	0.0	0.0	0.0	0.0	0.0	0.0	0.0	5.0	1.0	2.0	0.0	0.0
49	0.0	0.0	0.0	0.0	0.0	0.0	0.0	0.0	-2.0	0.0	2.0	0.0	0.0
50	0.0	0.0	0.0	0.0	'0.0	2.0	0.0	0.0	0.0	0.0	0.0	0.0	0.0

Figure IV.1 Constraints and Objective Function for a Mixture



Constraints:

$$6x_1 + 4x_{11} + x_{13} + x_{14} + x_{16} + x_{19} + x_{21} + x_{22} = b_1$$

$$4x_{11} + 2x_{13} + 3x_{14} = b_2$$

$$4x_{11} + 3x_{16} + 2x_{19} + x_{21} = b_3$$

$$3x_{22} = b_4$$

$$6x_1 - 2x_{11} - x_{13} - x_{14} = b_5$$

Objective Function, F:

$$\begin{aligned} F = & (x_{22} - C13_1)^2 + (x_{16} - C13_2)^2 + (x_{19} - C13_3)^2 + (2x_{11} - C13_4)^2 \\ & + (x_{19} + x_{13} + 2x_{11} - C13_5)^2 + (x_{21} - C13_7)^2 \\ & + (6x_1 - x_{13} - x_{14} - 2x_{11} - C13_8)^2 + (x_{13} + x_{14} + 2x_{11} - C13_9)^2 \end{aligned}$$

$$b_1 = (\text{Wt \% C}) / (\text{Atomic Weight of C})$$

$$b_2 = (\text{Wt \% H}) \cdot (\% \text{ Alpha-H}) / (\text{Atomic weight of H})$$

$$b_3 = (\text{Wt \% H}) \cdot (\% \text{ Beta-H}) / (\text{Atomic weight of H})$$

$$b_4 = (\text{Wt \% H}) \cdot (\% \text{ Gamma-H}) / (\text{Atomic weight of H})$$

$$b_5 = (\text{Wt \% H}) \cdot (\% \text{ Aromatic-H}) / (\text{Atomic weight of H})$$

$$C13_1 = (\text{Wt \% C}) \cdot (\% \text{ C in band } 1) / (\text{Atomic weight of C})$$

$$x_j = \text{concentration of group } j \text{ in moles/100 gram of sample}$$

5. Application of FGA to Known Mixtures

To examine the accuracy of FGA mixtures of known group concentrations were prepared from a number of simple organic compounds containing hydrocarbon functional groups representative of gas oils. The methodology outlined in chapter 4 was applied to each sample to obtain the structural profiles. Comparison of the spectral information with known values provided an estimate of error for the analytical methods. Structural profiles of samples served to develop error bounds on the functional group concentrations.

5.1 Sample Preparation and Analytical Methods

A total of eight samples were prepared for analysis. The description of each sample and the organic compounds used in preparing the samples are presented in Table V.1. The samples were divided into four categories. Samples S1 and S2 contained linear and cyclic saturated structures. MA1 and MA2 were monoaromatics and contained substituted benzene structures as well as linear and cyclic saturates. PA1 was a polyaromatic mixture containing one, two, and three ring aromatics, hydroaromatic ring, and linear structures. TS1, TS2, and TS3 contained substituted benzenes and linear structures as well as dibenzothiophene.

In the analysis of the the above samples, the known weight percent of elements for each sample were used. Some of the organic compounds listed in Table V.1 are quite volatile and may cause a gross error in the elemental analysis which would not be indicative of the actual error.

for the less volatile oil samples. For the oil samples, the elemental analyses were performed by the University of Alberta Microanalytical Laboratory and the reported error for each element analysis was 0.01 % .

The ^1H -NMR spectra for the known samples were recorded on a 60 MHz Varian spectrometer as described in chapter 3. The ^{13}C -NMR spectra of the mixtures were obtained from the University of Alberta High Field NMR Laboratory using a 200 MHz Bruker WH-200 spectrometer.

5.2 Peak Assignment for ^{13}C -NMR Spectra

For each known mixture, the ^{13}C -NMR spectrum provided the position of signals measured in ppm from TMS as internal reference, and the integration results for individual peaks. The ^{13}C -NMR band assignment discussed in chapter 3, together with the expected number of signals for each band were used to define bands for the spectrum where signals for particular types of carbons may appear. The chemical shift range of bands for S1, MA2, PA1, and TS2, representing the various categories of mixtures, are presented in the first column of Tables V.2 to V.5, respectively. These tables also provide the position of signals and their integrals for the above samples. Each peak was assigned to a particular type of carbon based on the published ^{13}C chemical shifts of the compounds present in the mixtures and the expected peak intensities from the known concentrations. The references for the chemical shifts of the model compounds are summarized in Table V.6. Tables V.2 to V.5 indicated that

for the model compounds used in this study, there were some overlaps between various bands as defined by Snape et al. (1979).

Spectral information from ^1H and $^{13}\text{C-NMR}$, and the structural profiles for each sample are summarized in Tables V.7 to V.14. For each sample, two sets of profiles are presented. One profile is based on the observed amount of carbon in the chemical shift range assigned to each band (B.A.). The other set of concentrations was obtained from the observed amount of carbon in various bands based on the individual assignment of peaks to each band (P.A.). For example, in the case of S1 and S2 samples, the chemical shift range for band 6 included 3 signals at 31.16, 32.35, and 33.79 ppm. Hence based on the band assignment, B.A., the relative amount of carbon in band 6 was obtained from the integration results for the above peaks. However, based on the individual peak assignments, P.A., band 6 carbons appeared at 21.95, 31.16, and 32.35 ppm.

5.3 Discussion of Results

5.3.1 $^1\text{H-NMR}$ Data

A typical characteristic of the $^1\text{H-NMR}$ spectra of S and MA samples was the broad band containing several peaks between 1.0 and 2.0 ppm which was due to the presence of cycloalkanes. For PA and TS samples the peaks in this range were rather sharp. Comparison of the relative amount of hydrogen in each band as obtained from the spectrum integration curve with known values, indicated that for all

samples, agreement between observed and known values was satisfactory. For the samples considered, the average percent error for intensities of $^1\text{H-NMR}$ bands varied between 4 and 6.5 % (Table V.15). These, however, were high estimates of error for $^1\text{H-NMR}$ data since there were possible losses of pentane due to evaporation during sample preparation. To minimize losses, samples were stored in a refrigerator prior to NMR analysis.

For the PA1 sample, the relative amount of hindered phenanthrene hydrogen, band 6, was determined by measuring the area of very small peaks centered about 8.3 ppm by planimetry. The area of these peaks relative to the total area of the spectra provided the percentage of hydrogen in band 6 which was in excellent agreement with the known value.

5.3.2 $^{13}\text{C-NMR}$ Data

The band assignment for the $^{13}\text{C-NMR}$ spectra is not as straight forward as that for the $^1\text{H-NMR}$ spectra because ^{13}C chemical shifts are extremely sensitive to molecular geometry. Unlike $^1\text{H-NMR}$ where only immediate groups or molecules influence the hydrogen chemical shift, in $^{13}\text{C-NMR}$, carbons separated by several bonds influence each other if they are geometrically close (Wehrli and Wirthlin, 1976). The band assignment presented by Snape et al. (1979) is thus subject to some uncertainty. The boundaries of such band assignments are not well defined and are subject to some overlap. Investigation of the chemical shifts of model

compounds in this study has clearly shown this overlap, in particular for the aliphatic region. For quantitative use of ^{13}C -NMR data in FGA, this limitation was recognized and as described in chapter 4, ^{13}C -NMR data were used to formulate the objective function for the optimization procedure.

Some of the bands in the ^{13}C -NMR spectra had well defined boundaries. One such band was the protonated aromatic carbon. For all the samples considered, the positions of signals for this carbon were in the expected range of 100 - 129.5 ppm. For aromatic carbon bound to other carbons (band 10) only the signals for substituted carbons in diethylbenzene appeared beyond 140 ppm. This would cause an overlap between band 10 and band 11 (aromatic carbon bound to heteroatoms) which may result in overestimation of carbon in band 11. On the other hand, the signal for carbon bound to sulphur in dibenzothiophene, was observed at 139 ppm.

Snape et al. (1979) assigned the chemical shift range between 129.5 and 148 ppm to aromatic carbon bonded to other carbon atoms. For the characterization of gas oils in this study, however, the upper limit of this band was set at 140 ppm. This was necessary in order to avoid underestimation of the relative amount of carbon in band 11 since the C-S signals in heteroaromatic sulphur structures are expected to appear around 140 ppm. Since aromatics and polar fractions of gas oils contained significant amounts of sulphur, typically between 5 and 8 weight %, any underestimation of

band 11 would result in lower concentration of thiophenoaromatics and higher concentration of aliphatic thioether. The overlap of aromatic carbon bound to alkyl substituents would give an overestimate for band 11 and an underestimate for band 10. The underestimate of band 10 would be corrected by data on alkyl substituents and phenanthrenes from $^1\text{H-NMR}$ spectra.

A large degree of overlap was also observed among bands in the aliphatic region. In the case of band 1 which contains methyl groups gamma or farther from aromatic rings, the relative amount of carbon can be underestimated if structures such as 2-methylpropane, isopentane, and 2-methylpentane are present. The observed chemical shift for the terminal methyl groups bound to methyne are 24.1, 21.8, and 22.3 ppm for the above compounds respectively (Levy et al., 1980) which are well out of the assigned range of 11 to 15 ppm for band 1. Other methyl groups such as those in t-butyl are shifted further down field to about 30 ppm (Levy et al., 1980). Hence, if a sample contains branches which are at least 2 carbons long, as would be the case for gas oils, the expected error in band 1 would be reduced. If both naphthenic methyl and gamma methyl in linear structures are included in the analysis, then the error in band 1 would affect the distribution of gamma hydrogen in the above groups. If gamma methyl is the only group with gamma hydrogen, then the error in band 1 would not affect the concentration of gamma methyl since it would be directly

obtained from the concentration of gamma hydrogen (band 1 in $^1\text{H-NMR}$ spectra). Rather, this error would affect the concentration of other groups. However, it is difficult to specify the group or groups which are affected by the error in band 1 of $^{13}\text{C-NMR}$ spectra.

The methylene group adjacent to the terminal methyl in n-pentane is shifted upfield to about 22 ppm and out of the expected range for band 6 (methylene groups in alkanes and alkyl branches). For other straight chain alkanes such as n-octane, n-butane, n-hexane, and n-decane, the signals for C2 methylene are observed at 22.7, 24.8, 22.7, and 22.8 respectively (Levy et al., 1980). If a sample contains very short chains, the percentage of methylene groups adjacent to terminal methyl is greater than that for a sample with longer chains. Hence, for oil samples containing long chains, the error in band 6 due to the upfield shift of such methylene groups would be reduced.

Among the bands in the aliphatic region, bands 2 and 3 representing terminal methyl beta and alpha to aromatic rings respectively, were consistent with the band assignments. The position of signals and the observed intensities of these bands were in satisfactory agreement with expected values.

The $^{13}\text{C-NMR}$ spectra of the aromatics fraction of Lloydminster Vacuum Gas Oil (LVGO) is presented in Figure V.1, which indicates the band assignments of Snape et al. (1979) and the extent of possible overlaps in the bands.

By introducing weighting factors for ^{13}C bands in FGA, it is possible to weight each band on the basis of accuracy. For bands which do not show any considerable overlap with other bands, such as bands 2, 3, and 9, one can assign weighting factors greater than 1. Weighting factors, typically 2 to 5, for the above bands would ensure a good agreement between the predicted and the observed concentration of carbon in such bands. A better agreement could be obtained by increasing the weighting factor for the above bands.

If the $^{13}\text{C-NMR}$ spectra is divided into bands using the band assignment of Snape et al. (1979), there would be error associated with the relative amount of carbon in each band due to the overlapping of bands. For the synthetic samples considered, using this band assignment (B.A.), the average absolute error in the intensities of aromatic bands (Table V.16) varied between 4 and 9 % while for the aliphatic region, the range for average absolute error for various bands was between 8 and 38 %. For the oil samples, the error in $^{13}\text{C-NMR}$ data is expected to be lower since unlike the model compounds examined in this study, gas oils contain longer chains and are thus less subject to overlap errors. Error in $^{13}\text{C-NMR}$ data was substantially reduced when individual peaks were assigned to bands thereby eliminating any overlapping of bands. Using the P.A. method, the average absolute error for the intensities of ^{13}C bands varied between 4 and 14 % except for band 4 (22 %). For S and MA

samples, band 4 represented naphthenic methyl. For these samples, intensities of band 4 were overestimated by 30 to 40 %. For PA and TS samples, band 4 represented beta carbons in hydroaromatic ring. For these samples, intensities of band 4 were overestimated by only 6 to 13 %. For S and MA samples containing saturated cyclic structures the errors in aliphatic bands were substantially higher compared with PA and TS samples which did not contain such structures. The error for P.A. method can be explained by another shortcoming of quantitative application of ^{13}C -NMR in that the intensities of signals are not exactly proportional to the amount of carbon. For example, considering the signals for toluene in the spectrum of MA2 sample, Table V.3, the ratios of peak integrals at 20.81, 124.81, 127.69, 128.48, and 137.11 ppm should be 1 : 1 : 2 : 2 : 1 respectively. However, the observed ratios were 1 : 1.05 : 2.74 : 2.13 : 1.01 indicating that protonated carbons had higher intensities. Adjusting the relaxation reagent or the pulse sequence could possibly reduce the error due to lack of proportionality; however, for gas oils such corrections would be difficult to verify.

Samples TS1, TS2, and TS3 were specially prepared to investigate the possible error in the intensity of the C-S signal in dibenzothiophene. The expected ratios for peak integrals at 120.99, 122.18, 123.71, 126.08, 134.96, and 138.90 ppm for TS2 sample, Table V.5, should be 1 : 1 : 1 : 1 : 1 : 1. The observed ratios were found to be 0.77 : 0.85

: 0.91 : 1.31 : 0.93 : 1. The observed ratios indicated that contrary to what was observed for toluene, the intensities of protonated aromatic carbons were low. The observed amounts of C-S carbon, band 11 in Tables V.12 to V.14, however, were in good agreement with the expected values.

For samples containing aromatic structures, Tables V.9 to V.14, the amounts of protonated aromatic carbon, band 9, obtained from the spectra, were consistently higher than the expected values. The error in the amount of carbon in band 9 was found to decrease from 14 to 5 % with increasing aromaticity of the sample. Although only 6 samples containing aromatic structures were considered in this study, the results suggest that it may be possible to establish correction factors for band 9 to minimize the error in ^{13}C -NMR data. One suitable parameter that such correction factors may be correlated with is aromaticity.

5.3.3 FGA Results

A summary of errors in the predicted functional group concentrations from FGA is presented in Table V.17. Using the B.A. method the predicted concentrations of some functional groups were within the range of $\pm 25\%$ of the actual group concentrations with average absolute errors between 4 and 13 %. These groups were gamma methyl, naphthenic methylene, beta methyl, hydroaromatic ring, and benzene. For the above groups, the range of error and the average absolute error remained relatively unchanged when the more accurate data from the P.A. method were used.

Using the B.A. method, naphthenic methyl, methyne, and chain_n methylene had a wide range of error and subsequently the average absolute error for these groups was in excess of 30 %. However, when the more accurate data from the P.A. method were used, the range of error and average absolute error for the above groups improved substantially suggesting that the concentrations of these groups were most subject to error in ¹³C-NMR data due to overlapping of bands.

While the predicted concentrations of alpha methyl from the B.A. method were consistently higher than the known concentrations, the predicted concentrations of alpha methylene were consistently lower than known values. The range and average error for these groups remained relatively unchanged when ¹³C-NMR data from the P.A. method were used. Both of the above groups contain alpha hydrogen and their combined concentrations (represented by alkyl substituents in Table V.17) were in good agreement with the known values.

Band 3 of ¹³C-NMR spectra contains signals from alpha methyl groups. The experimental concentrations of carbon in band 3 were slightly higher than the actual values (Table V.16) with an average error of 8 %. In order to obtain a good estimate for the concentration of alpha methyl, one may include the balance equation for band 3 of ¹³C-NMR spectra as an additional constraint in the optimization procedure, or assign band 3 with a high weighting factor.

In the case of PA1 sample, using the P.A. data resulted in a different split between benzene and naphthalene,

suggesting that distinction between these groups was not accurate on the basis of NMR data. As shown in Table V.17, the combined concentrations of benzene and naphthalene representing aromatic carbon in mono + diaromatics were in excellent agreement with known values.

The average absolute error in the predicted functional group concentrations indicated that with the exception of naphthenic methyl, only moderate improvement in the profiles were obtained when the more accurate ^{13}C data from the P.A. method were used, suggesting that the analysis was relatively insensitive to overlaps in ^{13}C band assignment. Although it is difficult to place error bounds on the individual functional group concentrations for unknown mixtures such as gas oils, examination of model compound profiles presented here provided some estimates for the degree of accuracy for the predicted concentrations of hydrocarbon functional groups. Concentrations of gamma methyl, naphthenic methylene, beta methyl, hydroaromatic rings, alkyl substituents, and mono + diaromatics were quite accurate and insensitive to overlaps in ^{13}C band assignment. For the above groups, the error for the predicted concentrations could be estimated at $\pm 15\%$. The predicted concentrations of chain methylene, methyne, and naphthenic methyl were less accurate with an estimated error of $\pm 40\%$.

Introducing weighting factors for bands with relatively low concentration of carbon representing a single group can improve the accuracy of the predicted functional group

concentrations. For such a band, using a weighting factor of 1.0 may result in very low predicted concentration for the group representing the band since the contribution of error to the objective function is low. In Table V.18 the predicted functional group concentrations for TS2 sample are compared with the actual concentrations using ^{13}C -NMR data from peak assignments. The first set of concentrations was obtained when weighting factors of 1.0 were assigned for all bands. The predicted concentrations were in satisfactory agreement with known values except for the aliphatic methyne group whose concentration was substantially underestimated. The second set of concentrations was obtained by assigning weighting factors of 2, 4, 2, and 4 for bands 2, 3, 4, and 7 respectively, which improved the predicted concentrations. For both set of profiles, the errors in the concentrations of alpha methyl and methylene were substantial; however, the combined concentrations represented by alkyl substituents were in good agreement with the known value. The choice of weighting factors for bands with small concentrations representing a single group is arbitrary. Weighting factors for these bands should be so chosen that the predicted concentrations approximate the experimental amount of carbon in such bands.

5.4 Summary

Comparison of the NMR data obtained for a number of synthetic mixtures with the expected values based on the known concentrations revealed that while for ^1H -NMR, the

data can be judged as fairly accurate, there is uncertainty in the ^{13}C -NMR data. The error in the ^{13}C -NMR data is associated with the overlap of bands particularly in the aliphatic region, and with the intensities of peaks which are not quite proportional to the amount of carbon representing the peaks.

The accuracy of the ^{13}C -NMR data could be substantially improved if individual peaks are assigned to particular type of carbons thereby eliminating the overlap of bands. This assignment is, however, difficult for complex hydrocarbon mixtures such as gas oils which contain a variety of complex structures. For the samples considered in this study, using the more accurate data based on the peak assignments, provided only moderate improvement in the predicted concentration of functional groups. This result can be explained by the fact that the error due to varying signal intensities cannot be completely eliminated. Also, the concentration of some functional groups are not sensitive to the ^{13}C -NMR data. The concentrations of alkyl substituents, and benzene and naphthalene should be summed into more general structural parameters.

Introduction of weighting factors for ^{13}C bands with small concentration allows the predicted concentration of groups representing such bands to approximate the experimental amounts of carbon. From the application of FGA to known mixtures, the analysis can be judged as fairly accurate. While for most hydrocarbon functional groups the

error in predicted concentrations could be estimated at ± 15 %, the predicted concentrations of chain methylene, methyne, and naphthenic methyl were less accurate with an estimated error of ± 40 %. In the next chapter, FGA will be used for structural characterization of Syncrude Coker Gas Oil (SCGO).

Table V.1 Composition of Synthetic Mixtures (weights in gram)

Compound	Sample					
	S1	S2	MA1	MA2	PA1	TS1
Decalin	0.9822	1.5297	0.8608	0.8150		
Methylcyclohexane	1.3876	1.2885	0.7434	0.7094		
n-Pentane	0.8368	0.8370	0.5564	0.5527	0.7285	0.4913
1-Pentane	0.4434	0.4905	0.4292	0.4654	0.4446	0.4441
Toluene			0.9016	2.5679		0.7686
Diethylbenzene			0.8232	2.3881	0.8144	0.8507
2-Methylnaphthalene					1.0215	0.8932
Phenanthrene					0.4914	
Tetralin					0.1076	
Dibenzothiophene					0.5857	0.7250
Wt% Carbon	85.13	85.36	87.24	88.59	88.12	88.05
Wt% Hydrogen	14.87	14.64	12.76	11.41	11.88	11.32
Wt% Sulfur					0.63	1.00
% Naphthalic carbon	60.24	67.02	34.36	18.50	45.54	51.71
Aromaticity			30.48	49.53		55.28
						56.01

Table V.2 Carbon-13 Peak and Band Assignment for S1

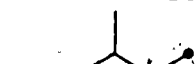
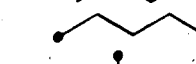
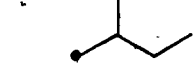
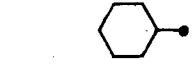
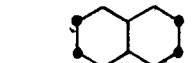
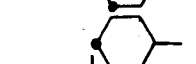
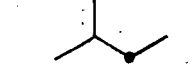
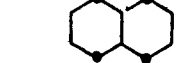
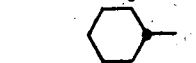
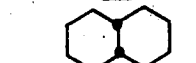
Range for Bands	Chemical shift (ppm) Observed	Literature	Integral	Ref.	Carbon Type	Band
1	11.18	11.3	2.743	a		1
	13.47	13.7	13.375	a		1
4	21.63	21.8	7.294	a		1
	21.95	22.2	14.084	a		6
5	22.32	23.3	10.148	b		4
	25.92	27.2	13.909	d		5
6	26.03	27.3	11.641	c		5
	26.33	27.1	9.943	c		5
7	29.30	29.7	5.583	a		7
	31.16	31.6	4.542	a		6
6	32.35	34.1	8.890	a		6
	33.79	34.7	15.409	d		5
7	35.03	36.3	17.068	c		5
	35.94	33.3	5.477	c		7
	43.15	44.2	3.651	d		7

Table V.3 Carbon-13 Peak and Band Assignment for MA2

Range for Bands	Chemical shift (ppm)	Observed	Literature	Integral	Ref.	Carbon Type	Band
1	11.21	11.3	0.512	a		1	
1	13.49	13.7	1.512	a		1	
2	14.76	15.8	0.391	e		2	
2	15.14	15.8	3.133	e		2	
3	20.81	20.4	2.998	a		3	
4	21.64	21.8	1.253	a		1	
4	21.91	22.2	1.734	a		6	
	22.34	23.3	1.068	b		4	
	24.98	29.2	0.431	e		6	
5	25.87	27.2	0.859	d		5	
5	25.99	27.3	1.552	c		5	
	26.28	27.1	1.337	c		5	
	28.00	29.2	1.207	e		6	
	28.42	29.2	2.476	e		6	
	29.24	29.7	0.870	a		7	
6	31.11	31.6	0.624	a		6	
6	32.27	34.1	0.822	a		6	
	33.73	34.7	2.017	d		5	
	34.96	36.3	1.563	c		5	
7	35.83	33.3	0.728	c		7	
	43.04	44.2	0.497	d		7	
	124.60	125.9	2.125	e		9	
9	124.81	125.6	3.162	a		9	
	125.44	125.9	0.391	e		9	

Table V.3 (Cont.)

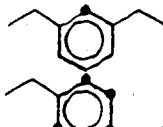
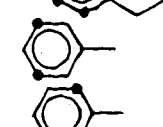
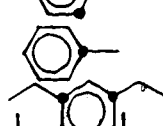
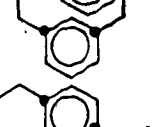
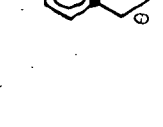
Range for Bands	Chemical shift (ppm)				Carbon Type	Band
	Observed	Literature	Integral	Ref.		
9	126.91	125.9	1.082	e		9
9	127.24	128.5	2.351	e		9
9	127.69	128.4	8.206	a		9
9	128.48	129.2	6.380	a		9
10	137.11	137.4	3.018	a		10
10	140.77	144.1	0.951	e		10
10	140.94	144.1	0.380	e		10
10	143.56	144.1	2.068	e		10

Table V.4 Carbon-13 Peak and Band Assignment for PA1

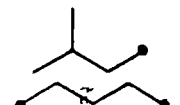
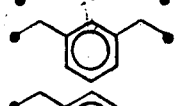
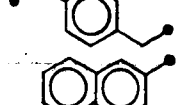
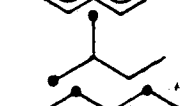
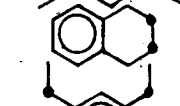
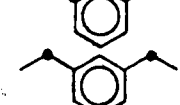
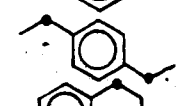
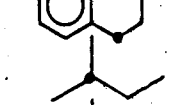
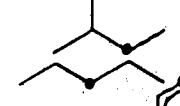
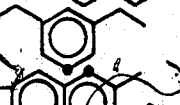
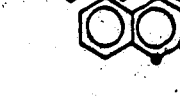
Range for Bands	Chemical shift (ppm) Observed	Chemical shift (ppm) Literature	Integral	Ref.	Carbon Type	Band
1	11.14	11.3	3.919	a		1
	13.63	13.7	14.745	a		1
2	14.89	15.8	1.002	e		2
	15.26	15.8	8.819	e		2
3	21.20	21.3	3.067	a		3
4	21.77	21.8	7.684	a		1
	22.04	22.2	16.021	a		6
	22.91	24.1	8.083	b		4
	25.09	29.2	0.980	e		6
6	28.11	29.2	2.653	e		6
	28.54	29.2	6.268	e		6
	29.02	30.3	7.356	b		6
	29.37	29.7	5.151	a		7
	31.24	31.6	4.000	a		6
7	33.83	34.7	7.021	a		6
	122.28	122.0	0.933	a		9
	124.53	124.8	2.678	a		9
	124.74	125.9	5.273	e		9
	125.04	126.0	8.724	b		9
9	125.43	125.7	3.120	a		9
	125.54	125.9	2.328	e		9
	126.13	126.7	2.928	a		9
	126.33	126.5	0.450	a		9
	126.49	126.9	4.185	a		9

Table V.4 (Cont.)

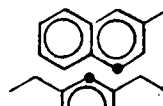
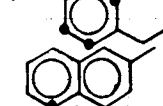
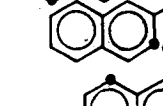
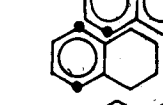
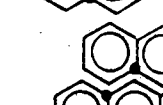
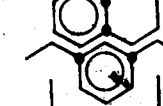
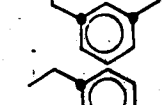
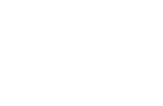
Range for Bands	Chemical shift (ppm) Observed	Chemical shift (ppm) Literature	Integral	Ref.	Carbon Type	Band
9	126.86	127.2	3.303	a		9
	127.07	125.9	2.441	e		9
	127.22	127.4	2.238	a		9
	127.36	128.5	9.250	e		9
	127.62	127.5	3.806	a		9
	127.90	127.9	4.778	a		9
	128.17	128.5	2.195	a		9
10	128.72	129.6	8.127	b		9
	130.00	131.0	1.047	a		10
	131.43	131.6	2.353	a		10
	131.73	133.0	1.349	a		10
	133.38	133.5	2.546	a		10
	134.83	135.2	2.445	a		10
	136.54	137.2	7.248	b		10
11	140.95	141.1	2.105	e		10
	141.12	144.1	1.626	e		10
12	143.74	144.1	5.208	e		10

Table V.5 Carbon-13 Peak and Band Assignment for TS2

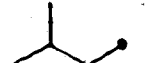
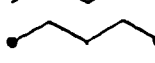
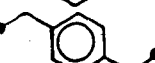
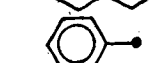
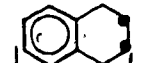
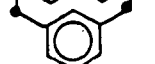
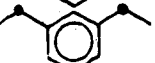
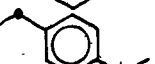
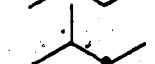
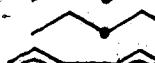
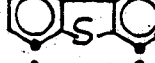
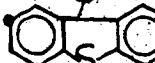
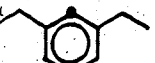
Range for Bands	Chemical shift (ppm)	Observed	Literature	Integral	Ref.	Carbon Type	Band
	11.14	11.3		2.269	a		1
1	13.43	13.7		3.888	a		1
	14.70	15.8		0.673	e		2
2	15.07	15.8		5.398	e		2
	20.76	20.4		4.836	a		3
3	21.57	21.8		6.316	a		1
	21.81	22.2		4.659	a		6
	22.70	24.1		5.346	b		4
	24.88	29.2		0.610	e		6
	27.90	29.2		1.827	e		6
6	28.33	29.2		3.738	e		6
	28.80	30.3		5.482	b		6
	29.14	29.7		3.358	a		7
	31.01	31.6		3.088	a		6
7	33.60	34.7		1.959	a		6
	120.99	122.6		0.842	f		9
	122.18	123.8		0.923	f		9
	123.71	124.3		0.991	f		9
	124.52	125.9		4.022	e		9
	124.74	125.6		4.319	a		9
9	124.83	126.0		5.648	b		9
	125.36	125.9		0.742	e		9
	126.08	124.4		1.432	f		9
	126.84	125.9		1.784	e		9

Table V.5 (Cont.)

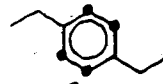
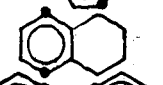
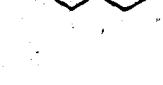
Range for Bands	Chemical shift (ppm) Observed	Literature	Integral	Ref.	Carbon Type	Band
9	127.17	128.5	3.945	e		9
	127.62	128.4	13.076	a		9
	128.41	129.2	9.748	a		9
10	128.48	129.6	6.357	b		9
	134.96	139.8	1.009	f		10
10	136.29	137.2	5.354	b		10
	137.05	137.4	4.691	a		10
11	138.90	139.9	1.090	f		11
	140.70	144.1	1.655	e		10
10	140.87	144.1	0.684	e		10
	143.49	144.1	3.513	e		10

Table V.6 References for ^{13}C Peak Assignments

- a) Levy et al. (1980); page 30 and page 111 for toluene, page 52 for isopentane, page 78 for pentane, page 116 for methylnaphthalene and phenanthrene.
- b) Ejcharh and Kozerski (1981) page 181 for methylcyclohexane, page 201 for téralin.
- c) Abraham and Loftus (1978) page 30 for cis-methylcyclohexane.
- d) Abraham and Loftus (1978) page 182 for trans-decalin.
- e) Diethylbenzene is a mixture of para and meta compounds, assignment of chemical shifts to carbons in para, meta, and other conformers were made based on the chemical shifts for ethylbenzene, Ejcharh and Kozerski (1981) page 201.
- f) Chemical shifts for benzothiophene (Levy et al., 1980, page 124) were used to assign peaks for dibenzothiophene.

Table V.7 Analytical Data and FGA Results for S1

1. H-NMR (% of total hydrogen)

Band	Actual	Observed	% Error
1	31.06	34.15	+9.95
2	68.94	65.85	-4.48

2. C13-NMR (% of total carbon)

Band	Actual	Observed(B.A.)	% Error	Observed(P.A.)	% Error
1	16.09	11.21	-30.33	16.29	+1.24
4	5.46	5.08	-6.96	7.06	+29.30
5	49.29	45.44	-7.81	47.29	-4.06
6	15.83	20.07	+26.78	19.14	+20.91
7	13.33	18.20	+36.53	10.22	-23.33

3. FGA Results

Concentrations in moles of functional group/100 g of sample
 Structure Actual Predicted % Error Predicted % Error

		(B.A.)		(P.A.)	
	1.122	1.429	+27.36	1.385	+23.44
	0.944	0.751	-20.44	0.643	-31.88
	1.141	1.330	+16.56	1.222	+7.10
	0.387	0.350	-9.56	0.458	+18.34
	3.493	3.227	-7.61	3.380	-3.24

Table V.8 Analytical Data and FGA Results for S2

1. H-NMR (% of total hydrogen)

Band	Actual	Observed	% Error
1	27.35	26.69	-2.41
2	72.65	73.31	+0.91

2. C13-NMR (% of total carbon)

Band	Actual	Observed(B.A.)	% Error	Observed(P.A.)	% Error
1	12.93	9.03	-30.16	13.55	+4.80
4	5.70	4.52	-20.70	7.68	+34.74
5	54.76	45.87	-16.23	51.40	-6.13
6	12.33	19.68	+59.61	16.48	+33.66
7	14.28	20.90	+46.36	10.89	-23.74

3. FGA Results

Concentrations in moles of functional group/100 g of sample
 Structure Actual Predicted % Error Predicted % Error

		(B.A.)		(P.A.)	
<chem>O=C(O)C</chem>	0.877	1.655	+88.71	1.343	+53.13
<chem>O=C</chem>	1.015	0.636	-37.34	0.640	-36.95
<chem>OCC</chem>	0.919	1.005	+9.36	1.010	+9.90
<chem>OCH3</chem>	0.405	0.296	-26.91	0.287	-29.13
<chem>OCH2O</chem>	3.891	3.515	-9.67	3.823	-1.75

Table V.9 Analytical Data and FGA Results for MA1

1. H-NMR (% of total hydrogen)

Band	Actual	Observed	% Error
1	22.43	23.94	+6.73
2	54.25	50.96	-6.06
3	9.87	11.20	+13.47
5	13.45	13.90	+3.34

2. C13-NMR (% of total carbon)

Band	Actual	Observed(B.A.)	% Error	Observed(P.A.)	% Error
1	10.62	6.83	-35.69	11.98	+12.81
2	3.91	3.41	-12.79	3.41	-12.79
3	3.12	3.72	+19.23	3.72	+19.23
4	2.42	5.15	+112.81	3.20	+32.23
5	27.97	25.12	-10.19	22.18	-20.70
6	13.19	14.43	+9.40	15.45	+17.13
7	8.29	8.81	+6.27	7.53	-9.17
9	23.44	26.15	+11.56	26.15	+11.56
10	7.04	6.38	-9.37	6.38	-9.37

3. FGA Results

Concentrations in moles of functional group/100 g of sample

Structure	Actual	Predicted (B.A.)	% Error (B.A.)	Predicted (P.A.)	% Error (P.A.)
<chem>c1ccccc1</chem>	0.369	0.378	+2.44	0.383	+3.79
<chem>CC</chem>	0.284	0.109	-61.61	0.200	-29.58
<chem>CH3</chem>	0.227	0.400	+76.21	0.339	+49.34
<chem>CH3C</chem>	0.284	0.310	+9.15	0.287	+1.05
<chem>CC(=O)C</chem>	0.674	0.942	+39.76	0.973	+44.36
<chem>CH(=O)C</chem>	0.602	0.396	-34.22	0.491	-18.44
<chem>CH3C(=O)C</chem>	0.771	0.597	-22.57	0.837	+8.56
<chem>CH3C(=O)C(=O)C</chem>	0.175	0.413	+136.00	0.173	-1.14
<chem>CC(=O)C(=O)C</chem>	2.032	1.828	-10.04	1.662	-18.21

Table V.10 Analytical Data and FGA Results for MA2

1. H-NMR (% of total hydrogen)

Band	Actual	Observed	% Error
1	14.81	15.37	+3.78
2	42.14	40.04	-4.98
3	18.24	18.97	+4.00
5	24.81	25.62	+3.26

2. C13-NMR (% of total carbon)

Band	Actual	Observed(B.A.)	% Error	Observed(P.A.)	% Error
1	6.27	4.19	-33.17	5.68	-9.41
2	6.43	5.43	-15.55	6.11	-4.98
3	5.04	5.20	+3.17	5.20	+3.17
4	1.31	2.17	+65.65	1.85	+41.22
5	15.06	18.48	+22.71	12.70	-15.67
6	11.76	7.51	-36.14	12.64	+7.48
7	4.60	4.83	+5.00	3.63	-21.09
9	38.06	41.07	+7.91	41.07	+7.91
10	11.47	11.12	-3.05	11.12	-3.05

3. FGA Results

Concentrations in moles of functional group/100 g of sample

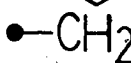
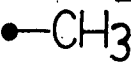
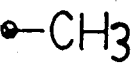
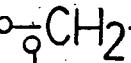
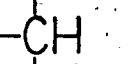
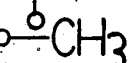
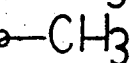
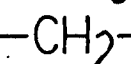
Structure	Actual	Predicted (B.A.)	% Error	Predicted (P.A.)	% Error
	0.609	0.622	+2.13	0.623	+2.30
	0.474	0.353	-25.53	0.411	-13.29
	0.372	0.481	+29.30	0.442	+18.82
	0.474	0.451	-4.85	0.483	+1.90
	0.392	0.216	-44.90	0.549	+40.05
	0.340	0.184	-45.88	0.194	-42.94
	0.462	0.388	-16.02	0.444	-3.90
	0.096	0.192	+100.00	0.136	+41.67
	1.111	1.378	+24.03	0.964	-13.23

Table V.11. Analytical Data and FGA Results for PA1

1. H-NMR (% of total hydrogen)

Band	Actual	Observed	% Error
1	31.04	29.84	-3.86
2	35.63	38.57	+8.25
3	14.01	13.40	-4.35
5	19.00	17.87	-5.95
6	0.32	0.32	0.00

2. C13-NMR (% of total carbon)

Band	Actual	Observed(B.A.)	% Error	Observed(P.A.)	% Error
1	16.62	10.38	-34.84	13.91	-16.30
2	5.21	4.65	-10.75	5.19	-0.38
3	1.49	1.62	+8.72	1.62	+8.72
4	3.81	4.06	+6.56	4.26	+11.81
6	24.68	26.69	+8.14	23.37	-5.31
7	2.65	3.71	+40.00	2.72	+2.64
9	31.03	35.25	+13.60	35.25	+13.60
10	14.51	13.68	-5.72	13.68	-5.72

3. FGA Results

Concentrations in moles of functional group/100 g of sample

Structure	Actual	Predicted (B.A.)	% Error	Predicted (P.A.)	% Error
	0.331	0.297	-10.27	0.267	-10.23
	0.109	0.114	+4.59	0.137	+24.77
	0.019	0.019	0.00	0.019	0.00
	1.149	1.331	+15.84	1.226	+6.70
	0.383	0.355	-8.53	0.389	+1.57
	0.140	0.148	+5.71	0.160	+14.29
	0.383	0.325	-15.14	0.280	-26.89
	1.219	1.172	-3.85	1.172	-3.85
	0.194	0.286	+47.42	0.288	+48.45
	0.109	0.112	+2.75	0.127	+16.51

Table V.12 Analytical Data and FGA Results for TS1

1. H-NMR (% of total hydrogen)

Band	Actual	Observed	% Error
1	25.19	22.22	-11.79
2	31.21	33.33	+6.79
3	18.92	19.56	+3.38
5	24.68	24.89	+0.85

2. C13-NMR (% of total carbon)

Band	Actual	Observed(B.A.)	% Error	Observed(P.A.)	% Error
1	12.86	7.36	-42.77	11.37	-11.58
2	5.08	4.41	-13.19	5.00	-1.57
3	3.34	3.56	+6.59	3.56	+6.59
4	4.40	4.61	+4.77	4.98	+13.18
6	20.14	22.00	+9.23	17.03	-15.44
7	2.47	2.31	-6.47	2.30	-6.88
9	37.82	41.38	+9.41	41.38	+9.41
10	13.36	13.87	+3.82	13.87	+3.82
11	0.53	0.49	-7.55	0.49	-7.55

3. FGA Results

Concentrations in moles of functional group/100 g of sample

Structure	Actual	Predicted	% Error	Predicted	% Error
(B.A.)				(P.A.)	

	0.593	0.594	+0.17	0.597	+0.67
	0.020	0.020	0.00	0.020	0.00
	0.161	0.159	-1.24	0.199	+23.60
	0.372	0.265	-28.76	0.224	-39.78
	0.245	0.344	+40.41	0.318	+29.80
	0.372	0.353	-5.11	0.422	+13.40
	0.781	0.949	+21.51	0.756	-3.20
	0.181	0.152	-16.02	0.171	-5.52
	0.943	0.832	-11.77	0.832	-11.77

Table V:13 Analytical Data and FGA Results for TS2

1. H-NMR (% of total hydrogen)

Band	Actual	Observed	% Error
1	22.58	20.67	-8.46
2	29.81	28.62	-3.99
3	20.21	21.38	+5.79
5	27.40	29.33	+7.04

2. C13-NMR (% of total carbon)

Band	Actual	Observed(B.A.)	% Error	Observed(P.A.)	% Error
1	11.12	5.77	-48.11	10.26	-7.73
2	5.47	4.29	-21.57	4.83	-11.70
3	3.62	3.85	+6.35	3.85	+6.35
4	4.02	5.02	+24.87	4.25	+5.22
6	17.74	22.36	+26.04	17.00	-4.17
7	2.30	1.56	-32.17	2.67	+16.09
9	40.47	42.83	+5.83	42.83	+5.83
10	13.96	13.45	-3.65	13.45	-3.65
11	0.85	0.87	+2.35	0.87	+2.35

3. FGA Results

Concentrations in moles of functional group/100 g of sample
 Structure Actual Predicted % Error Predicted % Error

	(B.A.)	(P.A.)
	0.614	0.654 +6.51
	0.031	0.031 0.00
	0.147	0.121 -17.69
	0.401	0.323 -19.45
	0.265	0.395 +49.05
	0.401	0.433 +7.98
	0.633	0.627 -0.95
	0.169	0.069 -59.17
	0.816	0.747 -8.45

Table V.14 Analytical Data and FGA Results for TS3

1. H-NMR (% of total hydrogen)

Band	Actual	Observed	% Error
1	22.74	21.95	-3.47
2	29.34	27.18	-7.36
3	19.94	21.60	+8.32
5	27.98	29.27	+4.61

2. C13-NMR (% of total carbon)

Band	Actual	Observed(B.A.)	% Error	Observed(P.A.)	% Error
1	11.04	6.32	-42.75	10.08	-8.69
2	4.79	3.84	-19.83	4.32	-9.81
3	3.40	3.50	+2.94	3.50	+2.94
4	4.63	4.24	-8.42	5.01	+8.21
6	17.80	22.74	+27.75	17.53	-1.51
7	2.33	1.92	-17.60	2.12	-9.01
9	40.74	42.72	+4.86	42.72	+4.86
10	14.04	13.52	-3.70	13.52	-3.70
11	1.23	1.20	-2.44	1.20	-2.44

3. FGA Results

Concentrations in moles of functional group/100 g of sample

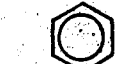
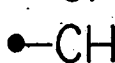
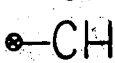
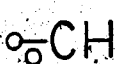
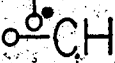
Structure	Actual (B.A.)	Predicted (B.A.)	% Error (B.A.)	Predicted (P.A.)	% Error (P.A.)
	0.593	0.619	+4.38	0.620	+4.55
	0.045	0.045	0.00	0.045	0.00
	0.169	0.132	-21.89	0.169	-2.37
	0.350	0.303	-13.42	0.228	-34.86
	0.249	0.388	+55.82	0.394	+58.23
	0.350	0.311	-11.14	0.343	-2.00
	0.613	0.681	+11.09	0.545	-11.09
	0.171	0.071	-58.48	0.117	-31.58
	0.807	0.779	-3.47	0.779	-3.47

Table V.15 % Error in H-NMR Band Intensities
 $\% \text{ Error} = (\text{observed} - \text{actual}) / (\text{actual}) \times 100$

Sample	1	2	3	4	5	6	Band #
S1	+9.95	-4.48					
S2	-2.41	+0.91					
MA1	+6.73	-6.06	+13.47	+3.34			
MA2	+3.78	-4.98	+4.00	+3.26			
PA1	-3.86	+8.25	-4.35	-5.95	0.00		
TS1	-11.79	+6.79	+3.38	+0.85			
TS2	-8.46	-3.99	+5.79	+7.04			
TS3	-3.47	-7.36	+8.32	+4.61			
Average Absolute Error	6.31	5.35	6.55	4.17			

Table V.16 % Error in C13-NMR Band Intensities
 % Error = $(\text{observed}-\text{actual})/(\text{actual}) \times 100$
 Average = Average Absolute Error

1-B.A. Method

Sample	1	2	3	4	5	6	7	8	9	10	11
S1	-30.33			-6.96	-7.81	+26.78	+36.35				
S2	-30.16			-20.70	-16.23	+59.61	+46.36				
MA1	-35.69	-12.78	+19.23	+112.81	-10.19	+9.40	+6.27	+11.56	-9.37		
MA2	-33.17	-15.55	+3.17	+68.65	+22.71	-36.14	+5.00	+7.91	-3.05		
PA1	-38.84	-10.75	+8.42	+6.56		+8.14	+40.00	+13.60	-5.72		
TS1	-42.77	-13.19	+6.59	+4.77		+9.23	-6.47	+9.41	+3.82	-7.55	
TS2	-48.11	-21.57	+6.35	+24.87		+26.04	-32.17	+5.83	-3.65	+2.35	
TS3	-42.75	-19.83	+2.94	-8.42		+27.75	-17.60	+4.86	-3.70	-2.44	
Average	37.23	15.61	7.83	31.34	14.23	25.39	23.78	8.86	4.88	4.11	

2-P.A. Method

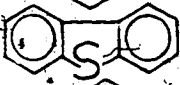
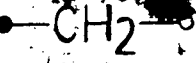
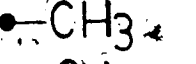
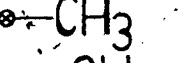
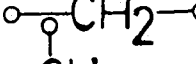
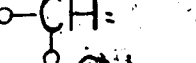
Sample	1	2	3	4	5	6	7	8	9	10	11
S1	+1.24			+29.30	-4.06	+20.91	-23.33				
S2	+4.80			+34.74	-6.13	+33.63	-23.74				
MA1	+12.81	-12.79	+19.23	+32.23	-20.70	+17.13	-9.17	+11.56	-9.37		
MA2	-9.41	-4.98	+3.17	+41.22	-15.67	+7.48	-21.09	+7.91	-3.05		
PA1	-16.30	-0.38	+8.72	+11.81		+5.31	+2.64	+13.60	-5.72		
TS1	-11.58	-1.57	+6.59	+13.18		-15.44	-6.38	+9.44	+3.82	-7.55	
TS2	-7.73	-11.70	+6.35	+5.72		-4.17	+16.09	+5.83	-3.65	+2.35	
TS3	-8.69	-9.81	+2.94	+8.21		-1.51	-9.01	+4.86	-3.70	-2.44	
Average	9.07	6.87	7.83	22.05	11.64	13.20	14.00	8.86	4.88	4.11	

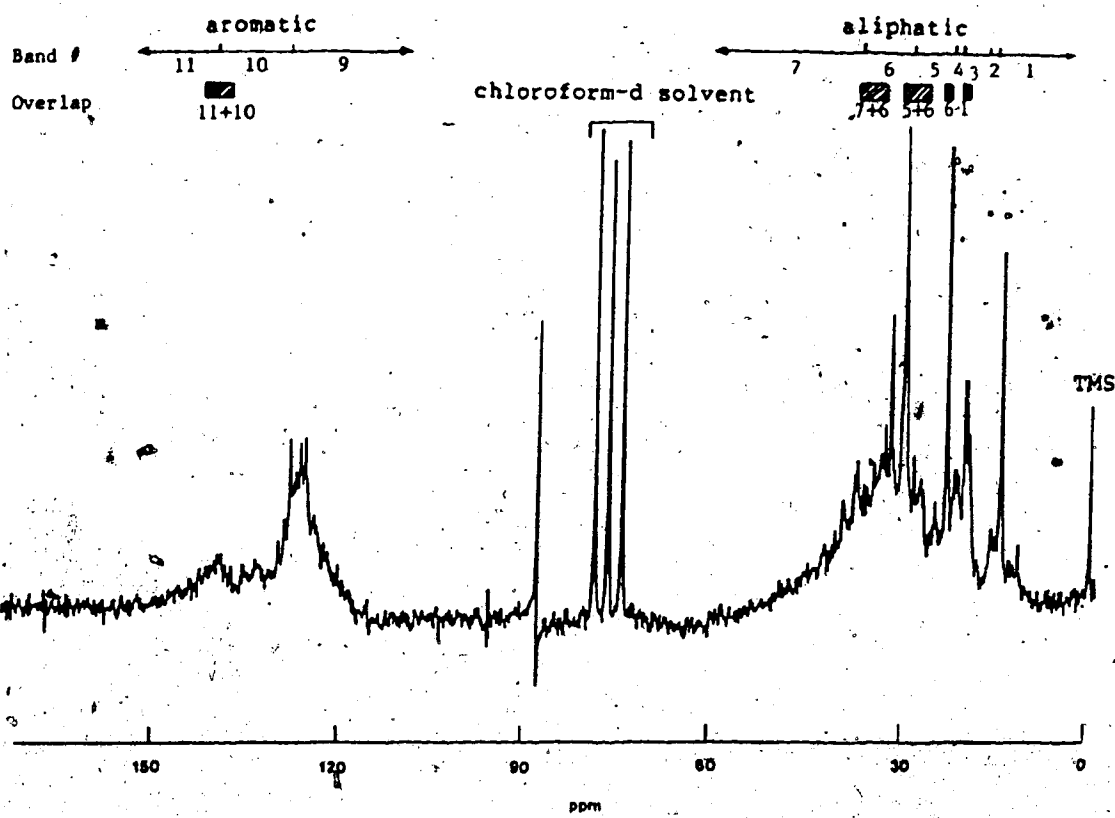
Table V.17 % Error in Predicted Group Concentrations
 $\% \text{Error} = ((\text{predicted}-\text{actual})/\text{actual}) \times 100$
 Average = Average Absolute Error

	$\bullet-\text{CH}_2-\text{O}$		$\bullet-\text{CH}_3$		Alkyl Substituents	
Sample	B.A.	P.A.	B.A.	P.A.	B.A.	P.A.
MA1	-61.61	-29.58	+76.21	+49.34	-0.39	+5.48
MA2	-25.53	-13.29	+29.30	+18.82	-1.41	+0.82
PA1	-15.14	-26.89	+2.75	+16.51	-11.18	-17.28
TS1	-28.76	-39.78	+40.41	+29.80	-1.30	-12.15
TS2	-19.45	-42.39	+49.05	+65.66	+7.80	+0.60
TS3	-13.42	-3.86	+55.82	+58.23	+15.36	+3.84
Average	27.32	31.13	42.25	39.72	6.24	6.69
					Mono + Diaromatics	
Sample	B.A.	P.A.	B.A.	P.A.	B.A.	P.A.
MA1	+2.44	+3.79	+4.59	+24.77	+2.44	+3.79
MA2	+2.13	+2.30			+2.13	+2.30
PA1	-10.27	-19.33			-5.01	-3.71
TS1	+0.17	+0.67			+0.17	+0.67
TS2	+6.51	+3.75			+6.51	+3.75
TS3	+4.38	+4.55			+4.38	+4.55
Average	4.32	5.73	4.59	24.77	3.44	3.13
	$\bullet-\text{CH}$		$\bullet-\text{CH}_2-\text{O}$		$\bullet-\text{CH}_3$	
Sample	B.A.	P.A.	B.A.	P.A.	B.A.	P.A.
S1	-20.44	-31.88	+27.36	+23.44	+16.56	+23.44
S2	-37.34	-36.95	+88.71	+53.13	+9.36	+9.90
MA1	-34.22	-18.44	+39.76	+44.36	-22.57	+8.56
MA2	-45.88	-42.94	-44.90	+40.05	-16.02	-3.90
PA1	+47.42	+48.45	+15.84	+6.70	-3.85	-3.85
TS1	-16.02	-5.52	+21.51	-3.20	-11.77	-11.77
TS2	-59.17	-18.93	-0.95	-9.00	-8.45	-8.45
TS3	-58.48	-31.58	+11.09	-11.09	-3.47	-3.47
Average	39.87	-29.34	31.27	23.87	11.51	7.12
	$\bullet-\text{CH}_3$		$\bullet-\text{CH}_2-\text{O}$		$\bullet-\text{CH}_3$	
Sample	B.A.	P.A.	B.A.	P.A.	B.A.	P.A.
S1	-9.56	+18.34	-7.61	-3.24		
S2	-26.91	-29.13	-9.67	-1.75		
MA1	+136.00	-1.14	-10.04	-18.21	+9.15	+1.05
MA2	+100.00	+41.67	+24.03	-13.23	-4.85	+1.90
PA1					-12.53	+1.57
TS1					-5.11	+13.44
TS2					+7.98	+5.73
TS3					+11.14	-2.00
Average	68.12	22.57	12.85	9.11	8.46	4.28
						
Sample	B.A.	P.A.				
PA1	+5.71	+14.29				
TS1	-1.24	+23.60				
TS2	-17.69	-8.84				
TS3	-21.89	-2.37				
Average	11.63	12.28				

Table V.18 Effect of Weighting Factors on TS2 Profiles

Concentrations in moles of functional group/100 g of sample

Structure	Actual	Predicted	% Error Without WF	Predicted % Error With WF
	0.614	0.646	+5.21	0.637 +3.75
	0.031	0.031	0.00	0.031 0.00
	0.147	0.131	-10.88	0.134 -8.84
	0.401	0.257	-31.42	0.231 -42.39
	0.265	0.425	+60.38	0.439 +65.66
	0.401	0.383	-3.24	0.424 +5.73
	0.633	0.677	+6.96	0.576 -9.00
	0.169	0.069	-59.17	0.137 -18.93
	0.816	0.747	-8.45	0.747 -8.45
Alkyl Substituents	0.666	0.682	+2.40	0.670 +0.60



■ Range for possible overlap

Figure V.1 Extent of overlap in ^{13}C bands of LVGO Aromatics

6. Application of FGA to Syncrude Coker Gas Oil (SCGO)

6.1 Analytical Data For SCGO

Functional Group Analysis was applied to obtain the structural profiles of various fractions of SCGO. Table VI.1 lists the results of conventional analysis of this oil. As a first step in the structural characterization, 10 grams of sample were subjected to the class separation scheme and about 97 % of the original sample was recovered in various fractions, as shown in Table VI.2. The three resin fractions made up about 50 % of the oil. All the fractions obtained from the class separation procedure, except for the asphaltenes which were recovered in very small amounts, were further analyzed by elemental analysis, $^1\text{H-NMR}$, and $^{13}\text{C-NMR}$. The elemental analyses for each fraction are presented in Table VI.3. As was expected from the class separation scheme, the heteroatom content increased from saturates to Polar III. The Polar III fraction was distinguished by its nitrogen and oxygen content which was distinctly higher than other fractions.

The relative amounts of hydrogen and carbon in various bands, as obtained from $^1\text{H-NMR}$ and $^{13}\text{C-NMR}$ spectra, are presented in Table VI.4 and Table VI.5, respectively. Peak areas for bands in $^1\text{H-NMR}$ spectra were obtained from the integration curve, and planimetry was used to obtain areas for small peaks such as olefins. For $^{13}\text{C-NMR}$ spectra, peak areas were obtained by planimetry since the behavior of the integration curve was poor. In order to minimize the error

in band intensities from ^{13}C -NMR spectra, the relative amount of carbon in band 9 (aromatic carbon bonded to hydrogen) was obtained directly from the amount of aromatic hydrogen as measured from ^1H -NMR spectra. The intensities of other bands were adjusted to account for this correction which minimized the possible errors in the ^{13}C -NMR peak areas due to relaxation effects.

6.2 Structural Characterization of SCGO by FGA

The structural profiles of SCGO fractions were obtained using the methodology outlined in Chapter 4. These profiles are presented in Table VI.6.

6.2.1 Saturates

The saturates fraction is made up of linear and cyclic aliphatic structures. As mentioned in Chapter 4, one is unable to distinguish between naphthenic methyne and methyne groups involved in linear structures. Hence one cannot determine the distribution of carbon in linear and saturated cyclic structures. The concentration of naphthenic methyl and methylene indicate that at least 30 % of carbon is involved in cyclic structures such as cyclohexanes, decalin, and perhydrophenanthrenes. This approximation is made assuming that at least one naphthenic methyne is present for every naphthenic methyl, for example in methylcyclohexane. The methyne group concentration includes the total concentration of methyne in structures such as alkylcyclohexanes, bridgehead methyne as in decalin, as well as methyne in linear structures. The high concentration of

methyne indicates a high degree of branching.

The heteroatom content of the saturates fraction is quite low. The small amounts of oxygen, sulphur, and nitrogen compounds contained in the saturates fraction are considered to be aliphatic ethers and thioethers, and non-basic nitrogen compounds respectively. These structures are among other equally valid groups such as alcohols and mercaptans to account for the presence of heteroatoms. However, the choice of groups for heteroatoms is limited due to insufficient analytical data. Since SCGO is a reacted oil, alcohols and mercaptans are less likely oxygen and sulphur groups, respectively, and are not included in the analysis. The choice of amine to represent nitrogen is unsatisfactory due to polarity, but no other nitrogen groups are known to be more likely. The presence of very small amounts of nitrogen in the saturates fraction can also be explained by possible error in the nitrogen analysis.

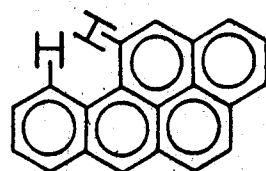
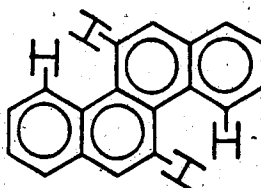
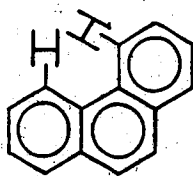
6.2.2 Aromatics

Aliphatic structures are dominant in the aromatics fraction of SCGO. Aliphatic carbon contributes to linear alkyl chains as well as saturated cyclic structures. The aromatic structures are mainly monoaromatics in the form of alkyl substituted benzene and benzothiophene. The relative concentration of substituents on aromatic rings to the total concentration of aromatic sites in groups such as benzene and heteroaromatics, provides an estimate of the degree of substitution on aromatic rings. For the aromatics fraction,

the degree of substitution is about 50 %. The relative concentration of alpha-methyl, to the total concentration of alpha-methyl and alpha-methylene, indicates that about 35 % of alkyl substituents on aromatic rings are methyl groups. Ethyl substituents on aromatic rings as obtained from beta-methyl concentration, contribute to 15 % of alkyl substitution. The remaining 50 % are long, branched chains, however; it is difficult to give an estimate of average chain length or the length between branches based on the structural profiles.

6.2.3 Polar I

In the Polar I fraction, aromatic structures dominate the profile and aliphatic structures mainly contribute to alkyl chains. The distinction between aliphatic carbon in linear structures and saturated rings is difficult due to the lack of analytical information about cyclic structures. FGA was unable to establish the concentration of naphthenic methylene but the presence of saturated rings could not be ruled out. The aromatic structures contain condensed ring systems such as naphthalene and phenanthrene as well as hydroaromatic rings. Phenanthrene was chosen as a representative structure for polycyclic aromatics. The aromatic hydrogen signal detected in band 6 of $^1\text{H-NMR}$ may belong to a number of polycyclic aromatic structures such as:



The choice of multi-ring structures is limited due to insufficient analytical data.

The degree of substitution on aromatic rings is about 40 % for the Polar I fraction and close to 40 % of alkyl substituents are methyl groups. It is difficult to estimate ethyl substitution on aromatic rings due to branching at the alpha position relative to the rings. The high concentration of methyne suggests that the remaining alkyl chains are highly branched and that cyclization may also be significant.

In the Polar I fraction, sulphur is involved in aromatic structures in the form of dibenzothiophene as well as aliphatic structures in the form of thioether. Aliphatic thioether can be involved in linear structures as well as cyclic sulfides identified by Payzant et al. (1983) in Athabasca bitumen. The ability of FGA to establish the concentration of various sulphur structures is particularly helpful since each structure may behave differently under reaction conditions. A small amount of olefins is also present in this fraction.

6.2.4 Polar II

In the Polar II fraction, the aromatic structures appear in condensed ring systems as marked by an increase in the concentration of phenanthrene, dibenzofuran and carbazole.

Dibenzofuran is the most likely oxygen group in Polar II as well as aromatics and Polar I fractions since no phenol or carbonyl bands were detected in the IR spectra of the above

fractions.

The degree of substitution on the aromatic rings in the Polar II fraction is about 40 %, which is similar to that of Polar I, with alpha methyl contributing to about 40 % of alkyl substituents on aromatic rings. The increase in the concentration of methyne groups suggests that the degree of branching is higher in the Polar II fraction compared with Polar I.

6.2.5 Polar III

The Polar III fraction is the only fraction which contains a substantial amount of nitrogen and oxygen. The IR spectrum of this fraction pointed to the presence of phenols and carbonyls. The ratio of phenols to carbonyls was obtained from the IR spectrum (as discussed in Chapter 4). This ratio was found to be 0.3 and was introduced in the computation scheme as an additional constraint. Aromatic structures present in the Polar III fraction are mainly aromatic ketones, phenols, aniline, and carbazole. Polyaromatics as well as hydroaromatic structures are also present in this fraction. The degree of substitution on aromatic ring is about 50 % which is higher than other polar fractions due to the presence of functionalized aromatic structures such as phenols and aniline. Sulphur is represented by aliphatic thioether structures while aniline and carbazole represent the nitrogen groups. Other heteroatom groups which may be present in this fraction cannot be accounted for due to the limited data.

Comparison of the structural profiles of various fractions revealed some trends in the structural features. The aliphatic groups in the saturates and aromatics fractions contribute to both saturated cyclic structures and linear chains while in the resin fractions aliphatic groups contribute mainly to alkyl chains. One measure of aromatic ring condensation is the ratio of the concentration of aromatic carbon bound to other aromatic carbon, to the total concentration of aromatic carbon. The degree of aromatic ring condensation increases from aromatics to Polar I, to Polar II, namely, 19, 27, and 30 %, respectively. For the Polar III fraction, however, aromatic ring condensation is about 19 % since functionalized benzene structures are the major aromatic structures. Benzothiophene is the most probable sulphur group present in the aromatics fraction while dibenzothiophene and aliphatic thioether are present in the polar fractions. The concentration of aliphatic thioether increases from Polar I to Polar III while that of dibenzothiophene decreases. A high degree of branching is observed for all resin fractions and an increase in the concentration of aliphatic thioether may suggest an increase in the average chain length from Polar I to Polar III.

The structural profiles of the individual fractions are combined in proportion to the separation yields to obtain the structural profile of the whole oil (Table VI.7). The profile excludes asphaltenes and the material not recovered in the separation procedure. From the concentration of

various functional groups, typical structural features such as aromaticity, degree of aromatic ring condensation, degree of substitution on aromatic rings, etc., can be obtained for the oil. The profiles also provide an estimate of the distribution of S, O, and N in various heteroatom functional groups.

FGA was used for structural characterization of SCGO without applying the class separation procedure. The analytical data for SCGO are summarized in Table VI.8 and the structural profile is presented in Table VI.7. Comparison of the two profiles in Table VI.7 pointed out that while the concentration of aliphatic groups remained relatively unchanged, the concentration of aromatic structures and the distribution of heteroatoms in various groups were strongly affected. The use of IR data for phenols and carbonyls was also excluded in the whole oil analysis, hence FGA was unable to establish any estimate of the concentration of the above groups. Class separation of gas oils is thus an important first step in the characterization procedure which allows the selection of different heteroatom groups representing the most likely structures for each fraction.

To obtain accurate structural profiles, one should have a reasonable knowledge of the major structures present in the sample so the selected set of functional groups represent the sample adequately. Based on the application of FGA to the mixtures of known concentration, the structural

profiles of the various fractions can be judged as fairly accurate; however, it is difficult to place an estimate of error on individual concentrations. Analytical data from ^{13}C -NMR spectra represent the largest source of error in the analysis. In Table VI.9, the relative amount of carbon in each band of ^{13}C -NMR spectra as obtained from FGA are compared with experimental values for the aromatics fraction. Most of the disagreement is in band 10 which includes signals from non-protonated aromatic carbon. This disagreement could be explained by the possible overlap of bands 10 and 11. As mentioned in chapter 5, signals for band 10 carbons could appear up to 148 ppm. The underestimation of band 10 and overestimation of band 11 were corrected by FGA as the predicted concentrations of carbon in the above bands were higher and lower than the experimental values respectively. Another explanation for this disagreement is that carbons in band 10 would be most subject to relaxation effects, indicating that the method of ^{13}C -NMR analysis should be improved.

6.3 Effect of ^{13}C -NMR Data on the Structural Profiles

The effect of ^{13}C -NMR data on the structural profiles of the various fractions of SCGO was investigated since analytical information from ^{13}C -NMR spectra provide the largest source of error in FGA. The relative amounts of carbon in each band were obtained from the spectrum integration curve. These are presented in Table VI.10 for various fractions. For most fractions, the behavior of the

integration curve was very poor. An example is presented in Figure VI.1 where the curve increases over a section of the baseline where no signals appear. The poor behavior is possibly due to the bowl shape base line of the spectrum which is typical of FT-¹³C-NMR.

Comparison of the analytical data as obtained by planimetry, Table VI.5, with those obtained from the integration curve, Table VI.10, indicates that the differences are within the expected error for ¹³C-NMR data. In the case of the Polar III fraction, the integration curve was very poor and it was difficult to obtain reliable data.

The structural profiles of each fraction were obtained using the data presented in Table VI.10. These profiles are presented in Table VI.11. Comparison of these profiles with those presented in Table VI.6, indicates that the concentrations of various groups in the saturates and aromatics fractions are least affected by the error in ¹³C-NMR data while the profiles of the polar fractions are more sensitive to the ¹³C-NMR data. The term "sensitive" is used for groups whose concentrations are forced to zero by small changes in ¹³C-NMR data. In the case of Polar I for example, the concentration of benzene and alpha methyne are forced to zero due to the differences between ¹³C-NMR data as obtained by planimetry and as obtained from the spectrum integration curve. Although the structural profiles of the Polar I and Polar II fractions are different from those presented in Table VI.6, the major structural features such

as aromaticity, the degree of substitution on aromatic rings, the degree of aromatic ring condensation, and the degree of branching are relatively unchanged.

Comparison of the profiles of the polar fractions indicates that the concentration of some groups such as gammâ methyl, hydroaromatic ring and polyaromatics are not affected by the error in $^{13}\text{C-NMR}$ data. The comparison also points out groups which are sensitive to $^{13}\text{C-NMR}$. The concentration of such groups should be lumped into a more general concentration which is not sensitive to error in analytical data. For example, the total methyne concentration, groups 15 and 21, is relatively unchanged while the individual concentrations of these groups are affected by the error in $^{13}\text{C-NMR}$ data. The total concentration of alkyl side chains on aromatic rings as obtained from alpha-methyl, alpha-methylene, and alpha-methyne is relatively unchanged but the individual concentrations of these groups are sensitive.

The profiles for the Polar I fraction point out that one cannot discriminate between benzene and naphthalene on the basis of NMR data. Hence the presence of structures such as alkyl benzenes may not be ruled out in the polar fractions. The split between sulphur groups is also affected by the error in the $^{13}\text{C-NMR}$ data. The analytical data presented in Table VI.10 indicate that the relative amounts of aromatic carbon bonded to heteroatoms, band 11 in $^{13}\text{C-NMR}$ spectra, are distinctly higher when the integration curve is

used, hence resulting in an increase in the concentration of dibenzothiophene. Model compounds studies presented in chapter 5 indicated that the intensity of the C-S signal for dibenzothiophene obtained from the area of the corresponding peak, was in excellent agreement with the known value. The higher content of band 11 carbon obtained from the integration curve suggests the incorrect interpretation of the spectrum integration curve. To obtain more accurate estimates of the amount of carbon in each band, the spectrum should be expanded allowing peak areas to be obtained by planimetry. Further model compound studies could provide an estimate for the accuracy of the predicted concentration of various sulphur groups from FGA.

6.4 Treatment of Resins

A problem that may be encountered in the analysis of gas oils is that some resin fractions, in particular Polar II and Polar III, are recovered in very small amounts. To obtain a reliable $^{13}\text{C-NMR}$ spectrum with adequate signal to noise ratio, at least one gram of sample should be dissolved in an equal volume of CDCl_3 . In the case of SCGO, sufficient amounts of each fraction were recovered in the class separation procedure to enable the analysis of individual fractions. However, the treatment of the resin fractions should depend on the amount of each fraction recovered. In cases where the Polar III fraction is recovered in small amounts, a heavy resin fraction containing Polar II and Polar III fractions should be

characterized by FGA. When both Polar II and Polar III are recovered in small amounts, less than one gram combined, then a total resin fraction containing all three polar fractions should be analyzed.

In Table VI.12 a comparison is made between the structural profiles of the resins of SCGO as obtained by:

1. combination of profiles of individual fractions
2. combination of Polar I and heavy resins profiles
3. structural profile from total resin analysis

The analytical data used for the combined fractions were obtained by summing information for individual fractions. This is a reasonable first approximation since in the NMR spectra, band intensities are additive and proportional to the amount of hydrogen or carbon present in the corresponding bonding environment. Results indicate that the agreement between the concentration of various functional groups for the three methods is satisfactory. In the combined fraction analysis, FGA was unable to establish estimates of the concentrations of some heteroatom groups. The differences between the structural profiles are due to the sensitivity of some groups to ^{13}C -NMR data as discussed in section 6.3. However, the major structural characteristics of the resins are relatively unchanged.

6.5 Summary

FGA was used to obtain the structural profile of SCGO. Data from ^1H -NMR, ^{13}C -NMR, IR, and elemental analysis were utilized to obtain the structural profiles of individual

fractions recovered from the class separation procedure. Structural features such as aromaticity, degree of aromatic ring condensation, degree of substitution on aromatic rings, etc., can easily be determined from the concentration of functional groups. FGA also provides an estimate of the distribution of sulphur in various groups as well as the concentration of aromatic and heteroaromatic structures. On the basis of NMR data, the distinction between mono and diaromatics is not possible.

Because of insufficient analytical data, the concentration of various polycyclic and saturated cyclic structures present in the oil cannot be determined. The choice of heteroatom functional groups is also limited. Functional groups representing the heteroatom content of various fractions are chosen to represent the most likely structures. Quantitative use of IR spectra, in particular for oxygen groups, to estimate concentrations directly from adsorption, would provide better estimates of the concentration of heteroatom groups. Introducing other sources of analytical data, in particular information on multi-ring structures, would also improve the profiles.

The structural profiles of the saturates and aromatics fractions were found to be least sensitive to error in analytical data from ^{13}C -NMR spectra. However, for the polar fractions, the structural profiles were quite sensitive to ^{13}C -NMR data. Although significant variations in individual group concentrations were observed for the polar fractions,

the major structural features were relatively unchanged. Alkyl substituents on aromatic rings, methyne groups, and benzene and naphthalene, should be lumped together to eliminate the sensitivity of the profiles to the analytical data.

Table VI.1 Properties of SCGO

Boiling range, °C	174 - 619
Specific gravity (15 °C)	0.9829
Sulphur, weight %	4.12
Nitrogen, weight %	0.305
Fraction, vol %.	
Naphtha (C7 - 177 °C)	0.54
Distillate (177 - 343 °C)	33.02
Fuel oil (343 °C +)	66.44

Table VI.2 Class Separation Results for SCGO

Fraction	Wt %
Saturates	25.28
Aromatics	20.92
Polar I	28.27
Polar II	12.38
Polar III	9.75
Asphaltenes	0.34
Recovery	96.94

Table VI.3 Elemental Analyses (Wt%) of SCGO Fractions

Element	Saturates	Aromatics	Polar I	Polar II	Polar III
C	85.89	85.61	84.14	83.96	79.91
H	13.57	11.04	8.42	7.72	8.47
O	0.37	0.18	0.52	0.66	4.66
N	0.07	0.03	0.05	0.29	2.20
S	0.10	3.14	6.87	7.37	4.76

Table VI.4 H-NMR Data for SCGO Fractions

Band #	% of Total Hydrogen				
	Saturates	Aromatics	Polar I	Polar II	Polar III
1	35.62	24.88	13.86	11.50	14.19
2	63.47	46.92	32.56	19.20	37.07
3	0.91	20.38	32.10	36.86	33.87
4			0.69		
5		7.82	19.40	20.25	12.81
6			1.39	2.19	2.06

Table VI.5 C13-NMR Data for SCGO Fractions

Band #	% of Total Carbon				
	Saturates	Aromatics	Polar I	Polar II	Polar III
1	7.45	5.61	7.65	5.05	7.24
2		2.25	4.53	2.91	3.30
3		5.04	6.87	6.50	5.03
4	5.11	3.10	4.10	3.88	4.68
5	20.56	14.81	10.63	8.38	9.56
6	35.40	27.49	17.51	15.80	21.63
7	31.48	16.04	8.35	13.57	15.72
9		12.02	24.79	24.59	18.78
10		8.74	12.26	15.49	10.50
11		4.87	3.31	3.83	3.56

Table VI.6 Structural Profiles of SCGO Fractions

Concentrations in moles of functional groups/100 g of sample							
Group#	Group name	Structure	Saturates	Aromatics	PolarI	PolarII	PolarIII
23	Naphthenic methyl		0.595	0.367			
24	Naphthenic methylene		1.317	0.837			
21	Aliphatic methyne		1.852	1.100	0.381	0.724	0.917
19	Chain methylene		2.327	1.149	0.550	0.297	0.337
22	Gamma methyl		1.004	0.541	0.386	0.294	0.397
13	Alpha methylene			0.592	0.097	0.162	0.260
14	Alpha methyl			0.352	0.414	0.399	0.292
15	Alpha methyne				0.281	0.276	
16	Beta methyl			0.149	0.247	0.145	0.174
11	Hydroaromatic ring				0.128	0.121	0.141
1	Benzene		0.186				0.227
2	Naphthalene				0.150	0.077	
3	Phenanthrene				0.058	0.084	0.087
5	Benzothiophene		0.098				
6	Dibenzothiophene				0.099	0.097	
33	Aliphatic thioether		0.003		0.115	0.133	0.148
50	Aliphatic ether		0.023				
7	Dibenzofuran			0.011	0.033	0.041	0.003
9	Carbazole			0.002	0.004	0.021	0.028
35	Aliphatic amine		0.005				
36	Aniline						0.129
30	Olefin				0.029		
43	Phenol						0.066
40	Aromatic carbonyl						0.221

Table VI.7 Structural Profiles for SCGO

Concentrations in moles of functional groups/100 g of sample

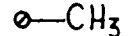
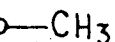
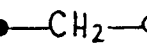
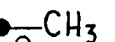
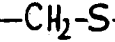
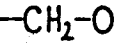
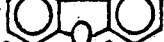
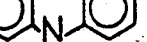
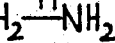
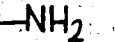
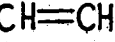
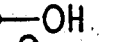
Group #	Group name	Structure	Combination of Fractions	Whole oil Analysis
23	Naphthenic methyl		0.235	0.350
24	Naphthenic methylene		0.526	0.521
21	Aliphatic methyne		1.020	1.159
19	Chain methylene		1.091	1.099
22	Gamma methyl		0.571	0.512
13	Alpha methylene		0.204	0.218
14	Alpha methyl		0.278	0.350
15	Alpha methyne		0.118	-
16	Beta methyl		0.141	0.178
11	Hydroaromatic ring		0.067	-
1	Benzene		0.063	0.020
2	Naphthalene		0.054	-
3	Phenanthrene		0.036	0.031
5	Benzothiophene		0.021	-
6	Dibenzothiophene		0.041	0.077
33	Aliphatic thioether		0.066	0.071
50	Aliphatic ether		0.006	-
7	Dibenzofuran		0.018	0.026
9	Carbazole		0.007	0.055
35	Aliphatic amine		0.001	-
36	Aniline		0.013	-
30	Olefin		0.008	0.023
43	Phenol		0.007	-
40	Aromatic carbonyl		0.022	-

Table VI.8 Analytical Data for SCGO (whole oil analysis)

1. Elemental Analysis

Element	Wt. %
C	83.88
H	10.19
O	0.41
N	0.77
S	4.75

2. H-NMR

Band #	% of total hydrogen
1	25.53
2	42.28
3	18.15
4	0.45
5	9.98
6	0.61

3. C13-NMR

Band #	% of total carbon
1	5.75
2	2.97
3	5.43
4	3.36
5	12.78
6	26.19
7	16.16
9	15.66
10	7.42
11	4.28

Table VI.9 Comparison of ^{13}C -NMR Data with
FGA Results for SCGO (% of total carbon)

Band #	Range, ppm.	Experimental	Predicted (FGA)
1	11 - 15	5.61	7.57
2	15 - 18	2.25	2.09
3	18 - 20.5	5.04	4.93
4	20.5 - 22.5	3.10	5.14
5	22.5 - 27.5	14.81	11.72
6	27.5 - 37	27.49	24.37
7	37 - 60	16.04	15.40
9	100 - 129.5	12.02	10.72
10	129.5 - 140	8.74	14.95
11	140 - 160	4.87	3.11

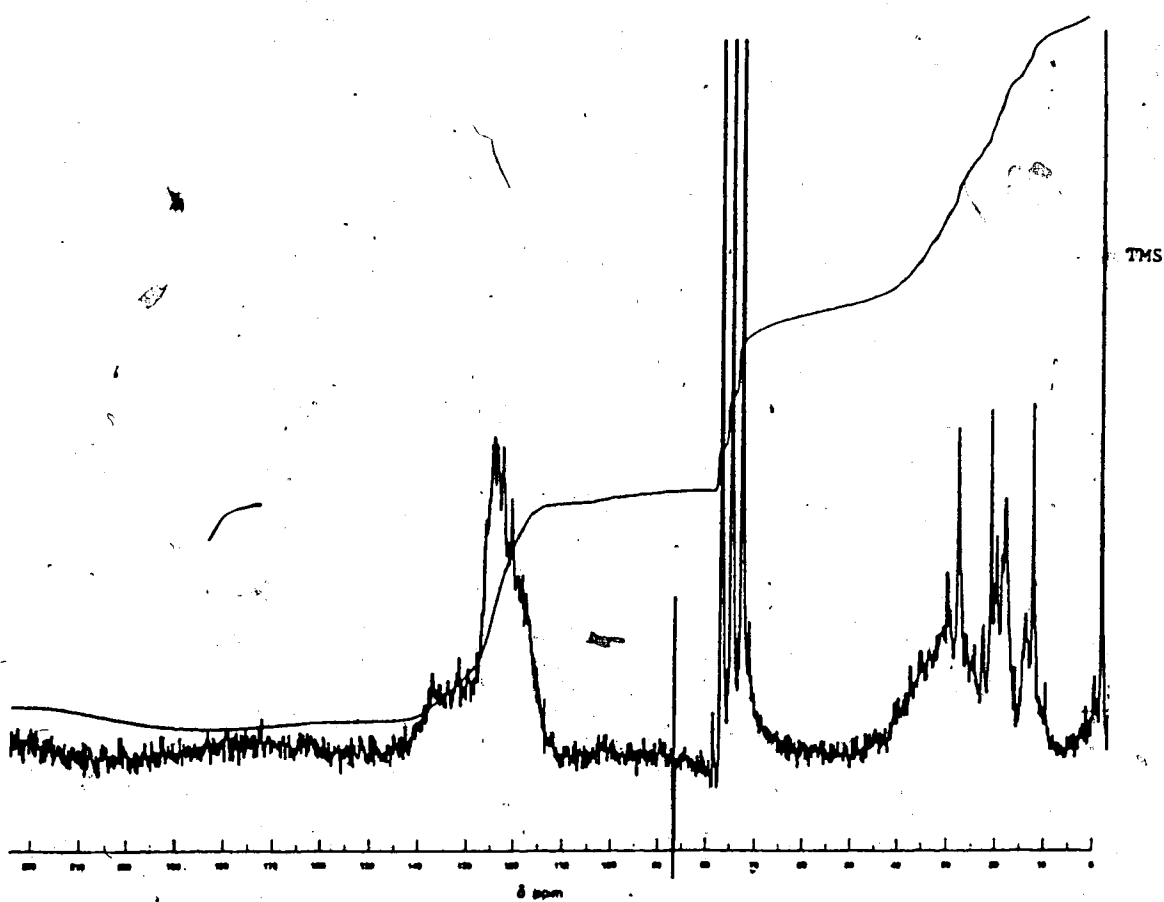


Figure VI.1 ¹³C-NMR Spectrum of SCGO Polar I

Table VI.10 C13-NMR Data for SCGO Fractions
 (data obtained from the spectrum integration curve)

Band #	% of Total Carbon			
	Saturates	Aromatics	Polar I	Polar II
1	7.29	5.96	2.63	3.14
2		2.38	5.92	3.92
3		4.77	5.92	5.88
4	6.48	3.28	3.95	3.14
5	22.27	14.30	9.87	8.63
6	32.38	27.10	15.79	14.90
7	31.58	15.78	10.52	14.90
9		12.02	24.79	24.59
10		8.41	15.34	16.59
11		6.01	5.26	4.31

Table VI.11 Structural Profiles of SCGO Fractions

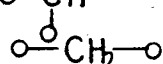
(C13-NMR Data from Spectrum Integration Curve)

Concentrations in moles of functional groups/100 g of sample

Group #	Group name	Structure	Saturates	Aromatics	Polar I	Polar II
23	Naphthenic methyl		0.611	0.359		
24	Naphthenic methylene		1.494	0.836		
21	Aliphatic methyne		1.836	1.089	0.691	0.911
19	Chain methylene		2.166	1.135	0.231	0.143
22	Gamma methyl		0.988	0.550	0.386	0.294
13	Alpha methylene			0.615	0.451	0.369
14	Alpha methyl			0.338	0.357	0.359
15	Alpha methyne					0.136
16	Beta methyl			0.165	0.357	0.219
11	Hydroaromatic ring				0.124	0.094
1	Benzene			0.189	0.085	
2	Naphthalene				0.023	0.065
3	Phenanthrene				0.058	0.084
5	Benzothiophene			0.098		
6	Dibenzothiophene				0.161	0.111
33	Aliphatic thioether		0.003		0.053	0.119
50	Aliphatic ether		0.023			
7	Dibenzofuran			0.011	0.033	0.041
9	Carbazole			0.002	0.004	0.021
35	Aliphatic amine		0.005			
30	Olefin				0.029	

Table VI.12 Structural Profiles of SCGO Resin Fraction

Concentrations in moles of functional groups/100 g of sample

Group#	Group name	Structure	Resin Fraction	Polar I + Heavy Resins	Polar I + II + III
21	Aliphatic methyne		0.738	0.626	0.569
19	Chain methylene		0.330	0.409	0.447
22	Gamma methyl		0.364	0.365	0.365
13	Alpha methylene		0.362	0.187	0.145
14	Alpha methyl		0.385	0.386	0.387
15	Alpha methyne			0.158	0.225
16	Beta methyl		0.207	0.209	0.208
11	Hydroaromatic ring		0.130	0.130	0.129
1	Benzene		0.116	0.042	0.044
2	Naphthalene			0.084	0.103
3	Phenanthrene		0.070	0.010	0.070
7	Dibenzofuran			0.023	0.029
43	Phenol		0.020	0.014	0.013
40	Aromatic carbonyl		0.065	0.047	0.043
30	Olefin		0.016	0.016	0.016
6	Dibenzothiophene		0.129	0.079	0.079
33	Aliphatic thioether		0.076	0.126	0.126
36	Aniline			0.025	
9	Carbazole		0.038	0.038	0.013

7. Structural Characterization of Alberta Gas Oils

7.1 Description of Gas Oils

FGA was used for the structural characterization of four different gas oils obtained from Alberta bitumen. Gas oils are middle distillates which are obtained during processing of raw bitumen by different methods. Cold Lake Gas Oil (CLGO) and Lloydminster Vacuum Gas Oil (LVGO) were obtained by direct distillation of the raw oil and were supplied by Petrocanada Exploration Ltd. Syncrude Coker Gas Oil (SCGOF2) was obtained from Athabasca bitumen which was first upgraded by thermal coking. The SCGO sample which was considered in chapter 6, was different from SCGOF2 in that the former was stored for over one year prior to analysis. Another sample that was analyzed in this study was a gas oil obtained from the Department of Energy, Mines, and Resources (EMRGO). This sample was obtained from Athabasca bitumen which was upgraded by the CANMET process prior to distillation.

The results from the conventional analysis of these gas oils (Chung, 1982; Man, 1981) are presented in Table VII.1. The Syncrude sample had the highest content of sulphur and nitrogen as well as a higher final boiling point. EMRGO was a lighter oil with lower initial and final boiling points and lower content of heteroatoms. In this chapter an attempt is made to use the structural profiles obtained from FGA as a basis to learn about the differences in chemical composition between these gas oils.

7.2 Analytical Data

The class separation yields for the gas oils considered in this study are presented in Table VII.2. For EMRGO, the overall recovery was below the expected value of approximately 95 %. The low recovery of EMRGO could be related to its low initial boiling point. Lighter gas oils gave poor material balance with the normal class separation method because the volatile components were evaporated with solvents. Also, they did not leave any appreciable colored compounds on the silica gel in the chromatography column, indicating that losses of higher boiling components were minimal. When such oils were dissolved in the chromatography solvents and then evaporated, between 5 and 10 % of the oil was lost with the solvents.

The materials lost during the class separation of EMRGO would mainly contribute to the naphtha fraction and to a good approximation the 82 % recovery represented about 95 % of gas oil in the boiling range of 177-491 °C. This illustrates one of the shortcomings of FGA in that the low boiling naphtha fraction could not be represented in the analysis. Such low boiling material can, however, be analyzed by other well established techniques such as gas chromatography.

The elemental analysis data for individual fractions are presented in Table VII.3. The results were consistent with the class separation scheme, and for all samples the heteroatoms content increased from saturates to Polar III.

Oxygen was present in all fractions but appeared in substantial amounts in the Polar III fraction of all samples.

Due to the limited amount of polar fractions obtained from the class separation of gas oils, a total resins fraction was prepared for each gas oil in which the amount of each polar fraction was proportional to the amounts recovered in the separation scheme. This procedure was necessary since at least one gram of each fraction was required for ^{13}C -NMR. The ^1H and ^{13}C NMR data for the gas oils are presented in Tables VII.4 and VII.5 respectively.

The IR spectrum of the Polar III fractions provided additional information on the concentration of phenols, carbonyls, and carbazole. The concentration of these groups in the Polar III fraction was obtained using the method described by McKay et al. (1975). These concentrations are presented in Table VII.6. In using this data in the analysis of the resins, the following assumptions were made:

1. that phenols and carbonyls appear in the Polar III fraction only. This is a reasonable approximation since these are the most polar oxygen groups. Also, the IR spectra of Polar I and Polar II fractions did not indicate the presence of these groups. Other less polar groups such as dibenzofuran are more likely to be present in Polar I and Polar II fractions.
2. that besides carbazole, aniline, a basic compound, is the other most likely nitrogen group in the Polar III

fraction. Hence, knowing the concentration of carbazole and the total nitrogen content of this fraction, the concentration of aniline could be obtained by difference. Other nitrogen groups such as quinoline may also be present in the Polar III fraction, but unless more specific information on heteroatom groups is available, the choice of such groups is limited.

7.3 FGA Results

The structural profiles of saturates, aromatics, and resins of SCGOF2, CLGO, LVGO, and EMRGO are presented in Tables VII.7 to VII.10 respectively. The profiles of the whole oils were obtained by combining the profiles of the individual fractions in proportion to the amounts recovered in the separation procedure. These profiles are also presented in Tables VII.7 to VII.10.

As mentioned in the previous chapters, the concentration of some groups which are sensitive to ¹³C-NMR data should be summed together to avoid ambiguity. The analysis of model compounds and SCGO indicated that alkyl substituents on aromatic rings should be considered as a single group. Differentiating between benzene and naphthalene was also not possible on the basis of NMR data. The profiles of various gas oils indicated that another uncertainty in FGA results may be the distinction between benzothiophene and dibenzothiophene. Although FGA provided a split between aliphatic thioether and thiophenes, for all the samples considered, sulphur in thiophenes was either

determined as benzothiophene or dibenzothiophene (the concentration of one group was always zero). Benzothiophene could be viewed as a representative group for less aromatic sulphur structures while dibenzothiophene could represent highly aromatic sulphur groups. As a further check, mixtures of model compounds containing both structures should be examined to see whether or not a distinction between these groups is possible on the basis of NMR data.

With the above limitations considered, the profiles of SCGOF2 (Table VII.7) were in good agreement with SCGO (Table VI.7). The difference between the concentration of various groups for the above samples were within the expected error in the FGA. This demonstrated the reproducibility of the analysis. Comparison of oxygen analyses for various fractions for the above samples indicated that the major difference between the two samples was a substantial decrease in the oxygen content of all the fractions of SCGO. This could be explained by the possible precipitation of some oxygen containing polar structures during the storage period, and by the variability in the feedstocks for the Syncrude process.

The profiles of the gas oils revealed some interesting structural features which could be related to their physical properties, i.e. boiling range. A summary of some of the major structural characteristics of the gas oils is presented in Table VII.11.

One of the differences between SCGOF2 and other gas oils was that the former had a significantly higher aromaticity. The concentration of heteroaromatics in SCGOF2 was also substantially higher compared with other gas oils, consistent with the higher content of resins in SCGOF2. Compared with saturates and aromatics, resins had a high content of N, O, and S which were mostly involved in heteroaromatic structures or functionalized aromatics such as phenols and anilines. Also, the structural profiles of resins of all gas oils were dominated by aromatic structures. For the samples considered, the aromaticity of resins was between 41 and 55 %. In general, resins may be viewed as highly aromatic in character, containing substantial amounts of poly and heteroaromatics. The class separation yields (Table VII.2) indicated that for SCGOF2, resins contributed to over 50 % of the whole oil which was significantly higher than other gas oils in which resins made up between 20 and 32 % of the oil.

The higher content of resins in SCGOF2 could be related to the higher final boiling point of the sample. The final boiling point of SCGOF2, CLGO, LVGO, and EMRGO were 619, 557, 556, and 491 °C, respectively, with resins contributing to 50, 32, 26, and 20 % of the oils respectively. Although fused aromatics and heteroatom groups which make up the resins could appear in a wide boiling range, such structures may be particularly abundant in 560-620 °C cut. This would also explain the significantly higher concentration of

heteroaromatics in the resins and aromatics of SCGOF2 compared with the corresponding fractions of other gas oils. The aromaticity of resins was also found to increase with increasing final boiling point of the samples; from 41 % for EMRGO, to 44 % for CLGO and LVGO, to 55 % for SCGOF2.

The concentration of total thiophenes was found to increase with the increasing final boiling point of the gas oils. On the other hand, the concentration of aliphatic thioether, which appeared in all class fractions; was not affected by the final boiling points. This would suggest the presence of aliphatic thioether in a wide boiling range.

The total concentration of functionalized aromatic structures, phenols and anilines, was also found to increase with increasing boiling range. The relatively high concentration of these groups in SCGOF2, could suggest that similar to heteroaromatic structures, functionalized aromatics were abundant in the 560-620 °C cut. The concentration of aniline in gas oils is of particular interest since as an organic base, it would tend to poison catalysts (Smith, 1970).

In Table II.1 the structural profiles of Cold Lake Tar Sands (Allen et al., 1985) were presented. This sample was a heavy atmospheric tower bottoms (ATB) with boiling point above 300 °C. The aromaticity of this sample was about 32 % and almost all of the aromatic carbons were involved in heterocyclic structures. Although the concentration of dibenzothiophene was overestimated because aliphatic sulphur

structures were not included in the analysis, the significantly higher concentration of various heteroatom groups in the Cold Lake ATB compared with CLGO would indicate the abundance of such functionalities in the 560 °C+ cut.

The structural profiles of Cold Lake ATB showed a significant increase in the concentration of alpha methyne and alpha methylene groups and a decrease in the concentration of alpha methyl compared with CLGO indicating that for lower boiling range samples, methyl substitution on aromatic rings would be significant. Also, a fraction of beta and beta(+) methyl, methylene, and methyne groups reported by Allen et al. (1985) should be involved in naphthenic structures such as those identified by Payzant et al. (1980) in the Cold Lake bitumen. The concentrations of benzene and naphthalene were considerably lower for Cold Lake ATB. This could be due to an overestimation of the concentration of dibenzothiophene since sulphur could also be present in aliphatic structures such as those identified by Payzant et al. (1983). The presence of sulphur in the saturates fraction was further evidence for the presence of aliphatic thioethers.

From the structural profiles of the gas oils, some relationships between chemical composition and their boiling range were observed. However, structural features should not merely be related to the boiling range. CLGO and LVGO were both obtained from distillation with no previous upgrading

and the boiling range for these oils were similar. However, LVGO was found to contain considerably more saturates and less resins. The aromaticity of CLGO was greater; it contained more hydroaromatic rings, less naphthenic carbon, and significantly more heteroatoms, both in the form of heteroaromatics and functionalized aromatic structures. The profiles of CLGO and LVGO obtained from FGA have clearly indicated that gas oils with very similar physical properties could have very different chemical composition which would affect their reactivity under processing conditions.

The structural profiles of the saturates fractions for the various gas oils were quite similar. All saturates fractions contained very low amounts of heteroatoms and the percentage of naphthenic carbon was about the same for all samples (between 28 and 31 % of total carbon). The degree of branching was slightly higher for LVGO as indicated by the greater concentration of methyne in linear structures. The estimate of branching was obtained by subtracting the approximate concentration of naphthenic methyne (obtained from naphthenic methyl concentration) from the total aliphatic methyne concentration.

The class separation yields indicated that for all the gas oils considered, the yields of the aromatics fraction were about the same (22 % of the oil). For aromatics, some of the structural features were quite similar for the various gas oils. For example, the percentage of naphthenic

carbon was found to vary between 15 and 17 %, and aromaticity ranged between 32 and 37 %. One of the significant differences between the profiles of aromatics was the distribution of aromatic carbon between heteroaromatics and mono * diaromatics. For the lighter oils, about 70 % of aromatic carbons were mono and diaromatics while for the heavier Syncrude sample, over 50 % of aromatic carbons were involved in heteroaromatic structures.

One of the interesting structural differences between the aromatics fractions was the approximate length of alkyl chains. An estimate of the relative chain length could be obtained from the ratio of the concentration of chain methylene, group 19, to the concentration of aliphatic methyne in linear structures. This ratio was found to be substantially higher for EMRGO and SCGOF2 indicating that these samples exhibited a lower degree of branching and longer average chain length. This difference could be related to the upgrading of the above samples prior to distillation which might have caused the removal of some alkyl branches. This point, however, should be further investigated by examining the structural profiles of gas oils in the same boiling range obtained from virgin Athabasca bitumen.

7.4 Summary

* For gas oils with low initial boiling point, FGA could not provide adequate structural profiles due to losses of

naphtha and other low boiling materials during the separation procedure. Application of FGA should be limited to gas oils with initial boiling points above 170 °C.

The profiles of the gas oils indicated that while the structures present in the resins fraction could appear in a wide boiling range, such structures, particularly various heteroaromatics, were most abundant in the 560-620 °C cut. The structural profiles of the saturates fraction were quite similar for all samples while aromatics and resins showed significant differences. The analysis of gas oils indicated that chemical composition could not be related merely to the boiling range. In the next chapter, the structural profiles of products obtained from a catalytic hydroprocessing reactor using SCGOF2 as the initial feedstock will be examined.

Table VII.1 Properties of Gas Oils

	SCGOF2	CLGO	LVGO	EMRGO
Boiling range, °C	174-619	186-557	192-556	132-491
Specific gravity (15 °C)	0.9829	0.9347	0.9239	0.9148
Sulphur, weight %	4.12	2.94	2.41	2.00
Nitrogen, weight %	0.305	-	-	0.05
Fraction, vol %				
Naphtha (C7-177 °C)	0.54	0.1	0.0	5.6
Distillate (177-343 °C)	33.02	32.5	37.2	50.1
Fuel oil (343 °C +)	66.44	67.4	62.8	44.3

Table VII.2 Class Separation Results (wt. % of the oil)

Fraction	SCGOF2	CLGO	LVGO	EMRGO
Saturates	24.18	38.88	44.82	39.62
Aromatics	21.37	22.63	22.76	22.23
Polar I	29.00	17.62	15.49	10.22
Polar II	10.87	7.33	5.89	4.93
Polar III	9.95	7.03	4.67	4.59
Asphaltenes	0.14	0.18	1.29	0.09
Recovery	95.51	93.67	94.92	81.68

Table VII.3 Elemental Analyses (Wt%) of gas oils

1. SCGOF2

Element	Fractions				
	Saturates	Aromatics	Polar I	Polar II	Polar III
C	85.56	84.63	83.93	83.65	79.35
H	13.65	10.56	7.94	7.92	8.50
O	0.61	0.78	1.21	0.72	5.53
N	0.08	0.04	0.01	0.48	2.21
S	0.10	3.99	6.91	7.23	4.41

2. CLGO

Element	Fractions				
	Saturates	Aromatics	Polar I	Polar II	Polar III
C	85.83	85.65	85.06	82.08	77.50
H	13.55	10.85	9.06	9.48	9.89
O	0.25	0.38	0.44	0.57	5.07
N	-	0.23	0.03	0.38	0.80
S	0.09	2.89	5.41	7.49	6.74

3. LVGO

Element	Fractions				
	Saturates	Aromatics	Polar I	Polar II	Polar III
C	85.63	86.19	85.65	81.91	76.93
H	13.73	10.99	8.55	9.79	9.87
O	0.44	0.50	0.62	0.78	5.47
N	0.01	-	0.04	0.25	0.52
S	0.19	2.32	5.14	7.27	7.21

4. EMRGO

Element	Fractions				
	Saturates	Aromatics	Polar I	Polar II	Polar III
C	85.93	86.15	83.75	79.15	77.04
H	13.46	10.84	8.76	10.12	9.91
O	0.30	0.56	1.11	0.90	6.77
N	0.18	-	0.11	0.28	0.70
S	0.13	2.45	6.27	9.55	5.58

Table VII.4 H-NMR Data for Gas Oils (% of total hydrogen)

1. SCGOF2

Band #	Saturates	Fractions		
		Aromatics		Resins
1	38.09	19.17		14.25
2	59.93	45.39		29.73
3	1.02	26.21		35.43
4	0.96	-		0.31
5	-	9.22		19.14
6	-	-		1.14

2. CLGO

Band #	Saturates	Fractions		
		Aromatics		Resins
1	35.31	21.18		19.80
2	62.08	43.35		40.03
3	2.61	26.11		25.96
4	-	-		-
5	-	9.36		13.64
6	-	-		0.57

3. LVGO

Band #	Saturates	Fractions		
		Aromatics		Resins
1	35.46	24.46		17.73
2	63.52	42.70		39.38
3	1.02	22.32		27.02
4	-	-		0.23
5	-	10.52		15.15
6	-	-		0.49

4. EMRGO

Band #	Saturates	Fractions		
		Aromatics		Resins
1	40.10	20.21		18.88
2	56.77	40.94		42.14
3	3.13	28.35		26.34
4	-	-		-
5	-	10.50		11.85
6	-	-		0.79

Table VII.5 C13-NMR Data for Gas Oils (% of total carbon)

1. SCGOF2

Band #	Saturates	Aromatics	Resins
1	6.38	5.63	6.75
2	-	3.09	3.65
3	-	4.10	6.44
4	8.51	3.49	3.12
5	19.06	12.87	10.00
6	35.01	29.02	15.23
7	29.22	12.91	12.05
9	0.91	13.71	23.45
10	0.91	8.26	11.32
11	-	6.92	7.99

2. CLGO

Band #	Saturates	Aromatics	Resins
1	11.90	7.44	5.76
2	-	3.44	3.85
3	-	5.65	6.71
4	10.67	3.51	3.30
5	18.68	14.93	11.05
6	37.76	25.13	16.78
7	20.99	16.48	13.94
9	-	14.13	19.12
10	-	6.32	15.95
11	-	2.97	3.54

3. LVGO

Band #	Saturates	Aromatics	Resins
1	7.22	5.29	4.71
2	-	2.30	2.31
3	-	4.63	3.81
4	5.90	3.46	2.61
5	24.20	13.85	10.90
6	35.08	23.92	18.40
7	27.60	19.35	16.68
9	-	15.99	20.31
10	-	8.03	11.49
11	-	3.18	8.78

4. EMRGO

Band #	Saturates	Aromatics	Resins
1	9.45	6.78	10.87
2	-	3.05	4.52
3	-	4.77	9.96
4	9.28	3.25	2.94
5	17.50	12.21	13.44
6	36.14	24.30	17.95
7	27.63	17.23	10.75
9	-	15.74	17.42
10	-	7.69	9.89
11	-	4.98	2.26

Table VII.6 Concentration (moles of functional groups/100 g of sample) of Polar III groups from IR

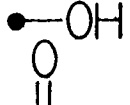
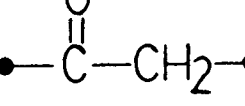
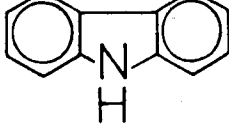
Group name	Structure	SCGOF2	CLGO	LVGO	EMRGO
Phenol		0.047	0.035	0.027	0.035
Carbonyl		0.173	0.126	0.117	0.223
Carbazole		0.060	0.029	0.017	0.034

Table VII.7 Structural Profiles of SCGOF2 Fractions

Concentrations in moles of functional groups/100 g of sample

Group #	Group name	Structure	Saturates	Aromatics	Resins	whole oil
19	Chain methylene		2.349	1.049	0.276	0.975
21	Aliphatic methyne		1.632	0.634	0.768	0.957
22	Gamma methyl		0.961	0.414	0.379	0.534
23	Naphthenic methyl		0.759	0.256		0.250
24	Naphthenic methylene		1.271	0.808		0.503
13	Alpha methylene			0.807	0.439	0.410
14	Alpha methyl			0.318	0.411	0.286
15	Alpha methyne					
16	Beta methyl			0.221	0.202	0.155
11	Hydroaromatic ring				0.091	0.048
1	Benzene		0.202	0.070	0.082	
2	Naphthalene					
3	Phenanthrene				0.046	0.024
5	Benzothiophene			0.079		0.018
6	Dibenzothiophene				0.128	0.067
33	Aliphatic thioether		0.003	0.045	0.074	0.050
7	Dibenzofuran			0.049	0.079	0.052
50	Aliphatic ether		0.026			0.007
40	Aromatic carbonyl				0.035	0.018
43	Phenol				0.009	0.005
9	Carbazole			0.003	0.019	0.011
35	Aliphatic amine		0.006			0.002
36	Aniline				0.020	0.010
30	Aromatic olefin				0.012	0.006
31	Terminal olefin		0.043			0.011

Table VII.8 Structural Profiles of CLGO Fractions

Group #	Group name	Structure	Concentrations in moles/100 g sample			
			Saturates	Aromatics	Resins	whole oil
19	Chain methylene		2.551	0.771	0.905	1.557
21	Aliphatic methyne		1.771	1.006	0.743	1.234
22	Gamma methyl		0.645	0.516	0.612	0.602
23	Naphthenic methyl		0.942	0.244		0.451
24	Naphthenic methylene		1.220	0.830		0.708
13	Alpha methylene			0.683	0.060	0.186
14	Alpha methyl			0.409	0.425	0.244
15	Alpha methyne				0.143	0.049
16	Beta methyl			0.233	0.223	0.133
11	Hydroaromatic ring				0.103	0.035
1	Benzene		0.263			0.064
2	Naphthalene				0.077	0.026
3	Phenanthrene				0.026	0.009
5	Benzothiophene		0.038			0.009
6	Dibenzothiophene				0.086	0.029
33	Aliphatic thioether		0.003	0.052	0.106	0.050
7	Dibenzofuran			0.024	0.057	0.025
50	Aliphatic ether		0.016			0.007
40	Aromatic carbonyl				0.028	0.010
43	Phenol				0.008	0.003
9	Carbazole			0.016	0.014	0.009
35	Aliphatic amine					
36	Aniline				0.006	0.002
30	Aromatic olefin					
31	Terminal olefin					

Table VII.9 Structural Profiles of LVGO Fractions

Concentrations in moles of functional groups/100 g of sample

Group #	Group name	Structure	Saturates	Aromatics	Resins	whole oil
19	Chain methylene		2.275	0.907	0.854	1.547
21	Aliphatic methyne		1.609	0.987	1.030	1.297
22	Gamma methyl		0.969	0.516	0.531	0.737
23	Naphthenic methyl		0.641	0.374		0.398
24	Naphthenic methylene		1.567	0.859		0.959
13	Alpha methylene			0.605	0.542	0.298
14	Alpha methyl			0.363	0.253	0.159
15	Alpha methyne					
16	Beta methyl			0.170	0.135	0.079
11	Hydroaromatic ring				0.084	0.023
1	Benzene		0.271	0.129		0.102
2	Naphthalene					
3	Phenanthrene				0.022	0.006
5	Benzothiophene			0.037	0.127	0.044
6	Dibenzothiophene					
33	Aliphatic thioether		0.006	0.035	0.059	0.028
7	Dibenzofuran			0.031	0.070	0.027
50	Aliphatic ether		0.028			0.013
40	Aromatic carbonyl				0.021	0.006
43	Phenol				0.005	0.001
9	Carbazole				0.008	0.002
35	Aliphatic amine		0.001			0.001
36	Aniline				0.004	0.001
30	Aromatic olefin				0.010	0.003
31	Terminal olefin					

Table VII.10 Structural Profiles of EMRGO Fractions

Concentrations in moles of functional groups/100 g of sample						
Group #	Group name	Structure	Saturates	Aromatics	Resins	whole oil
19	Chain methylene		2.308	0.823	1.273	1.653
21	Aliphatic methyne		1.939	0.524	0.745	1.265
22	Gamma methyl		0.817	0.503	0.585	0.675
23	Naphthenic methyl		1.012	0.221		0.552
24	Naphthenic methylene		1.020	0.859		0.729
13	Alpha methylene			0.858		0.234
14	Alpha methyl			0.418	0.463	0.226
15	Alpha methyne				0.127	0.031
16	Beta methyl			0.246	0.099	0.091
11	Hydroaromatic ring				0.059	0.014
1	Benzene		0.296			0.081
2	Naphthalene				0.046	0.011
3	Phenanthrene				0.036	0.009
5	Benzothiophene			0.054		0.015
6	Dibenzothiophene				0.046	0.011
33	Aliphatic thioether		0.004	0.023	0.170	0.049
7	Dibenzofuran			0.035	0.088	0.031
50	Aliphatic ether		0.019			0.009
40	Aromatic carbonyl				0.052	0.013
43	Phenol				0.008	0.002
9	Carbazole				0.017	0.004
35	Aliphatic amine		0.013			0.006
36	Aniline				0.004	0.001
30	Aromatic olefin					
31	Terminal olefin					

Table VII.11 Summary of the Important Structural Features
of gas oils

(concentrations in moles / 100 grams of sample)

	SCGOF2	CLGO	LVGO	EMRGO
1. Whole Oil				
Naphthenic carbon	10.8 %	16.5 %	19.2 %	18.1 %
Aromaticity	36.3 %	22.7 %	19.8 %	19.8 %
Mono + di aromatics	0.492	0.644	0.612	0.596
Polyaromatics	0.336	0.126	0.084	0.126
Heteroaromatics	1.704	0.828	0.700	0.672
Thiophenes	0.085	0.038	0.044	0.026
Thioether	0.050	0.050	0.028	0.049
Hydroaromatic rings	0.048	0.035	0.023	0.014
Phenols + Anilines	0.015	0.005	0.002	0.003
2. Resins				
Aromaticity	55.1 %	44.3 %	44.0 %	41.1 %
Mono + di aromatics	0.420	0.770	0.774	0.460
Polyaromatics	0.644	0.346	0.308	0.504
Heteroaromatics	2.712	1.884	1.952	1.812
3. Aromatics				
Naphthenic carbon	15.1 %	15.0 %	17.3 %	15.1 %
Aromaticity	34.9 %	33.0 %	32.1 %	36.9 %
Mono + di aromatics	1.212	1.578	1.626	1.776
Heteroaromatics	1.256	0.784	0.668	0.852
Linear methyne	0.378	0.762	0.613	0.303
Chain methylene	1.049	0.771	0.907	0.828
Ratio CH / CH ₂	2.8	1.0	1.5	2.7
4. Saturates				
Naphthenic carbon	28.5 %	30.2 %	31.0 %	28.4 %
Linear methyne	0.873	0.829	0.968	0.927

8. Structural Characterization of Hydroprocessed Syncrude Coker Gas Oil

FGA was used for structural characterization of a product oil, SC-101, from catalytic hydroprocessing of SCGOF2 over a commercial Ni-Mo catalyst. The equipment, analytical methods, and pretreatment of catalysts for hydrotreating of SCGOF2 are given by Rangwala et al. (1984). Hydrotreatment was carried out at 400 °C under 13.9 MPa of hydrogen pressure. For typical runs, they obtained 60 to 90 % sulphur conversion, 20 to 60 % nitrogen conversion, and 17 to 44 % pitch conversion, where pitch was defined as the liquid fraction having a boiling point range of 343 and 524 °C. Gases produced during hydrotreating included C1 to C5 hydrocarbons as well as hydrogen sulfide. For the SC-101 run, 0.8 % of carbon in the feed was converted to gaseous products.

The analytical data used in FGA for structural characterization of SC-101 are presented in Table VIII.1. SC-101 was distilled for four hours at 160 °C prior to the class separation to stabilize the oil and 3.07 % of the sample was recovered as light volatiles. The residue was then subjected to the separation procedure and about 95 % of the sample was recovered in the various class fractions. The methodology described in chapter 7 was applied to obtain the structural profiles of saturates, aromatics, and resins,

8.1 Comparison of Structural Profiles of SC-101 with SCGOF2

The structural profiles of the individual class fractions of SC-101 are presented in Table VIII.2. These profiles were combined to give the whole oil profiles for SC-101 which are presented along with the profiles of SCGOF2 in Table VIII.3. Comparison of the profiles pointed to major structural changes in the product oil, SC-101, resulting from hydroprocessing of the original feedstock. Some of these changes are discussed here.

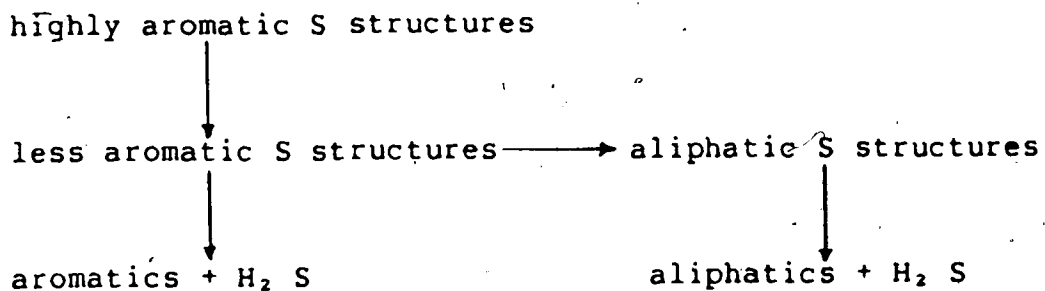
The profiles of the whole oil indicated a decrease in the concentration of phenanthrene and an increase in the concentration of benzene. This would suggest the hydrogenation of phenanthrene (condensed-rings aromatics in general) to give less condensed aromatic structures. Wu and Haynes (1975) proposed three major reaction pathways for catalytic hydrocracking of phenanthrene with tetralins, naphthalenes, and biphenyls as intermediates and benzene and alkylbenzenes as products. The hydrogenation of polyaromatics to alkylbenzenes would also explain the increase in the concentration of aliphatic structures and a decrease in aromaticity; from 36.3 % for SCGOF2 to 28.5 % for SC-101. The increase in the concentration of benzene could also be related to the desulphurization of benzothiophene and dibenzothiophene to give ethylbenzene and biphenyl, respectively (Nag et al., 1979).

The profiles of SC-101 indicated that over 70 % of sulphur was removed from the feed. The concentration of

various heteroatom groups suggested that desulphurization was the primary reaction. Examination of individual sulphur groups revealed that while the concentration of benzothiophene and aliphatic thioether were reduced by about 66 %, over 75 % of dibenzothiophenes had undergone desulphurization. This was contrary to previous work in hydrodesulphurization of model compounds (Nag et al., 1979). They found that desulphurization of dibenzothiophene proceeded less rapidly than benzothiophene under typical hydroprocessing conditions. Any speculation would be premature; however, one possible explanation could be that benzothiophene and/or aliphatic thioether were intermediates in the desulphurization of dibenzothiophene. In the case of thioether being a reaction intermediate, a possible reaction would be the hydrogenation of aromatic rings prior to sulphur removal. As reported by Nag et al., 1979, bicyclohexyl would be the product for such reaction scheme. The above observation could be related to two cases:

1. > that the predicted distribution of sulphur in various groups is inaccurate. One way to check this would be to use other chemical methods which identify different sulphur types.
2. that the reactions of model compounds are not appropriate for desulphurization of gas oils.

One approach for modelling hydrodesulphurization of gas oils would be to consider the reaction sequence as follows:



The substituents on aromatic rings which could include long alkyl chains as well as other functionalities could also affect the desulphurization reactions. Katti et al. (1984) found that methyl substitution on dibenzothiophene in the 4 position reduced the pseudo first order rate constant while methyl substitution in other positions increased the rate constant. The effect of longer chains on desulphurization of thiophenoaromatics has not been reported.

The percentage of naphthenic carbon was found to increase from 10.8 % for SCGOF2 to 15.3 % for SC-101. This increase could be explained by hydrogenation of aromatic structures. Cycloparaffins could react under hydroprocessing conditions to give lower molecular weight cycloparaffins and butanes, (Sullivan and Meyer, 1975). This reaction and the dealkylation of alkylaromatics with short alkyl chains would account for the light volatiles which were recovered during the hydroprocessing reaction and from distillation of SC-101 prior to class separation. Reduction in the beta methyl concentration was further evidence for cracking of ethyl substituents on aromatic rings to give ethane. Dealkylation of aromatics with long side chains and hydrogenation of

various aromatic structures would be responsible for the increase in the content of saturates fraction for SC-101 compared with SCGOF2.

The removal of organonitrogen, 35 %, and organooxygen, 38 %, were substantially lower than the percentage of the total sulphur removed. The concentration of carbazole remained unchanged while anilines and aliphatic amines were largely removed. Olefins were also completely hydrogenated as the ¹H-NMR spectra of various fractions of SC-101 did not indicate the presence of olefinic hydrogen.

An interesting observation was the decrease in the concentration of dibenzofuran and an increase in the concentration of aliphatic ether, suggesting that the latter could possibly be an intermediate in the deoxygenation of dibenzofuran. Furimsky (1978) proposed the reaction scheme for catalytic hydrodeoxygenation of dibenzofuran. It consisted of the hetero-ring opening to give biphenyl-1-ol. Dehydroxylation would either follow immediately to give biphenyl, or it would proceed via preliminary ring hydrogenation to give cyclohexylbenzene. Neither of the above reaction schemes would explain the increase in the concentration of oxygen structures in the saturates fraction. As in the case of desulphurization, a possible explanation would be the hydrogenation of the aromatic rings prior to the hetero-ring opening. In FGA, oxygen in the saturates fraction was represented only by aliphatic ether since the choice of heteroatom groups was limited due to

insufficient analytical data. Aliphatic ether would be a possible intermediate, however; further investigation of oxygen types in the saturates fraction could provide some information on the reaction pathways for dibenzofuran. For example, dicyclohexylether is a likely intermediate in such reactions and may possibly appear in the saturates fraction.

The lower concentration of hydroaromatic rings and a higher concentration of alpha methylene indicated the opening of the hydroaromatic rings in structures such as tetralin during the hydrotreatment. Other reactions involving tetralin, however, should not be excluded. For example, tetralin could be converted to naphthalene when it loses its hydrogens (Aarts et al., 1978). The structural profiles obtained from FGA can neither confirm nor rule out the latter reaction scheme since distinction between naphthalene and benzene was not possible on the basis of NMR data.

8.2 Summary

Examination of the structural profiles of SC-101 and SCGOF2 revealed some changes in the concentration of various groups. These changes could be explained by the various reactions involving the functional groups. Additional information, in particular for heteroatom groups and condensed aromatics, could provide more insight into the reactions occurring during hydropyrolysis of gas oils. FGA can be judged as a promising tool to examine the chemical changes in a feedstock due to processing.

Table VIII.1 Analytical Data for SC-101
1. Class Separation Yields

Fraction	% of total oil
Saturates	35.03
Aromatics	33.13
Polar I	16.80
Polar II	5.46
Polar III	4.29
Asphaltenes	-
Recovery	94.71

2. Elemental Analyses (Wt %)

Element	Saturates	Aromatics	Polar I	Polar II	Polar III
C	85.96	87.63	87.96	87.03	79.77
H	13.23	10.88	8.41	8.13	9.18
O	0.55	0.50	0.48	0.90	6.62
N	0.03	0.06	0.04	1.18	2.25
S	0.23	0.93	3.11	2.76	2.18

3. H-NMR (% of total hydrogen)

Band #	Saturates	Aromatics	Resins
1	34.92	25.40	14.53
2	61.90	40.32	20.94
3	3.18	24.20	40.17
5	-	10.08	22.86
6	-	-	1.50

4. C13-NMR (% of total carbon)

Band #	Saturates	Aromatics	Resins
1	8.09	8.82	6.21
2	-	2.38	4.09
3	-	4.65	7.87
4	7.32	3.34	3.98
5	22.51	12.67	9.44
6	37.93	24.26	12.60
7	24.14	13.96	6.86
9	-	14.91	28.48
10	-	12.74	15.50
11	-	5.27	4.97

5. Concentration (moles of functional groups/100 g of sample) of Polar III groups from IR

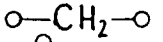
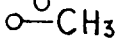
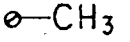
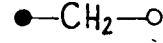
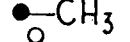
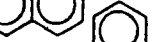
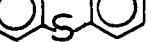
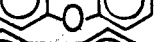
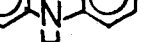
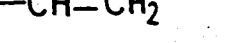
Group name	Structure	Concentration
Phenol		0.048
Carbonyl		0.217
Carbazole		0.087

Table VIII.2 Structural Profiles of SC-101 Fractions

Concentrations, in moles of functional groups/100 g of sample

Group #	Group name	Structure	Saturates	Aromatics	Resins
19	Chain methylene	<chem>O=C=O</chem>	2.179	0.822	0.203
21	Aliphatic methyne	<chem>O=C</chem>	2.207	1.025	0.534
22	Gamma methyl	<chem>O=CCH3</chem>	0.773	0.545	0.407
23	Naphthenic methyl	<chem>O=CCH3</chem>	0.755	0.369	
24	Naphthenic methylene	<chem>O=C=O</chem>	1.158	0.784	
13	Alpha methylene	<chem>C=C</chem>		0.807	0.714
14	Alpha methyl	<chem>C=C</chem>		0.337	0.433
15	Alpha methyne	<chem>C=C</chem>			
16	Beta methyl	<chem>C=C</chem>	0.162		0.116
11	Hydroaromatic ring	<chem>c1ccccc1</chem>			0.101
1	Benzene	<chem>c1ccccc1</chem>	0.298	0.299	
2	Naphthalene	<chem>c1ccc2ccccc2c1</chem>			
3	Phenanthrene	<chem>c1ccc2cc3ccccc3cc2c1</chem>			0.063
5	Benzothiophene	<chem>c1ccsc1</chem>		0.017	
6	Dibenzothiophene	<chem>c1cc2ccsc2c1</chem>		0.012	0.043
33	Aliphatic thioether	<chem>CS</chem>	0.007		0.047
7	Dibenzofuran	<chem>c1ccc2c(c1)oc3ccccc23</chem>		0.031	0.055
50	Aliphatic ether	<chem>CCOC</chem>	0.034		
40	Aromatic carbonyl	<chem>C=O</chem>			0.035
43	Phenol	<chem>Oc1ccccc1</chem>			0.008
9	Carbazole	<chem>c1ccncc1</chem>		0.004	0.033
35	Aliphatic amine	<chem>CH2NH2</chem>	0.002		
36	Aniline	<chem>NH2</chem>			0.012

Table VI.3 Structural Profiles for SC-101 and SCGOF2
Concentrations in moles of functional groups/100 g of sample

Group #	Group name	Structure	Concentration	
			SCGOF2	SC-101
19	Chain methylene		0.975	1.150
21	Aliphatic methyne		0.957	1.324
22	Gamma methyl		0.534	0.591
23	Naphthenic methyl		0.250	0.408
24	Naphthenic methylene		0.503	0.702
13	Alpha methylene		0.410	0.482
14	Alpha methyl		0.286	0.239
15	Alpha methyne		-	-
16	Beta methyl		0.155	0.089
11	Hydroaromatic ring		0.048	0.028
1	Benzene		0.082	0.188
2	Naphthalene		-	-
3	Phenanthrene		0.024	0.018
5	Benzothiophene		0.018	0.006
6	Dibenzothiophene		0.067	0.016
33	Aliphatic thioether		0.050	0.016
50	Aliphatic ether		0.007	0.013
7	Dibenzofuran		0.052	0.026
9	Carbazole		0.011	0.011
35	Aliphatic amine		0.002	0.001
36	Aniline		0.010	0.003
43	Phenol		0.005	0.002
40	Aromatic carbonyl		0.018	0.010
30	Aromatic olefin		0.006	-
31	Terminal olefin		0.011	-

9. Conclusions and Recommendations

9.1 Conclusions

The following conclusions were made from this study:

1. The uncertainty in ^{13}C -NMR data was due to the overlap in the band assignments and to the intensities of signals which were not quite proportional to the amount of carbon. Adjustment of the relaxation reagent or the pulse sequence would possibly reduce the error due to lack of proportionality; however, for gas oils such corrections would be difficult to verify. These limitations were recognized and ^{13}C -NMR data were used to formulate an objective function.
2. Wolfe's algorithm for quadratic programming was used in the optimization procedure. This provided a direct check for the uniqueness of the solution.
3. The choice of heteroatom groups was limited due to the lack of analytical data. Quantitative analysis of the IR spectra provided information which were used as additional constraints.
4. The contributions of ^{13}C bands to the objective function were weighted. By assigning greater weights for bands containing relatively small amounts of carbon, the predicted concentrations of carbon in such bands approximated the expected values.
5. Application of FGA to mixtures of known group concentrations indicated that the predicted concentrations of hydrocarbon functional groups such as

gamma methyl, beta methyl, hydroaromatic ring, naphthenic methylene, total alkyl substituents, and mono + diaromatics were fairly accurate with an estimated error of $\pm 15\%$. The concentrations of chain methylene, methyne, and naphthenic methyl were less accurate with an estimated error of $\pm 40\%$.

6. Distinction between mono and diaromatics and alkyl substituents was not possible on the basis of NMR data.
7. FGA provided an estimate for the distribution of sulphur in thiophenoaromatics and aliphatic structures.
8. Class separation by column chromatography provided fractions enriched in selected functional groups. Nitrogen and oxygen groups such as anilines, phenols, and carbonyls were concentrated in the Polar III fraction while sulphur groups were present in considerable amounts in all class fractions. The separation procedure facilitated the choice of appropriate heteroatom groups representing the most likely structures for individual fractions. In the whole oil analysis, the choice of heteroatoms was limited.
9. Gas oils with low initial boiling points, were treated prior to the class separation scheme to remove naphtha and low-boiling materials which could be analyzed by other methods such as gas chromatography. Otherwise such materials would be lost in the separation procedure during solvent extraction.
10. Structural profiles of gas oils from different crude oil

sources and produced by different processes indicated that samples with similar physical properties exhibited appreciable differences in chemical composition.

11. Heteroaromatic structures appeared in a wide boiling range, but they were most abundant in the 560-620°C cut.
12. Structural profiles of hydroprocessed SCGO indicated significant differences in the functional group concentrations from the original feedstock. The changes could be explained by a number of reactions that occur during hydrotreatment. FGA could be judged as a promising tool to examine chemical changes due to processing of feedstocks.

9.2 Recommendations

The following recommendations should be considered for future work.

1. Asphaltenes can be ignored in the characterization of oil samples when they are present in very small amounts. However, appropriate NMR methods should developed for asphaltenes so they could be included in the analysis when they are present in significant amounts (in excess of 5 % by weight).
2. The method of ^{13}C -NMR analysis should be improved to obtain more reliable peak intensities. One alternative would be to use longer pulse delays.
3. The distribution of sulphur in benzothiophene, dibenzothiophene, and aliphatic thioether should be examined by using FGA to characterize synthetic mixtures

containing such groups. Other chemical methods which distinguish between different sulphur types should also be considered.

4. Data from Mass Spectroscopy on fused aromatics and heteroaromatic structures could be included in FGA. This would involve the development of a method to assign and relate the concentration of peaks to specific structures. If such concentration data are accurate, they could be introduced as additional constraints. Otherwise, the mathematical formulation of FGA should be modified to include Mass Spectroscopy data as part of the objective function.
5. Nitrogen was abundant in the Polar III fraction (0.5 to 2.2 % by weight). Analytical data from potentiometric titration would provide more accurate estimates for the concentration of basic nitrogen groups such as carbazole, aniline, and quinoline.
6. FGA should be applied to a number of gas oil samples from similar sources to further examine the analysis for accuracy and reproducibility.

List of References

Chung, S.Y.K., M. Sc. Thesis: "Thermal hydroprocessing of heavy gas oils", Department of Chemical Engineering, University of Alberta, 1982.

Beuther, H., and Schmid, B.K., Proceedings of the Sixth World Petroleum Congress, Vol. III, 297, 1963.

Metzger, K.J., Christman, R.D., and Marmo, J.F., API Proc., Div. Refining, 51, 72, 1971.

Schuit, G.C.A., and Gates, B.C., AICHE J., 19, 47, 1973.

Brown, J.K., and Ladner, W.R., Fuel, 39, 87, 1960.

Oka, M., Chang, H., and Gavalas, G.R., Fuel, 56, 3, 1977.

Allen, D.T., Ph. D. Thesis: "Modelling the reactions of coal liquids", California Institute of Technology, 1983.

Petrakis, L., Allen, D.T., Gavalas, G.R., and Gates, B.C., Anal. Chem., 55, 1557, 1983.

Allen, D.T., Grandy, D.W., Jeong, K.M., and Petrakis, L., I&EC Proc. Des. Dev., 24(3), 737, 1985.

Le, T.T., M. Sc. Thesis: "Structural characterization and

property estimation of complex liquid mixtures", University of California, Los Angeles, 1985.

Allen, D.T., Gray, M.R., and Le, T.T., Liq. Fuels Tech., 2(3), 327, 1984.-

Payzant, J.D., Rubenstein, I., Hogg, A.M., and Strausz, O.P., Chem. Geol., 29, 73, 1980.

Strausz, O.P., Rubenstein, I., Hogg, A.M., and Payzant, J.D., in "Atomic and nuclear methods in fossil energy research", Ed. Filby, R.H., et al., pp 401-431, Plenum, 1982.

Selucky, M.L., Chu, Y., Ruo, T.C.S., and Strausz, O.P., Fuel, 57, 9, 1978.

Payzant, J.D., Montgomery, D.S., and Strausz, O.P., Tetr. Lett., 24(7), 651, 1983.

Strausz, O.P., Journal of the Japan Petroleum Institute, 27(2), 89, 1984.

Bunger, J.W., Thomas, K.P., and Dorrence, S.M., Fuel, 57, 9, 1979.

Selucky, M.L., Ph. D. Thesis: "Chemical composition of

Athabasca bitumen", Department of Chemistry, University of Alberta, 1976.

Selucky, M.L., Chu, Y., Ruo, T.C.S., and Strausz, O.P., Fuel, 56, 369, 1977.

Chamberlain, N.F., "The practice of NMR spectroscopy", Plenum, New York, 1974.

Snape, C.E., Ladner, W.R., and Bartle, K.D., Anal. Chem., 51(13), 2189, 1979.

Abraham, R.J. and Loftus, P., "Proton and ^{13}C NMR spectroscopy: An integrated approach", Heyden & Son Ltd., London, 1978.

Bunger, J.W., "Characterization of Utah tar sand bitumen", in ACS symp. series #151, Ed. Yen, T.F., pp 121-136, 1976.

Allen, D.T., Petrakis, L., Grandy, D.W., Gavalas, G.R., and Gates, B.C., Fuel, 63, 803, 1984.

Wolfe, P., Econometrica, 27(3), 382, 1959..

Kunzi, P.K., Tzaschach, H.G., and Zehnder, C.A., "Numerical methods of mathematical optimization", Academic Press, 1968.

Luus, R., and Jaakkola, T.H.I., AICHE J., 19(4), 760, 1973.

Dantzig, G.B., "Linear programming and extensions", Princeton U. Press, Princeton, 1963.

Marquardt, D.M., J. Soc. Indust. Appl. Maths., 11(2), 431, 1963.

Wehrli, F.W., and Wirthlin, T., "Interpretation of carbon-13 NMR spectra", Heyden & Son Ltd., London, 1976.

Levy, G.C., Licher, R.L., and Nelson, G.L., "Carbon-13 Nuclear Magnetic Resonance Spectroscopy", P. 52, 2nd ed., John Wiley & Sons, New York, 1980.

Levy, G.C., Licher, R.L., and Nelson, G.L., ibid., P. 78.

Ejcharh, A., and Kozerski, L., "Spektrometria Magnetycznego Resonansu Jadrowego ^{13}C ", Państwowe Wydawnictwo Naukowe, Warsaw, 1981.

Man, G.P., M. Sc. Thesis: "Hydroprocessing of heavy gas oil in a continuous stirred tank reactor", Department of Chemical Engineering, University of Alberta, 1981.

McKay, J.F., Cogswell, T.E., Weber, J.H., and Latham, D.R., Fuel, 54, 50, 1975.

Smith, J.M., "Chemical Engineering Kinetics", 2nd Ed., McGraw-Hill Kogakusha, Tokyo, 1970.

Rangwala, H.A., Dalla Lana, I.G., Otto, F.D., and Wanke, S.E., "Catalysis on the Energy Scene", Kaliaguine, S., and Mahay, A., Editors, pp 537-544, Elsevier Science Publishers B.V., Amsterdam, 1984.

Wu, W.L., and Haynes Jr., H.W., ACS Symposium Series #20, Ed. Ward, J.W., and Qader, S.A., 1975.

Nag, N.K., Sapre, A.V., Broderick, D.H., and Gates, B.C., Catalysis, 57, 509, 1979.

Katti, S.S., Westerman, D.W.B., Gates, B.C., Youngless, T., and Petrakis, L., Ind. Eng. Chem. Process Des. Dev. 23(4), 773, 1984.

Sullivan, R.F., and Meyer, J.A., ACS Symposium Series #20, Ed. Ward, J.W., and Qader, S.A., 1975.

Furimsky, E., Fuel, 57, 494, 1978.

Aarts, J.J.B., Ternan, M., and Parsons, B.I., Fuel, 57, 473, 1978.

Forsythe, G.E., and Moller, C.B., "Computer solution of

linear algebraic systems", Prentice-Hall, Englewood Cliffs,
NJ, 1967.

Appendix A : Modifications to the Quadratic Programming Algorithm

A.1. Description of the Algorithm

In applying Wolfe's algorithm for quadratic programming, some modifications were necessary to ensure that the optimum solution was obtained. Details of the algorithm is given elsewhere (Wolfe, 1959). A brief discussion is presented here.

Consider a system of n variables and m linear constraints. For simplicity, the constraints are taken to be equalities, however, inequality constraints can be handled by introducing appropriate slack variables. Rewriting equation (1) in matrix notation:

$$\mathbf{A} \underline{\mathbf{x}} = \mathbf{b} \quad (6)$$

\mathbf{A} : mxn matrix of coefficients for constraints

$\underline{\mathbf{x}}$: $nx1$ vector for unknown group concentrations

\mathbf{b} : $mx1$ vector of analytical data

For simplicity, consider the objective function given by equation (4) :

$$F = \sum_{k=1}^{13} \{ C13_k - \sum_{j=1}^n C0_{kj} \underline{x}_j \}^2 \quad (4)$$

The above objective function can be expressed in terms of $\underline{\mathbf{x}}$ given by equation (7) .:

$$F(\mu, \underline{\mathbf{x}}) = \mu \mathbf{P} \underline{\mathbf{x}} + (\underline{\mathbf{x}}^T \mathbf{C} \underline{\mathbf{x}})/2 \quad (7)$$

where \mathbf{C} is an nxn symmetric positive semidefinite matrix defining the quadratic part of the objective function. \mathbf{P} is a $1xn$ matrix and μ is a non-negative parameter which together define the linear part of the objective function.

For $\mu = 1.0$, the objective function can be expressed by equation (8) :

$$F = \sum_j P_j X_j + (\sum_i \sum_k X_i X_j C_{i,j})/2 \quad (8)$$

From equations (4) and (8) the coefficients for matrix C and P can be obtained for $\mu = 1.0$:

$$C_{i,j} = 2 \left\{ \sum_{k=1}^3 CO_{kj} CO_{ki} \right\} \quad (9)$$

$$P_j = -2 \left\{ \sum_{k=1}^3 C13_k CO_{kj} \right\} \quad (10)$$

Wolfe showed that by introducing variables \underline{v} and \underline{u} where \underline{v} is $n \times 1$ and \underline{u} is $1 \times m$, the solution to the following system of equations is the solution to the optimization problem :

$$\underline{v} \underline{x} = \underline{0}$$

$$C \underline{x} - \underline{v} + A^T \underline{u} + P^t = \underline{0} \quad (11)$$

The algorithm then proceeds by introducing artificial variables \underline{z}^1 , \underline{z}^2 , and \underline{w} and uses the simplex method to obtain the solution. The initial tableau for the algorithm is :

$$A \underline{x} + \underline{w} = \underline{b}$$

$$C \underline{x} - \underline{v} + A^T \underline{u} + \underline{z}^1 - \underline{z}^2 + P^t = \underline{0} \quad (12)$$

where \underline{z}^1 , \underline{z}^2 , and \underline{w} are n , n , and m component vectors respectively.

Wolfe's algorithm consists of three phases. In phase I, the linear form $\sum_{i=1}^m w_i$ is minimized to give an initial feasible solution. The initial tableau for phase I is a $(m+n)$ by $(4n+2m+1)$ matrix with the standard coefficients of Wolfe's algorithm in which \underline{z}^1 and \underline{w} constitute the initial basis. The columns of the initial tableau consist of

X, Z', Z², W, V, U, and μ respectively. The algorithm then proceeds by choosing a non-basic variable to replace a basic variable in the basis by applying the standard selection rules of simplex method with the condition that no U, V, and μ are allowed to enter the basis. Phase I terminates after a finite number of basis changes when all artificial variables W are non-basic, hence, the linear form $\sum_{i=1}^m w_i$ is minimized to zero.

In phase II, W, and non-basic Z' and Z² variables are dropped and the linear form $\sum_{k=1}^n z_{*k}$ is minimized where Z* constitute the n basic Z' and Z² variables from phase I. At the end of phase II, all Z*, become non-basic. The conditions for phase II are that μ is not allowed to enter the basis and that corresponding X, and V, cannot be in the basis simultaneously. The solution at the end of phase II minimizes the objective function, F, with $\mu = 0$.

In phase III, μ is maximized to obtain the solution for a specified positive μ^* , where :

$$\mu^j < \mu^* < \mu^{j+1} \quad (13)$$

and the solution X* is a linear combination of solutions X^j and X^{j+1}, where j is the step counter for the progress of the algorithm. The value of μ^* is chosen to be 1.0 based on the objective function specified by equation (8).

A.2. Modifications to the Algorithm

Considering the conditions for phase II, that corresponding X, and V, cannot be in the basis simultaneously and that μ remains non-basic, then at the end

of phase II, all of the m U_i as well as n non-corresponding X_i and V_i are basic. Consider that at some stage during phase II, there are a total of n non-corresponding X_i and V_i in the basis. At such a point no X_i or V_i outside the basis can qualify to become basic. Now suppose that at this point, there still remains some Z^* , in the basis. The simplex method rule for selecting a non-basis variable to enter the basis is to choose the variable with the least negative d_j , (d_j is the sum of the column entries in the tableau, see Dantzig, 1963). At this point since no X_i and V_i can enter the basis, only the non-basis U_i can become basic. But if at this point, none of the non-basis U_i have corresponding negative d_j , termination occurs since no variables can enter the basis.

At such a termination point, there are equal number of Z^* , in the basis as there are non-basic U_i . The approach taken was to remove Z^* , variables from the basis one by one and replace them by an appropriate U_i .

One additional modification was necessary. Consider the case where the total number of basic X_i and V_i is less than n at a "would-be termination point". At this point, the total number of basic Z^* , is greater than the number of non-basic U_i . If all the non-basis U_i are made basic in the expense of basic Z^* , there would still remain some Z^* , in the basis. The number of basic Z^* , after all U_i are made basic is equal to the difference between n and the total number of basic X_i and V_i . The approach taken for such a

case was to replace basic z^* , by appropriate non-basic U_i , as well as non-basic X_i and V_i .

The above approaches ensure the completion of phase II, but they may result in some sign restrictions to be violated. However, the violations are corrected in phase III when the optimum solution is obtained.

A.3. Correction of Sign Violations

In Wolfe's algorithm, z^* , V , and X are non-negative vectors. The sign restriction on these variables may be violated by applying the strategies mentioned above. Sign violations for z^* , are corrected when the solution for phase II is obtained since at the end of phase II all z^* , are non-basic and hence equal to zero. However, some basic X_i and V_i may be negative at the end of phase II.

Phase III of Wolfe's algorithm is initiated by dropping all z^* , and proceeding to obtain the solution for $\mu=1.0$. The same conditions as those for phase II are applied with the exception that μ is allowed to enter the basis and hence be maximized. If phase III, begins by allowing μ to enter the basis, as in normal procedure, μ may take a negative value, even though it is a non-negative parameter. Another uncharacteristic behavior is that μ may decrease after a change of basis. These effects are thought to be caused by the fact that some basic X_i and V_i are negative. The approach taken was to correct all sign violations (by interchange of negative basic X_i and V_i with appropriate non-basic variables) before μ is allowed to enter the basis.

Hence, μ remains zero (i.e. non-basic) so long as there are sign violations in the basis. Then μ is allowed to enter the basis and be maximized by applying the normal procedure of Wolfe's algorithm until the solution is obtained for $\mu=1.0$.

Appendix B : Program Listing and Documentation

Two computer programs written in FORTRAN were used in FGA. One of the programs, START, is a short, interactive program for data entry via the terminal keyboard. The other program, OPTIMA, performs the computations involved in FGA. Three optimization algorithms are used by the program. These are:

1. Wolfe's algorithm for quadratic programming
2. Direct search method of Luus and Jaackola
3. Marquardt least square parameter estimation algorithm

Description of the programs and related subroutines together with the program listings are presented here.

```

C
C     Program START
C
C     This program is an interactive program which allows
C     data entry via the terminal keyboard. The program
C     writes all the information supplied by the user in
C     to a file for subsequent use by the main program.
C
C     Description of Variables
C
C     EA      : array containing the elemental analyses data
C     HNMR   : array containing H-NMR data
C     CNMR   : array containing C13-NMR data
C     N       : number of groups representing a sample
C     KNC    : array containing the group numbers
C     M2     : Number of inequality constraints ( < or = )
C     NR     : Number of groups with known concentration from
C             other analysis such as IR
C     KRC    : array containing group numbers for functional
C             groups with known concentration
C     CONC   : array containing the concentration of groups
C             with known concentration
C     WF     : array containing the weighting factors for
C             each band of C13-NMR spectra
C     COMOP  : flag for option of combining band 5 and 6 in
C             C13-NMR spectra
C     IRPC   : indicator when ratio of phenol to carbonyl
C             is known from IR analysis
C     RAPC   : ratio of phenol to carbonyl obtained from IR
C
C
REAL EA(5),HNMR(7),CNMR(12),CONC(50)
INTEGER KRC(50),KNC(50)
INTEGER WF(50),COMOP
INTEGER IRPC
REAL RAPC
C
C     WRITE(6,10)
10  FORMAT(/, 'HOW MANY GROUPS ARE PRESENT?', /)
READ(5,15) N
15  FORMAT(I6)
        WRITE(10,15) N
        WRITE(6,20)
20  FORMAT(/, 'ENTER GROUP NUMBERS.', /)
DO 30 J=1,N
        READ(5,15) KNC(J)
        WRITE(10,15) KNC(J)
30  CONTINUE
        WRITE(6,40)
40  FORMAT(/, 'ENTER THE NUMBER OF INEQUALITIES', /)
        READ(5,15) M2
        WRITE(10,15) M2
        WRITE(6,50)
50  FORMAT(/, 'ENTER NUMBER OF GROUPS ANALYZED BY IR.', /)

```

```

READ(5,15) NR
WRITE(10,15) NR
IF(NR .EQ. 0) GOTO 70
WRITE(6,55)
55 FORMAT(/, 'ENTER THE GROUP NUMBER FOR IR GROUPS.', /)
DO 56 J=1,NR
READ(5,15) KRC(J)
WRITE(10,15) KRC(J)
56 CONTINUE
WRITE(6,58)
58 FORMAT(/, 'ENTER CONCENTRATIONS OF THESE GROUPS', /)
DO 60 J=1,NR
READ(5,65) CONC(J)
WRITE(10,65) CONC(J)
65 FORMAT(F10.3)
60 CONTINUE
70 WRITE(6,75)
75 FORMAT(/, 'ENTER WT. % OF ELEMENTS IN THIS ORDER:')
WRITE(6,76)
76 FORMAT('C,H,O,N,S', /)
DO 80 I=1,5
READ(5,85) EA(I)
WRITE(10,85) EA(I)
85 FORMAT(F6.2)
80 CONTINUE
WRITE(6,90)
90 FORMAT(/, 'ENTER H-NMR DATA AS % H IN EACH BAND', /)
DO 95 I=1,7
READ(5,100) HNMR(I)
WRITE(10,100) HNMR(I)
100 FORMAT(F6.2)
95 CONTINUE
WRITE(6,110)
110 FORMAT(/, 'ENTER C13-NMR DATA AS % C IN EACH BAND', /)
DO 120 I=1,13
READ(5,125) CNMR(I)
WRITE(10,125) CNMR(I)
125 FORMAT(F6.2)
120 CONTINUE
WRITE(6,130)
130 FORMAT(/, 'ENTER WEIGHTING FACTOR FOR C13-NMR BANDS', /)
DO 140 I=1,13
READ(5,15) WF(I)
WRITE(10,15) WF(I)
140 CONTINUE
WRITE(6,150)
150 FORMAT(/, 'ENTER 1 TO COMBINE BAND 5 AND 6, OR ELSE 0', /)
READ(5,15) COMOP
WRITE(10,15) COMOP
WRITE(6,200)
200 FORMAT(/, 'ENTER 1 IF PHENOL/CARBONYL RATIO IS KNOWN')
WRITE(6,210)
210 FORMAT('ENTER 0 OTHERWISE')
READ(5,15) IRPC

```

```
      WRITE(10,15) IRPC
      IF(IRPC .EQ. 0) GOTO 250
      WRITE(6,220)
220   FORMAT(/, 'ENTER RATIO OF PHENOL TO CARBONYL')
      READ(5,230) RAPC
      WRITE(10,230) RAPC
230   FORMAT(F10.3)
250   CONTINUE
      STOP
      END
```

B.1. Program OPTIMA

OPTIMA addresses the task of setting up matrices of constraints and the objective function using the information supplied by the user for subsequent use by the optimization algorithms. The tasks of this program are:

1. to obtain information supplied by the user and the constraint coefficients for each group, as presented in chapter 4, to set up the constraint matrix. The constraint coefficients are read from a file referred to as unit 9.
2. to set up the right hand side vector of the constraint matrix using elemental analyses and $^1\text{H-NMR}$ data as well as the molecular weight of each element.
3. to introduce appropriate slack variables when inequality constraints are present.
4. to set up equality constraints for groups whose concentrations are known from other analysis, e.g. IR analysis.
5. to discard unnecessary information, i.e. delete rows with no entries in the constraint matrix.
6. to introduce secondary inequality constraints to ensure that the solution is physically reasonable, and equality constraint if the ratio of phenols to carbonyls is known.
7. to rearrange the columns of the constraint matrix so that no singularity is observed in the dependent variables sub-matrix. This singularity check is a

requirement if the direct search method is to be implemented. In the direct search algorithm, the independent variables are determined at random at each iteration and then the dependent variables are solved using Gaussian elimination which requires that the diagonal elements of the dependent variables sub-matrix be non-zero. Hence, the columns and rows of the constraint matrix must be rearranged to ensure the above criteria. The columnwise rearrangement involves including a variable corresponding to each constraint in the dependent variables sub-matrix. Systematically, slack variables corresponding to inequality constraints (i.e. single element columns), and one variable for each of the remaining constraints make up the dependent variables sub-matrix. Rearrangement of the rows is performed by subroutine AROW.

8. to obtain the objective function coefficients as presented in chapter 4 and set up the objective function matrix. The objective function coefficients are obtained from a file referred to as unit 8.
9. to delete rows with no entries in the objective function matrix (i.e. exclude bands with no signals), incorporate weighting factors in the objective function, and combine information for bands 5 and 6 if so specified by the user.
10. to call subroutine MAINP which performs the optimization procedure.

```

C
C Program OPTIMA
C
C Description of Variables
C
C HNMR : array containing H-NMR data
C CNMR : array containing C13-NMR data
C EA : array containing elemental analyses data
C A,AA : constraint matrix coefficients
C AT : transpose of A
C CO,CCO: objective function matrix coefficients
C CT : transpose of CO
C RHS : array containing total concentration for each
C       constraint ( right hand side of equations)
C C13 : array containing the total concentration of
C       carbon in each band of C13-NMR spectra
C NR : number of groups with known concentrations
C KRC : array containing the group number for groups
C       with known concentration
C CONC : array containing the concentration of groups
C       with known concentrations
C N : number of selected groups for a sample
C KNC : array containing the group numbers
C NG : total number of available functional groups
C M2 : number of inequality constraints
C M1 : number of equality constraints
C MM : total number of constraints
C NCB : number of C13-NMR bands detected in the spectra
C WF : array containing the weighting factors for
C       each band in the C13-NMR spectra
C COMOP : flag for option of combining band 5 and 6 in
C       C13-NMR spectra
C IRPC : indicator when ratio of phenol to carbonyl is
C       known from IR analysis
C RAPC : ratio of phenol to carbonyl obtained from IR
C RMS,RMC,RMO,RMH,RMN : atomic weight of S, C, O, H, N
C KRC2,RNEW,SAVE,COUNT,CNT : intermediate arrays for
C       storing information
C
C
REAL AT(120,120),CT(120,120),HNMR(7),CNMR(13),CONC(120)
REAL AA(120,120),A(120,120),CO(120,120),CCO(120,120)
REAL SAVE(120),C13(13)
REAL RHS(120),EA(5)
INTEGER ANC(120),KRC(120),KRC2(120),COUNT(120),CNT(120)
REAL RNEW(120)
INTEGER WF(13)
INTEGER COMOP
INTEGER IRPC
REAL RAPC
C
C
NG=50
DO 1 J=1,NG
  READ(9,2) (AT(J,I),I=1,13)
 2 FORMAT(13F6.1)

```

```

1   CONTINUE
DO 3 I=1,13
DO 3 J=1,NG
AA(I,J)=AT(J,I)
3   CONTINUE
READ(10,7) N
7   FORMAT(I6)
DO 10 J=1,N
READ(10,7) KNC(J)
10  CONTINUE
READ(10,7) M2
READ(10,7) NR
IF(NR .EQ. 0) GOTO 15
DO 11 J=1, NR
READ(10,7) KRC(J)
11  CONTINUE
DO 12 J=1, NR
READ(10,13) CONC(J)
13  FORMAT(F10.3)
12  CONTINUE
15  DO 18 I=1,5
READ(10,16) EA(I)
16  FORMAT(F6.2)
18  CONTINUE
DO 19 I=1,7
READ(10,16) HNMR(I)
19  CONTINUE
DO 20 I=1,13
READ(10,16) CNMR(I)
20  CONTINUE
DO 17 I=1,13
READ(10,7) WF(I)
17  CONTINUE
DO 21 I=1,13
RHS(I)=0.0
21  CONTINUE
READ(T0,7) COMOP
READ (10,7) IRPC
IF(IRPC .EQ. 0) GOTO 25
READ(10,24) RAPC
24  FORMAT(F10.3)
25  CONTINUE

```

C
C ALL THE REQUIRED DATA HAVE BEEN OBTAINED TO SET UP
C THE CONSTRAINT MATRIX A

RMH=1.0079
RMC=12.01115
RMO=15.9994
RMN=14.0067
RMS=32.064
RHS(1)=EA(1)/RMC
RHS(2)=(EA(2)/RMH)*(HNMR(5)/100.)
RHS(3)=(EA(2)/RMH)*(HNMR(6)/100.)

```

RHS(4)=(EA(2)/RMH)*(HNMR(7)/100.)
RHS(5)=(EA(2)/RMH)*(HNMR(1)/100.)
RHS(6)=(EA(2)/RMH)*(HNMR(2)/100.)
RHS(7)=(EA(2)/RMH)*(HNMR(3)/100.)
RHS(10)=(EA(2)/RMH)*(HNMR(4)/100.)
RHS(11)=EA(3)/RMO
RHS(12)=EA(5)/RMS
RHS(13)=EA(4)/RMN

```

C
 DO 29 J=1,N
 DO 27 I=1,13
 A(I,J)=AA(I,KNC(J))
 27 CONTINUE
 29 CONTINUE

C
 C INTRODUCE SLACK VARIABLES FOR INEQUALITY CONSTRAINTS
 C

```

N1=N+1
IF(M2.EQ.0) GOTO 50
NN=N+M2
N1=N+1
DO 30 J=N1,NN
DO 35 I=1,13
A(I,J)=0.0
35 CONTINUE
30 CONTINUE
IF(M2.EQ.2) GOTO 40
IF(M2.EQ.3) GOTO 45
A(2,N+1)=1.0
A(6,N+2)=1.0
A(7,N+3)=1.0
A(8,N+4)=1.0
A(9,N+5)=1.0
RHS(8)=RHS(2)
RHS(9)=RHS(6)+RHS(7)
GOTO 50
40 A(2,N+1)=1.0
A(8,N+2)=1.0
RHS(8)=RHS(2)
GOTO 50
45 A(6,N+1)=1.0
A(7,N+2)=1.0
A(9,N+3)=1.0
RHS(9)=RHS(7)+RHS(6)

```

C
 C SET UP EQUATIONS FOR GROUPS WITH KNOWN CONCENTRATIONS
 C

```

50 MM=13
NN=N+M2
IF(NR.EQ.0) GOTO 100
DO 80 J=1,NR
DO 55 K=1,NG
IF(KRC(J).NE.K) GOTO 55
MM=MM+1

```

```

RHS(MM)=CONC(J)
DO 60 JJ=1,NN
A(MM,JJ)=0*0
IF(JJ .GT. N) GOTO 60
IF(KNC(JJ) .EQ. KRC(J)) A(MM,JJ)=1.0
IF(KNC(JJ) .EQ. KRC(J)) KC=JJ
60 CONTINUE
MM2=MM-1
DO 65 I=1,MM2
IF(A(I,KC) .EQ. 0.0) GOTO 65
RHS(I)=RHS(I)-RHS(MM)*A(I,KC)
A(I,KC)=0.0
65 CONTINUE
55 CONTINUE
KRC2(J)=KRC(J)
KRC(J)=0
80 CONTINUE
C
C SPECIAL CASE FOR PHENOLIC AND ALCOHOLIC HYDROGEN IF
C THE CONCENTRATION OF THEIR GROUPS ARE KNOWN FROM IR.
C
DO 90 J=1,NR
IF(KRC(J) .EQ. 43) GOTO 91
IF(KRC(J) .EQ. 44) GOTO 95
IF(KRC(J) .EQ. 45) GOTO 95
GOTO 90
91 RHS(2)=RHS(2)-CONC(J)
GOTO 90
95 RHS(6)=RHS(6)-(0.5*CONC(J))
RHS(7)=RHS(7)-(0.5*CONC(J))
90 CONTINUE
C
C AT THIS STAGE WE HAVE ADDED APPROPRIATE SLACK
C VARIABLES AND ADJUSTED THE COEFFICIENT MATRIX A WHEN
C GROUPS WITH KNOWN CONCENTRATION FROM IR ARE PRESENT
C (I.E. EXTRA CONSTRAINTS)
C
C DELETE ROWS WITH NO ELEMENTS
C
100 DO 105 I=1,MM
COUNT(I)=0
DO 110 J=1,NN
IF(A(I,J) .LE. 0.0) GOTO 110
COUNT(I)=COUNT(I)+1
110 CONTINUE
105 CONTINUE
DO 125 I=1,MM
IF(COUNT(I) .GT. 0) GOTO 125
COUNT(I)=0
DO 115 J=1,NN
IF(A(I,J) .EQ. 0.0) GOTO 115
COUNT(I)=COUNT(I)+1

```

```

115 CONTINUE
IF(COUNT(I) .EQ. 0) GOTO 125
WRITE(6,120)
120 FORMAT(/, 'WARNING: ROW WITH -IVE COEFFICIENTS ONLY', /)
STOP
125 CONTINUE
MKT=13
145 MT=MKT
DO 150 I=1,MT
CNT(I)=0
DO 131 J=1,NN
IF(A(I,J) .NE. 0.0) CNT(I)=CNT(I)+1
131 CONTINUE
IF(CNT(I) .GT. 0) GOTO 150
I2=1
MM3=MM-1
DO 130 K=I2,MM3
DO 135 J=1,NN
A(K,J)=A(K+1,J)
135 CONTINUE
RHS(K)=RHS(K+1)
130 CONTINUE
MM=MM-1
MKT=MT-1
GOTO 145
150 CONTINUE
C
C     INTRODUCE SECONDARY EQUALITY AND
C     INEQUALITY CONSTRAINTS
C
C     FOR AROMATIC SITES
C
M21=M2
IAR=0
DO 500 J=1,N
IF(KNC(J) .EQ. 1) IAR=1
500 CONTINUE
IF(IAR .EQ. 0) GOTO 531
IF(M2 .EQ. 2) GOTO 531
IF(M2 .EQ. 5) GOTO 531
MM=MM+1
M2=M2+1
DO 505 J=1,N,
A(MM,J)=AA(2,KNC(J))*(-1.0)
IF(AA(2,KNC(J)) .EQ. 0.0) A(MM,J)=0.0
505 CONTINUE
DO 506 I2=1,M2
A(MM,N+I2)=0.0
506 CONTINUE
A(MM,N+M2)=1.0
DO 510 I=1,MM
IF(I .EQ. MM) GOTO 510
A(I,N+M2)=0.0
510 CONTINUE

```

C
 C FOR CHAIN TERMINATING GROUPS
 C
 531 I22=0
 DO 532 J=1,N
 IF(KNC(J) .EQ. 22) I22=1
 532 CONTINUE
 IF(I22 .EQ. 0) GOTO 541
 MM=MM+1
 M2=M2+1
 DO 535 J=1,N
 A(MM,J)=0.0
 IF(KNC(J) .EQ. 22) A(MM,J)=1.0
 IF(KNC(J) .EQ. 19) A(MM,J)=-1.0
 IF(KNC(J) .EQ. 17) A(MM,J)=-1.0
 IF(KNC(J) .EQ. 21) A(MM,J)=-2.0
 IF(KNC(J) .EQ. 46) A(MM,J)=-2.0
 IF(KNC(J) .EQ. 39) A(MM,J)=1.0
 IF(KNC(J) .EQ. 35) A(MM,J)=1.0
 IF(KNC(J) .EQ. 45) A(MM,J)=1.0
 IF(KNC(J) .EQ. 32) A(MM,J)=-1.0
 535 CONTINUE
 RHS(MM)=0.0
 DO 536 I2=1,M2
 A(MM,N+I2)=0.0
 536 CONTINUE
 A(MM,N+M2)=1.0
 DO 540 I=1,MM
 IF(I .EQ. MM) GOTO 540
 A(I,N+M2)=0.0
 540 CONTINUE
 C
 C EQUALITY CONSTRAINT WHEN RATIO OF PHENOL TO CARBONYL
 C IS KNOWN
 C
 541 IF(IRPC .EQ. 0) GOTO 580
 MM=MM+1
 RHS(MM)=0.0
 DO 560 J=1,N
 A(MM,J)=0.0
 IF(KNC(J) .EQ. 40) A(MM,J)=RAPC
 IF(KNC(J) .EQ. 43) A(MM,J)=-1.0
 560 CONTINUE
 DO 565 I2=1,M2
 A(MM,N+I2)=0.0
 565 CONTINUE
 NR=NR+1
 KRC2(NR)=43
 580 NN=N+M2
 DO 582 I=1,MM
 IF(RHS(I) .EQ. 0.0) RHS(I)=ABS(RHS(I))
 582 CONTINUE
 NT=N

C
C
C START REARRANGING THE COLUMNS.
C SLACK VARIABLES ARE ALREADY IN PLACE.
C FIRST CONSIDER GROUPS WITH KNOWN CONCENTRATION,
C
C

```
IF(NR .EQ. 0) GOTO 172
DO 170 J=1,NR
DO 155 K=1,NG
IF(KRC2(J) .NE. K) GOTO 155
DO 160 JJ=1,N
IF(KNC(JJ) .EQ. KRC2(J)) KC=JJ
160 CONTINUE
DO 165 I=1,MM
SAVE(I)=A(I,NT)
A(I,NT)=A(I,KC)
A(I,KC)=SAVE(I)
165 CONTINUE
TEMP=KNC(NT)
KNC(NT)=KNC(KC)
KNC(KC)=TEMP
KRC2(J)=0
NT=NT-1
155 CONTINUE
170 CONTINUE
```

C
C
C M2 SLACK VARIABLES AND NR IR-DETERMINED GROUPS ARE
C IN THEIR PROPER LOCATION IN THE MATRIX. THE REMAINING
C (MM-NR-M2) SHOULD BE PLACED IN THE APPROPRIATE
C COLUMNS IN THE DEPENDENT MATRIX.
C
C

```
172 NT=N-NR
IC=0
MK=MM-NR-(M2-M21)
DO 220 I=1,13
IN=13-I+1
IF(COUNT(IN) .EQ. 0) GOTO 220
NS=0
IF(M2 .EQ. 0) GOTO 180
DO 175 J=N1,NN
IF(A(MK,J) .EQ. 1.0) NS=NS+1
175 CONTINUE
180 IF(NS .GT. 0) GOTO 210
CNT(MK)=0
DO 185 J=1,NT
IF(A(MK,J) .EQ. 0.0) GOTO 185
CNT(MK)=CNT(MK)+1
IF(A(1,J) .EQ. 0.0) IC=1
185 CONTINUE
DO 190 J=1,NT
IF(A(MK,J) .EQ. 0.0) GOTO 190
```

```

IF(IC .EQ. 0) GOTO 193
IF(A(1,J) .EQ. 0.0) KC=J
IF(A(1,J) .EQ. 0.0) GOTO 195
193 IF(A(MK,J) .GT. 0.0) KC=J
190 CONTINUE
195 DO 200 K=1,MM
    SAVE(K)=A(K,NT)
    A(K,NT)=A(K,KC)
    A(K,KC)=SAVE(K)
200 CONTINUE
    TEMP=KNC(NT)
    KNC(NT)=KNC(KC)
    KNC(KC)=TEMP
    NT=NT-1
210 MK=MK-1
220 CONTINUE
    MLAST=MM
    NLAST=N+M2
    DO 600 K=1,M2
    DO 605 I=1,MM
        IF(A(I,NLAST) .EQ. 0.0) GOTO 605
        JJ=I
        GOTO 606
605 CONTINUE
606 DO 610 J=1,NN
    SAVE(J)=A(JJ,J)
    A(JJ,J)=A(MLAST,J)
    A(MLAST,J)=SAVE(J)
610 CONTINUE
    TEMP=RHS(JJ)
    RHS(JJ)=RHS(MLAST)
    RHS(MLAST)=TEMP
    MLAST=MLAST-1
    NLAST=NLAST-1
600 CONTINUE
    DO 901 J=1,M2
    KNC(J+N)=100+J
901 CONTINUE
C
C      THE COLUMNWISE REARRANGEMENT OF THE CONSTRAINT
C      MATRIX IS COMPLETE
C
C      WRITE(6,905) (KNC(J),J=1,NN)
C905 FORMAT(20I6,/)
C      WRITE(6,904)
C904 FORMAT(/)
C      DO 1000 I=1,MM
C      WRITE(6,1005) (A(I,J),J=1,NN)
C1005 FORMAT(20F6.1)
C1000 CONTINUE
C      DO 1100 I=1,MM
C      WRITE(6,1200) RHS(I)
C1200 FORMAT(F10.3)
C1100 CONTINUE

```

C
C SET UP THE OBJECTIVE FUNCTION MATRIX
C

```
DO 250 J=1,NG
READ(8,255) (CT(J,I),I=1,13)
255 FORMAT(13F6.1)
250 CONTINUE
DO 260 I=1,13
DO 260 J=1,NG
CCO(I,J)=CT(J,I)
260 CONTINUE
DO 270 I=1,13
C13(I)=(EA(1)/RMC)*(CNMR(I)/100.)
270 CONTINUE
DO 280 J=1,N
DO 275 I=1,13
CO(I,J)=CCO(I,KNC(J))
275 CONTINUE
280 CONTINUE
```

C
C INTRODUCE WEIGHTING FACTORS
C

```
DO 281 I=1,13
DO 282 J=1,N
CO(I,J)=CO(I,J)*WF(I)
282 CONTINUE
C13(I)=C13(I)*WF(I)
281 CONTINUE
IF(COMOP.EQ.0) GOTO 289
```

C
C OPTION TO COMBINE BAND 5 AND 6 IN THE C13-NMR SPECTRA
C

```
DO 271 J=1,N
RNEW(J)=0.0
DO 272 I=5,6
RNEW(J)=RNEW(J)+CO(I,J)
272 CONTINUE
271 CONTINUE
DO 273 I=5,6
DO 273 J=1,N
CO(I,J)=0.0
273 CONTINUE
DO 274 J=1,N
CO(5,J)=RNEW(J)
274 CONTINUE
C13(5)=C13(5)+C13(6)
289 NKCB=13
290 NCB=NKCB
DO 330 I=1,NCB
CNT(I)=0
DO 300 J=1,N
IF(CO(I,J).NE.0.0) CNT(I)=CNT(I)+1
300 CONTINUE
IF(CNT(I).GT.0) GOTO 330
```

```
I2=I  
I3=NCB-1  
DO 310 K=I2,I3  
DO 315 J=1,N  
CO(K,J)=CO(K+1,J)  
315 CONTINUE  
C13(K)=C13(K+1)  
310 CONTINUE  
NKCB=NCB-1  
GOTO 290  
330 CONTINUE  
C  
C THE OBJECTIVE FUNCTION MATRIX IS SET UP  
C  
C WRITE(6,400) (KNC(J),J=1,N)  
C400 FORMAT(20I6)  
C WRITE(6,401)  
C401 FORMAT(/)  
C DO 410 I=1,NCB  
C WRITE(6,415) (CO(I,J),J=1,N)  
C415 FORMAT(20F6.2)  
C410 CONTINUE  
C DO 420 I=1,NCB  
C WRITE(6,425) C13(I),  
C425 FORMAT(F10.3)  
C420 CONTINUE  
M1=MM-M2  
CALL MAINP(M1,M2,N,NCB,RHS,C13,CO,A,EA,KNC)  
STOP  
END
```

B.2. Subroutine MAINP

This subroutine addresses the task of calling other subroutines used in the optimization procedure. The algorithm for the direct search method is also included in this subroutine. In the optimization procedure, first an optimum solution is obtained from Wolfe's quadratic programming algorithm by calling subroutine QUAD. Detailed description of the algorithm is discussed by Wolfe (1959). A brief discussion and modifications to the algorithm is presented in Appendix A. The optimum solution from Wolfe's algorithm is tested by the direct search method. Detailed description of the algorithm is given by Luus and Jaackola (1973).

In applying the direct search method several subroutines are called. These are:

1. AROW

This subroutine rearranges the rows in the constraint matrix so that all the diagonal elements of the dependent variables sub-matrix are non-zero.

2. RANDU

This is a SSP library system subroutine which generates random numbers between 0.0 and 1.0. This allows the independent variables to be determined at random at each iteration.

3. DECOMP and SOLVE

These subroutines were obtained from Forsythe et al. (1967) and use Gaussian elimination to solve for the

dependent variables once the independent variables are determined at each iteration.

```
SUBROUTINE MAINP(M1,M2,N,NCB,RHS,C13,CO,A,EA,KNC)
```

C This subroutine performs the direct search
C optimization method and calls subroutines which
C perform other optimization algorithms.

C Description of variables

C M2 : number of inequality constraints of the
C form less than or equal to
C M3 : number of inequality constraints of the
C form greater than or equal to
C M1 : number of equality constraints
C N : number of functional groups
C MM : total number of constraints
C NIN : number of independent variables
C NCB : number of bands in the C13-NMR spectra
C R : random number generated by RANDU
C EP : size reduction factor for search region
C C : square matrix of the dependent variables
C CO : objective function matrix
C C13 : array containing the total concentration
C of carbon in each band
C EA : array containing the elemental analyses
C KNC : array containing the group numbers
C BOUND : array defining the bounds for independent
C variables in the direct search method
C GMAX : array containing concentrations yielding
C the minimum in the objective function
C MID : array defining the center of the feasible
C space in the direct search method
C RJ : Jacobian matrix of the objective function
C matrix
C FF,X : arrays containing the functional group
C concentrations
C FUN,SMINI,FUN2,RF : value of objective function
C A,AA,AO,AOO,AO2,AAO : arrays for the constraint
C matrix coefficients
C B,BB,BBB,BBO,B3,RHS : arrays containing the right
C hand side of constraints

```
REAL A(120,120),AA(120,120),AOO(120,120)
```

```
REAL AO(120,120),AO2(120,120),AAO(120,120)
```

```
REAL RHS(120),B(120),BB(120),BBB(120),BBO(120)
```

```
REAL CO(120,120);C13(120),CB(120),RJ(120,120)
```

```
REAL GMAX(120),FF(120),X(120),MID(120),BOUND(120)
```

```
REAL EA(5),B3(120),C(120,120)
```

```
INTEGER KNC(120),IPVT(120)
```

```
REAL WORK(120)
```

```
REAL COND,CONDPI
```

C

```
NDIM=120
```

```
LL=1
```

```
M3=0
```

```
NN=N+M2+M3
```

```

      MM=M1+M2+M3
      NIN=N-M1
C
C     SAVE THE CONSTRAINT MATRIX AND THE RIGHT HAND SIDE
C     VECTOR FOR LATER USE.
C
      DO 9 I=1,MM
      DO 9 J=1,NN
      9   AAO(I,J)=A(I,J)
      DO 78 I=1,MM
      B(I)=RHS(I)
      BB(I)=B(I)
      BBO(I)=B(I)
      BBB(I)=B(I)
      DO 79 J=1,NN
      AO(I,J)=A(I,J)
      79   CONTINUE
      78   CONTINUE
      DO 69 I=1,MM
      DO 69 J=1,N
      AA(I,J)=A(I,J)
      69   CONTINUE
C
C     OBTAIN THE OPTIMUM SOLUTION USING THE QUADRATIC
C     PROGRAMMING ALGORITHM
C
      CALL QUAD(AA,CO,C13,B,N,NCB,M1,M2,M3,X,FUN,KNC)
      IL=0
C
C     STOP IF NO FURTHER CHECK BY THE DIRECT SEARCH
C     OR MARQUARDT ALGORITHM IS REQUIRED.
C
      IF(IL.EQ.0) STOP
      IEVAL=0
      IX=999
C
C     USE RESULTS FROM THE QUADRATIC PROGRAMMING ALGORITHM
C     AS THE INITIAL VALUES FOR THE DIRECT SEARCH METHOD.
C
      DO 298 J=1,NN
      MID(J)=X(J)
      FF(J)=X(J)
      GMAX(J)=MID(J)
      298   CONTINUE
C
C     REARRANGE THE CONSTRAINTS SO NO DIAGONAL
C     ELEMENTS ARE ZERO
C
      CALL AROW(AO,BB,NDIM,N,M1,M2,M3,C)
C
C     USE DECOMP TO DECOMPOSE THE DEPENDENT SUBMATRIX, C,
C     BY GAUSSIAN ELIMINATION. USE SOLVE TO COMPUTE THE
C     DEPENDENT VARIABLES WHEN THE INDEPENDENT VARIABLES
C     ARE DETERMINED.

```

```

C   CALL DECOMP(NDIM,MM,C,COND,IPVT,WORK)
C   CONDP1=COND+1
C   IF(CONDP1 .EQ. COND) WRITE(6,4)
4   FORMAT('MATRIX C IS SINGULAR TO WORKING PRECISION')
C   IF(CONDP1 .EQ. COND) STOP

C   SAVE THE REARRANGED CONSTRAINT MATRIX AND THE RIGHT
C   HAND SIDE VECTOR (FROM AROW) FOR LATER USE.

C   DO 128 I=1,MM
    BBB(J)=BB(I)
    DO 129 J=1,NN
      AOO(I,J)=AO(I,J)
      AO2(I,J)=AO(I,J)
      CONTINUE
      CONTINUE

C   ESTABLISH BOUNDS ON INDEPENDENT VARIABLES

C   DO 290 J=1,NIN
    IF(AAO(1,J) .EQ. 0) BOUND(J)=EA(3)/RMO
    IF(AAO(1,J) .EQ. 0) GOTO 290
    BOUND(J)=BBO(1)/(AAO(1,J))
290  CONTINUE
    SMINI=FUN
292  LL=1.
    EP=0.05

C   MINIMIZATION ROUTINE BY DIRECT SEARCH

C   DO 380 L=1,150
    DO 381 K=1,200
    DO 301 J=1,NIN
      CALL RANDU(IX,IY,R)
      IX=IY
      FF(J)=MID(J)+(R-0.5)*BOUND(J)*2.
      IF(FF(J) .LT. 0.0) GOTO 381
301  CONTINUE

C   INDEPENDENT VARIABLES HAVE BEEN DETERMINED

C   DO 385 I=1,MM
    B(I)=BBB(I)
    DO 390 J=1,NIN
      B(I)=B(I)-FF(J)*AO2(I,J)
390  CONTINUE
385  CONTINUE

C   CALL SOLVE TO COMPUTE DEPENDENT VARIABLES.

C   CALL SOLVE(NDIM,MM,C,B,IPVT)
DO 409 J=1,MM
  FF(J+NIN)=B(J)

```

```

409  CONTINUE
NIN1=NIN+1
DO 410 J=NIN1,NN
IF (FF(J) .LT. 0.0) GOTO 381
410  CONTINUE
IL=IL+1
C
C
C      MINIMIZATION FUNCTION SHOULD BE EVALUATED HERE
C
C
DO 3025 I=1,NCB
CB(I)=C13(I)
DO 3026 J=1,N
IF(CO(I,J) .EQ. 0.0) GOTO 3026
CB(I)=CB(I)-CO(I,J)*FF(J)
3026  CONTINUE
CB(I)=CB(I)**2
3025  CONTINUE
FUN2=0.0
DO 3027 I=1,NCB
FUN2=FUN2+CB(I)
3027  CONTINUE
FUN=FUN2
IF(FUN .GT. SMINI) GOTO 381
SMINI=FUN
DO 415 J=1,NN
GMAX(J)=FF(J)
415  CONTINUE
381  CONTINUE
C
C
DO 420 J=1,NIN
MID(J)=GMAX(J)
420  CONTINUE
IEVAL=IEVAL+IL
421  IL=0
C
C      RLT=(L/10)-LL
C      IF(RLT) 379,52,379
C52   LL=LL+1
C      WRITE(6,53) SMINI,L
C53   FORMAT(E12.5,5X,I3)
C      DO 43 J=1,NN
C      WRITE(6,44) J,GMAX(J)
C43   CONTINUE
C44   FORMAT('X',I2,'=',F12.5)
379   DO 425 J=1,NIN
      BOUND(J)=(1.0-EP)*BOUND(J)
425   CONTINUE
380   CONTINUE
IF(IEVAL .EQ. 0) GOTO 430
GOTO 435
430   WRITE(6,431)

```

```
431 FORMAT('NO FURTHER IMPROVEMENT BY DIRECT SEARCH')
STOP
435 DO 440 J=1,NN
      X(J)=GMAX(J)
      IF(J .NE. N+1) GOTO 4351
      WRITE(6,4352)
4352 FORMAT('/', 'SLACK VARIABLES', '/')
4351 WRITE(6,438) KNC(J), GMAX(J)
438 FORMAT('X', I3, '=', F12.5)
440 CONTINUE
      WRITE(6,441) SMINI
441 FORMAT('/', F12.5, '/')
C
C      USE MARQUARDT ALGORITHM FOR FURTHER CHECK. THE
C      INITIAL SOLUTION IS THAT FROM THE DIRECT SEARCH.
C
9323 CALL JACC(A00,X,C0,C13,RJ,BB,B3,MM,NIN,NCB)
      RF=SMINI
      CALL MARQ(X,C,C13,RJ,BBB,AO2,IPVT,NDIM,N,M1,NCB,NIN,
      $,RF,M2,M3,KNC)
      STOP
      END
```

```

SUBROUTINE QUAD(AA,CO,C13,B,N,NCB,M1,M2,M3,X,FUN,KNC)
C
C This subroutine contains Wolfe's algorithm.
C The algorithm is briefly explained in Appendix A.
C For more details see the reference (Wolfe, 1959).
C
C Description of variables
C
C M1   : number of equality constraints
C M2   : number of inequality constraints (< or = )
C M3   : number of inequality constraints (> or = )
C N    : number of functional groups
C NCB  : number of bands in C13-NMR spectra
C FUN  : value of the objective function
C KNC  : array containing the group number of the
C        functional groups
C CO   : objective function matrix
C C13  : right hand side vector of the objective
C        functional equations
C CB   : sum of squares of the objective function
C        equations
C AA   : constraint matrix
C AAT  : transpose of AA
C A    : tableau for quadratic programming
C P    : vector defining the linear part of the
C        objective function
C C    : matrix defining the quadratic part of the
C        objective function
C B,RHS: right hand side vector of the constraints
C KROW : row number for key row
C KC   : column number for key column
C D    : array for storing the sum of column entries
C        used in determining the key column
C DD   : array for storing D corresponding to the key
C        column
C SD   : array for storing D
C AS   : array for storing entries of the key column
C Q,QQ,RATIO: ratio of the right hand side to the key
C        column entries to determine the key row
C RMU  : value of MU in phase III
C RRMU : array for storing the latest 3 values of RMU
C X    : functional group concentrations
C XT   : array for storing the latest 3 functional
C        group concentrations in phase III
C BNDX : array containing the index for basic variables
C IFLAG: flag for using modified version of phase I
C WO   : sum of artificial variables W to be
C        minimized in phase I
C ZO   : sum of artificial variables Z* to be
C        minimized in phase II
C PVT  : pivot element
C KKC  : array for storing the column numbers of two
C        columns which provide the same improvement
C        to the objective function in phase I

```

```

C      KT : array used to identify basic Z1 and Z2
C      variables at the end of phase I
C
REAL A(120,120),AA(120,120),AAT(120,120),RHS(120)
REAL D(120),DD(120),AS(120,120),X(120),B(120)
REAL P(120),C(120,120)
REAL SAVE(120,120),W(2)
REAL SD(120),RATIO(120)
REAL RRMU(3),XT(3,120)
REAL C13(120),CB(120),CO(120,120)
INTEGER KKC(2),BNDX(120),KT(120),KNC(120)
C
TOL=0.002
TOLD=-0.0001
IFLAG=0
M=M1
MM=M+M2+M3
NN=N+M2+M3
KC=0
C
C      DEFINE MATRIX C AND VECTOR P TO SET UP THE
C      INITIAL TABLEAU
C
70   DO 1 J=1,NN
      P(J)=0.0
1    CONTINUE
DO 3 I=1,N
DO 3 J=1,N
      C(I,J)=0.0
3    CONTINUE
DO 20 J=1,N
DO 30 K=1,N
DO 40 I=1,NCB
      C(J,K)=C(J,K)+(2.*(CO(I,J)*CO(I,K)))
40   CONTINUE
30   CONTINUE
20   CONTINUE
DO 50 J=1,N
DO 60 I=1,NCB
      P(J)=P(J)-(2.*(C13(I)*CO(I,J)))
60   CONTINUE
50   CONTINUE
N2=MM+N
N3=MM+(2*N)+M2+M3
N4=MM+(3*N)+M2+M3
N5=MM+(4*N)+M2+M3
KK=(4*N)+M2+M3+(2*MM)+1
MM2=MM+1
C
C      SET UP THE INITIAL TABLEAU FOR PHASE I
C
DO 75 I=1,N2
      RHS(I)=0.0
DO 76 J=1,KK

```

```

      A(I,J)=0.0
760 CONTINUE
750 CONTINUE
      DO 80 I=1,MM
      RHS(I)=B(I)
      DO 90 J=1,N
      A(I,J)=AA(I,J)
      IF(I .EQ. J) A(I,J+NN)=1.0
90  CONTINUE
80  CONTINUE
      IF(M2 .EQ. 0) GOTO 93
      DO 91 I=1,M2
      A(I+M,I+N)=1.0
91  CONTINUE
93  IF(M3 .EQ. 0) GOTO 96
      DO 92 I=1,M3
      A(I+M+M2,I+N+M2)=-1.0
92  CONTINUE
96  DO 95 I=1,N
      DO 95 J=1,MM
      AAT(I,J)=AA(J,I)
95  CONTINUE
      DO 100 I=MM2,N2
      I2=I-MM
      A(I,KK)=P(I-MM)
      DO 105 J=1,N
      A(I,J)=C(I-MM,J)
      IF(I2 .EQ. J) A(I,J+N2+M2+M3)=1.0
      IF(I2 .EQ. J) A(I,J+N3)=-1.0
      IF(I2 .EQ. J) A(I,J+N4)=-1.0
105 CONTINUE
100 CONTINUE
      DO 120 I=MM2,N2
      DO 125 J=1,MM
      A(I,J+N5)=AAT(I-MM,J)
125 CONTINUE
120 CONTINUE
      DO 126 I=1,N2
      DO 126 J=1,MM
      SAVE(J,I)=A(I,J+NN)
126 CONTINUE
      NN1=NN+1
      NN3=3*N+M2+M3
      DO 127 I=1,N2
      DO 128 J=NN1,N4
      A(I,J)=A(I,J+MM)
128 CONTINUE
127 CONTINUE
      DO 129 I=1,N2
      DO 129 J=1,MM
      A(I,J+NN3)=SAVE(J,I)
129 CONTINUE
      DO 130 I=1,MM
      BNDX(I)=NN3+I

```

```

130 CONTINUE
DO 132 I=1,N
BNDX(I-MM)=NN+I
132 CONTINUE
C DO 135 I=1,N2
C WRITE(6,136) (A(I,J),J=1,KK)
C135 CONTINUE
C136 FORMAT(25F9.3)
C
C THE INITIAL TABLEAU IS SET UP, PHASE I
C BEGINS HERE. CHECK TO SEE IF A FEASIBLE
C SOLUTION EXISTS AND PROCEED WITH THE ITERATIVE,
C PROCEDURE.
C
DO 150 J=1,KK
D(J)=0.0
DO 160 I=1,MM
D(J)=D(J)-A(I,J)
160 CONTINUE
150 CONTINUE
WO=0.0
DO 170 I=1,MM
WO=WO-RHS(I)
170 CONTINUE
C
IF(KC .GT. 0) GOTO 205
IT=0
C
C A MODIFICATION TO PHASE I OF THE ALGORITHM WOULD
C BE TO FORCE W'S OUT OF THE INITIAL BASIS.
C THIS AND THE SUBSEQUENT PROCEDURE IN PHASE II
C MAY RESULT IN VIOLATIONS IN THE SIGN RESTRICTION
C HOWEVER, THESE VIOLATIONS WOULD BE DEALT WITH IN
C PHASE III BEFORE A SOLUTION IS OBTAINED. FOR THIS
C METHOD (SET IFLAG TO 1), AT EACH STEP THE KEY ROW
C WOULD CORRESPOND TO A "W" REMAINING IN THE BASIS.
C
IF(IFLAG .EQ. 1) IW=0
IF(IFLAG .EQ. 0) IW=1000
C
C ITERATIVE PROCEDURE FOR PHASE I STARTS HERE.
C DETERMINE KEY COLUMN AND KEY ROW.
C
1000 IO=0
C DO 171 I=1,N2
C171 WRITE(6,172)(A(I,J),J=1,KK)
C172 FORMAT(25F9.3)
C WRITE(6,173)(D(J),J=1,KK)
C173 FORMAT(/,25F9.3,/)
C DO 176 I=1,N2
C WRITE(6,177) RHS(I)
C176 CONTINUE
C177 FORMAT(F10.4)

```

```

C      WRITE(6,174) WO
C174  FORMAT(/,F10.3,/)

C
DO 180 J=1,NN3
IF(D(J) .LT. TOLD) GOTO 182
GOTO 180
182 IO=IO+1
180 CONTINUE
IF(IW .LT. MM) GOTO 850
IF(IO .GT. 0) GOTO 850
IF(IO .EQ. 0) GOTO 1100
IF(WO .GT. 0.0) GOTO 190
GOTO 192
190 WRITE(6,191)
191 FORMAT('NO FEASIBLE SOLUTION')
STOP
192 IF(WO .EQ. 0.0) GOTO 1100
C
C      DETERMINE PIVOT ELEMENT
C
850 IW=IW+1
IF(IW .GT. MM) GOTO 880
KROW=IW
KC=0
VLST=10000.0
DO 855 J=1,NN
IF(A(KROW,J) .EQ. 0.0) GOTO 855
IF(D(J) .LT. VLST) KC=J
IF(D(J) .LT. VLST) VLST=D(J)
855 CONTINUE
GOTO 205
880 KS=NN
IK=0
NS=NN3
DO 750 J=1,NN
IF(D(J) .LT. TOLD) GOTO 755
GOTO 750
755 IK=IK+1
750 CONTINUE
IF(IK .EQ. 0) GOTO 950
C
C      IF TWO VARIABLES PROVIDE THE SAME CHANGE IN THE
C      SUM OF INFEASIBILITIES, THEN A MAIN VARIABLE IS
C      CHOSEN OVER AN ARTIFICIAL VARIABLE TO ENTER THE
C      BASIS.
C
DO 790 K=1,2
VLST=0.0
KC=0
DO 760 J=1,KS
IF(D(J) .GE. 0.0) GOTO 760
IF(D(J) .GT. VLST) GOTO 760
VLST=D(J)
KC=J

```

```

      KKC(K)=KC
760   CONTINUE
      KROW=0
      ST=1000.0
      COUNT=0
      DO 770 I=1,N2
      IF(A(I,KC)) 770,770,774
774   Q=RHS(I)/A(I,KC)
      COUNT=COUNT+1
      IF(Q-ST) 778,770,770
778   ST=Q
      KROW=I
770   CONTINUE
      IF(COUNT .EQ. 0) GOTO 780
      GOTO 785
780   IF(K .EQ. 1) GOTO 950
      WRITE(6,781)
781   FORMAT('UNBOUND SOLUTION')
      STOP
785   PVT=A(KROW,KC)
      W(K)=WO-((D(KC)*RHS(KROW))/PVT)
      KS=NN3
790   CONTINUE
      IF(KKC(1) .EQ. KKC(2)) GOTO 950
      IF(W(1) .GE. W(2)) NS=NN
950   VLST=0.0
      KC=0
      DO 200 J=1,NS
      IF(D(J) .GE. 0.0) GOTO 200
      IF(D(J) .GT. VLST) GOTO 200
      VLST=D(J)
      KC=J
200   CONTINUE

205   DO 210 I=1,N2
      AS(I,KC)=A(I,KC)
      DD(KC)=D(KC)
210   CONTINUE
      IF(IW .LE. MM) GOTO 233
      DO 211 I=1,N2
      SD(I)=A(I,KC)
211   CONTINUE
      KROW=0
212   ST=1000.0
      COUNT=0
      DO 220 I=1,N2
      IF(A(I,KC)) 220,220,215
215   Q=RHS(I)/A(I,KC)
      COUNT=COUNT+1
      IF(Q-ST) 218,220,220
218   ST=Q
      KROW=I
220   CONTINUE
      DO 224 I=1,N2

```

```

A(I,KC)=SD(I)
224 CONTINUE
IF(COUNT .EQ. 0) GOTO 225
GOTO 230
225 WRITE(6,223)
223 FORMAT('UNBOUND SOLUTION')
STOP
230 CONTINUE
C
233 PVT=A(KROW,KC)
BNDX(KROW)=KC
C
C PIVOT ELEMENT IS DETERMINED, TRANSFORM THE TABLEAU.
C
RHS(KROW)=RHS(KROW)/PVT
DO 240 I=1,N2
IF(I .EQ. KROW) GOTO 240
RHS(I)=RHS(I)-A(I,KC)*RHS(KROW)
240 CONTINUE
C
WO=WO-D(KC)*RHS(KROW)
IF(ABS(WO) .LE. TOL) GOTO 245
GOTO 246
245 WO=0.0
246 CONTINUE
DO 250 J=1,KK
A(KROW,J)=A(KROW,J)/PVT
250 CONTINUE
DO 260 J=1,KK
D(J)=D(J)-DD(KC)*A(KROW,J)
IF(ABS(D(J)) .LE. TOL) D(J)=0.0
260 CONTINUE
DO 270 I=1,N2
IF(I .EQ. KROW) GOTO 270
DO 280 J=1,KK
A(I,J)=A(I,J)-A(KROW,J)*AS(I,KC)
280 CONTINUE
270 CONTINUE
C
DO 290 J=1,KK
DO 290 I=1,N2
XX=A(I,J)
IF(ABS(XX) .GT. TOL) GOTO 290
A(I,J)=0.0
290 CONTINUE
IT=IT+1
GOTO 1000
1100 JK=NN+1
JK2=N*3+M2+M3
KJZ=0
DO 1105 J=JK,JK2
DO 1110 I=1,N2
IF(BNDX(I) .EQ. J) KJZ=KJZ+1
1110 CONTINUE

```

```

1105 CONTINUE
  IF(KJZ .LE. N) GOTO 1150
  JK=N*4+MM+1+M2+M3
  JK2=N*4+MM+MM+M2+M3
  DO 1120 J=JK,JK2
  DO 1125 I=1,N2
    IF(BNDX(I) .EQ. J) GOTO 1120
1125 CONTINUE
  KC=J
  GOTO 70
1120 CONTINUE
1150 DO 300 J=1,NN
  DO 305 I=1,N2
    IF(J .EQ. BNDX(I)), GOTO 310
    GOTO 305
310 X(J)=RHS(I)
  GOTO 300
305 CONTINUE
  X(J)=0.0
300 CONTINUE
C  DO 320 J=1,NN
C  WRITE(6,325) X(J)
C320 CONTINUE
  325 FORMAT(F10.4)
C
C  END OF PHASE I.
C  PROCEED BY OBTAINING THE INITIAL TABLEAU FOR
C  PHASE II.
C
  N2Z=NN+N
  DO 400 J=NN1,NN3
  KT(J)=0
  DO 405 I=1,N2
    IF(A(I,J) .NE. 0.0) GOTO 406
    GOTO 405
406 KT(J)=KT(J)+1
405 CONTINUE
400 CONTINUE
  KP=1
  N1Z=NN+N
  DO 410 J=NN1,NN3
    IF(KT(J) .GT. 1) GOTO 410
    DO 407 I=1,N2
      IF(A(I,J) .EQ. 0.0) GOTO 407
      IF(A(I,J) .EQ. 1.0) KI=I
      IF(A(I,J) .EQ. 1.0) GOTO 408
407 CONTINUE
    GOTO 410
408 DO 409 I=1,N2
  A(I,NN+KP)=0.0
  IF(I ,EQ. KI) A(I,NN+KP)=1.0
409 CONTINUE
  KP=KP+1.
410 CONTINUE

```

```

NZ=KP-1
NZ1=NN+NZ+1
NZ2=(2*N)-NZ+MM
NK=NN3+MM+1
DO 420 J=NK,KK
DO 425 I=1,N2
A(I,J-NZ2)=A(I,J)
425 CONTINUE
420 CONTINUE
DO 421 I=1,N2
IF(BNDX(I) .GT. N5) BNDX(I)=BNDX(I)-(2*N-NZ)-MM
421 CONTINUE
KK2=NN+NZ+N+MM+1
C DO 430 I=1,N2
C430 WRITE(6,435) (A(I,J),J=1,KK2)
C435 FORMAT(14F6.2)
C DO 438 I=1,N2
C WRITE(6,439) RHS(I)
C438 CONTINUE
C439 FORMAT(F6.2)
NNZ=NN+NZ
DO 441 J=1,NNZ
KT(J)=0
DO 442 I=1,N2
IF(A(I,J) .EQ. 0.0) GOTO 442
KT(J)=KT(J)+1
442 CONTINUE
441 CONTINUE
DO 443 J=1,NNZ
IF(KT(J) .NE. 1) GOTO 443
DO 444 I=1,N2
IF(A(I,J) .EQ. 0.0) GOTO 444
BNDX(I)=J
444 CONTINUE
443 CONTINUE
C DO 440 I=1,N2
C440 WRITE(6,445) BNDX(I)
C445 FORMAT(I5)
C
C INITIAL TABLEAU FOR PHASE II IS OBTAINED.
C
C PHASE II BEGINS NOW.
C
NNZ=NN+NZ
ZN2=2*N+NZ+M2+M3+M
KK=N*2+NZ+MM+M2+M3
KKM=KK+1
C
ZO=0.0
DO 490 I=1,N2
IF(BNDX(I) .LE. NN) GOTO 490
IF(BNDX(I) .GT. NNZ) GOTO 490
ZO=ZO-RHS(I)
490 CONTINUE

```

```

C
DO 510 J=1,KKM
D(J)=0.0
DO 505 I=1,N2
IF(BNDX(I) .LE. NN) GOTO 505
IF(BNDX(I) .GT. NNZ) GOTO 505
D(J)=D(J)-A(I,J)
505 CONTINUE
510 CONTINUE

C
DO 508 J=1,NNZ
DO 509 I=1,N2
IF(BNDX(I) .EQ. J) D(J)=0.0
509 CONTINUE
508 CONTINUE

C
NU1=NN+N+NZ+1
NU2=NN+N+NZ+MM
IT2=0

C
C START THE ITERATIVE PROCEDURE FOR PHASE II.
C
500 IO=0
C DO 511 I=1,N2
C511 WRITE(6,512) (A(I,J),J=1,KKM)
C512 FORMAT(25F9.3)
C WRITE(6,513) (D(J),J=1,KKM)
C513 FORMAT(/,25F9.3,/)

C DO 514 I=1,N2
C514 WRITE(6,515) RHS(I)
C515 FORMAT(F10.4)
C WRITE(6,516) ZO
C516 FORMAT(/,F10.4,/)

C
C
DO 520 J=1,KK
IF(D(J) .LT. TOLD) GOTO 522
GOTO 520
522 IO=IO+1
520 CONTINUE
IF(IO .GT. 0) GOTO 550
IF(IO .EQ. 0) GOTO 680
IF(ZO .GT. 0.0) GOTO 525
GOTO 530
525 WRITE(6,526)
526 FORMAT('NO FEASIBLE SOLUTION')
STOP
530 IF(ZO .EQ. 0.0) GOTO 680.

C
C DETERMINE KEY COLUMN
C
550 DO 555 J=1,KKM
SD(J)=D(J)
555 CONTINUE

```

```

556 VLST=0.0
KC=0
DO 560 J=1,KK
IF(D(J) .GE. 0.0) GOTO 560
IF(D(J) .GT. VLST) GOTO 560
VLST=D(J)
KC=J
560 CONTINUE
IF(KC .EQ. 0) GOTO 1800
C
C DETERMINE KEYROW
C
C WHEN TWO VARIABLES ARE INVOLVED IN A TIE IN
C CHOOSING THE KEY ROW, THEN THE KEY ROW IS
C DETERMINED SUCH THAT THE LEAVING BASIC VARIABLE
C IS AN ARTIFICIAL VARIABLE RATHER THAN A MAIN
C VARIABLE.
C
561 KROW=0
ST=1000.0
COUNT=0
DO 565 I=1,N2
IF(A(I,KC)) 565,565,563
563 Q=RHS(I)/A(I,KC)
COUNT=COUNT+1
IF(Q-ST) 564,565,565
564 ST=Q
KROW=I
565 CONTINUE
IF(BNDX(KROW) .LE. NN) GOTO 5000
GOTO 5005
5000 DQ 5010 I=1,N2
RATIO(I)=-1.0
IF(A(I,KC) .EQ. 0.0) GOTO 5010
IF(A(I,KC) .LT. 0.0) GOTO 5010
RATIO(I)=RHS(I)/A(I,KC)
5010 CONTINUE
DO 5020 I=1,N2
IF(RATIO(I) .LT. 0.0) GOTO 5020
IF(I .EQ. KROW) GOTO 5020
IF(RATIO(I) .EQ. RATIO(KROW)) GOTO 5025
GOTO 5020
5025 IF(BNDX(I) .GT. NN) KROW=I
5020 CONTINUE
C
C
C CHECK FOR CONDITION 2 OF PHASE II
C
C
5005 IF(KC .LE. NN) GOTO 570
IF(KC .LE. NNZ) GOTO 590
IF(KC .GT. ZN2) GOTO 587
570 IF(KC .GT. NN) GOTO 580
IF(KC .GT. N) GOTO 576

```

```

KJ=KC+NZ+NN
DO 575 I=1,N2
IF(BNDX(I) .EQ. KJ) D(KC)=10000.0
IF(BNDX(I) .EQ. KJ) GOTO 556
575 CONTINUE
GOTO 590
576 KJ=KC+NZ+NN+M
DO 577 I=1,N2
IF(BNDX(I) .EQ. KJ) D(KC)=10000.0
IF(BNDX(I) .EQ. KJ) GOTO 556
577 CONTINUE
GOTO 590
580 KJ=KC-NN-NZ
DO 585 I=1,N2
IF(BNDX(I) .EQ. KJ) D(KC)=10000.0
IF(BNDX(I) .EQ. KJ) GOTO 556
585 CONTINUE
GOTO 590
587 KJ=KC-NZ-NN-M
DO 588 I=1,N2
IF(BNDX(I) .EQ. KJ) D(KC)=10000.0
IF(BNDX(I) .EQ. KJ) GOTO 556
588 CONTINUE
GOTO 590
C
C
590 IF(COUNT .EQ. 0) GOTO 592
GOTO 596
592 WRITE(6,594)
594 FORMAT('UNBOUND SOLUTION')
STOP
596 CONTINUE
DO 598 J=1,KKM
D(J)=SD(J)
598 CONTINUE
DO 600 I=1,N2
AS(I,KC)=A(I,KC)
600 CONTINUE
DD(KC)=D(KC)
PVT=A(KROW,KC)
BNDX(KROW)=KC
C
C
C TRANSFORM THE TABLEAU
C
C
RHS(KROW)=RHS(KROW)/PVT
DO 605 I=1,N2
IF(I .EQ. KROW) GOTO 605
RHS(I)=RHS(I)-A(I,KC)*RHS(KROW)
605 CONTINUE
ZO=ZO-D(KC)*RHS(KROW)
IF(ABS(ZO) .LE. TOL) ZO=0.0
DO 610 J=1,KKM

```

```

A(KROW,J)=A(KROW,J)/PVT
610 CONTINUE
DO 615 J=1,KKM
D(J)=D(J)-DD(KC)*A(KROW,J)
IF(ABS(D(J)) .LE. TOL) D(J)=0.0
615 CONTINUE
DO 620 I=1,N2
IF(I .EQ. KROW) GOTO 620
DO 625 J=1,KKM
A(I,J)=A(I,J)-A(KROW,J)*AS(I,KC)
625 CONTINUE
620 CONTINUE
C
DO 630 J=1,KKM
DO 630 I=1,N2
XX=A(I,J)
IF(ABS(XX) .GT. TOL) GOTO 630
A(I,J)=0.0
630 CONTINUE
IT2=IT2+1
GOTO 500
C
C MODIFICATION FOR PHASE II TO AVOID TERMINATION.
C FOR DETAILS SEE APPENDIX A.
C
1800 DO 1802 J=1,KKM
D(J)=SD(J)
1802 CONTINUE
NNZ1=NN+1
NNZ2=NN+NZ
NV1=NN+NZ+1
KU=NN+NZ+N+M
DO 1900 JJ=NNZ1,NNZ2
DO 1805 II=1,N2
IF(BNDX(II) .EQ. JJ) GOTO 1820
1805 CONTINUE
GOTO 1900
1820 KROW=II
DO 1821 J=1,KKM
SD(J)=D(J)
1821 CONTINUE
1822 KC=0
VLST=10000.0
DO 1830 K=1,NU2
IF(K .LE. NN) GOTO 1831
IF(K .GT. NNZ2) GOTO 1831
GOTO 1830
1831 IF(ABS(A(KROW,K)) .LE. TOL) GOTO 1830
IF(D(K) .LT. VLST) KC=K
IF(D(K) .LT. VLST) VLST=D(K)
1830 CONTINUE
IF(KC .LE. KU) GOTO 1832
KJ=KC-NZ-NN-M
DO 1826 I=1,N2

```

```

    IF(BNDX(I) .EQ. KJ) D(KC)=20000.0
    IF(BNDX(I) .EQ. KJ) GOTO 1822
1826 CONTINUE
    GOTO 1836
1832 IF(KC .GE. NU1) GOTO 1836
    IF(KC .LE. NN) GOTO 8341
    KJ=KC-NN-NZ
    DO 1834 I=1,N2
    IF(BNDX(I) .EQ. KJ) D(KC)=20000.0
    IF(BNDX(I) .EQ. KJ) GOTO 1822
1834 CONTINUE
    GOTO 1836
8341 IF(KC .LE. N) GOTO 8345
    KJ=KC+NZ+M+NN
    DO 8342 I=1,N2
    IF(BNDX(I) .EQ. KJ) D(KC)=20000.0
    IF(BNDX(I) .EQ. KJ) GOTO 1822
8342 CONTINUE
    GOTO 1836
8345 KJ=KC+NN+NZ
    DO 8346 I=1,N2
    IF(BNDX(I) .EQ. KJ) D(KC)=20000.0
    IF(BNDX(I) .EQ. KJ) GOTO 1822
8346 CONTINUE
1836 DO 1833 J=1,KKM
    D(J)=SD(J)
1833 CONTINUE

```

C
C TRANSFORM THE TABLEAU
C

```

    DO 1835 I=1,N2
    AS(I,KC)=A(I,KC)
1835 CONTINUE
    DD(KC)=D(KC)
    PVT=A(KROW,KC)
    BNDX(KROW)=KC
    C
    RHS(KROW)=RHS(KROW)/PVT
    DO 1840 I=1,N2
    IF(I .EQ. KROW) GOTO 1840
    RHS(I)=RHS(I)-A(I,KC)*RHS(KROW)
1840 CONTINUE
    ZO=ZO-D(KC)*RHS(KROW)
    IF(ABS(ZO) .LE. TOL) ZO=0.0
    DO 1845 J=1,KKM
    A(KROW,J)=A(KROW,J)/PVT
1845 CONTINUE
    DO 1850 J=1,KKM
    D(J)=D(J)-DD(KC)*A(KROW,J)
    IF(ABS(D(J)) .LE. TOL) D(J)=0.0
1850 CONTINUE
    DO 1860 I=1,N2
    IF(I .EQ. KROW) GOTO 1860
    DO 1865 J=1,KKM

```

```

A(I,J)=A(I,J)-A(KROW,J)*AS(I,KC)
1865 CONTINUE
1860 CONTINUE
C
    DO 1870 J=1, KKM
    DO 1870 I=1, N2
    XX=A(I,J)
    IF(ABS(XX) .GT. TOL) GOTO 1870
    A(I,J)=0.0
1870 CONTINUE
C    DO 1871 I=1, N2
C1871 WRITE(6,1872) (A(I,J), J=1, KKM)
C1872 FORMAT(25F9.3)
C    WRITE(6,1873) (D(J), J=1, KKM)
C1873 FORMAT(/,24F9.3,/ )
C    DO 1874 I=1, N2
C1874 WRITE(6,1875) RHS(I)
C1875 FORMAT(F10.4)
C    WRITE(6,1876) ZO
C1876 FORMAT(/,F10.5,/ )
1900 CONTINUE
680  DO 690 J=1, NN
    DO 695 I=1, N2
    IF(J .EQ. BNDX(I)) GOTO 698
    GOTO 695
698  X(J)=RHS(I)
    GOTO 690
695  CONTINUE
    X(J)=0.0
690  CONTINUE
C    DO 697 J=1, NN
C    WRITE(6,699) X(J)
C697  CONTINUE
C699  FORMAT(F10.4)
C
C    END OF PHASE II
C    PROCEED TO OBTAIN THE INITIAL TABLEAU FOR PHASE III.
C
    NN2=2*N+M2+M3
    NM=NN+NZ+1
    KM=NN+N+M
    DO 900 J=NM, KKM
    DO 905 I=1, N2
    A(I,J-NZ)=A(I,J)
905  CONTINUE
900  CONTINUE
    DO 909 I=1, N2
    IF(BNDX(I) .GT. NN) BNDX(I)=BNDX(I)-NZ
909  CONTINUE
C
C    INITIAL TABLEAU FOR PHASE III IS OBTAINED.
C
    KMU=2*N+MM+M2+M3+1
    RMU=0.0

```

```

DO 908 J=1,KMU
D(J)=0.0
IF(J .EQ. KMU) D(J)=-1.0
908 CONTINUE
C
DO 907 J=1,NN
XT(1,J)=X(J)
907 CONTINUE
RRMU(1)=RMU
C
IT3=0
C
C START THE ITERATIVE PROCEDURE FOR PHASE III.
C DO NOT ALLOW MU TO ENTER THE BASIS UNTIL ALL
C SIGN VIOLATIONS ARE CORRECTED.
C
910 IO=0
C DO 911 I=1,N2
C911 WRITE(6,912) (A(I,J),J=1,14)
C912 FORMAT(14F9.3)
C WRITE(6,913) (D(J),J=1,14)
C913 FORMAT(/,14F9.3,/)
C DO 914 I=1,N2
C WRITE(6,915) RHS(I)
C915 FORMAT(F10.4)
C914 CONTINUE
WRITE(6,916) RMU
916 FORMAT(/,F10.4,/)

C
DO 920 J=1,KMU
IF(D(J) .LT. TOLD) GOTO 922
GOTO 920
922 IO=IO+1
920 CONTINUE
IF(RMU .GE. 1.0) GOTO 1500
IF(IO .GT. 0) GOTO 930
IF(RMU .LT. 0.0) GOTO 925
GOTO 930
925 WRITE(6,926)
926 FORMAT('MU IS UNBOUNDED')
STOP
930 IF(IT3 .EQ. 0) GOTO 931
IF(IT3 .EQ. 1) GOTO 928
IF(RMU .LE. 0.0) GOTO 928
IF(ABS(RRMU(2)-RRMU(3)) .LE. 0.0001) GOTO 1600
928 DO 927 J=1,NN
XT(3,J)=XT(1,J)
XT(1,J)=XT(2,J)
927 CONTINUE
RRMU(3)=RRMU(1)
RRMU(1)=RRMU(2)
931 DO 935 J=1,KMU
SD(J)=D(J)
935 CONTINUE

```

```

C
C      DETERMINE KEYCOLUMN
C
936  VLST=0.0
      KC=0
      KJ=0
      DO 960 J=1, KMU
      IF(D(J) .GE. 0.0) GOTO 960
      IF(D(J) .GT. VLST) GOTO 960
      VLST=D(J)
      KC=J
960  CONTINUE
C
C      DETERMINE KEYROW
C
      KC1=KC
      NVO=NN+N
      NROW=N+MM
      DO 9600 I2=1,NROW
      I=NROW-I2+1
      IF(BNDX(I) .GT. NVO) GOTO 9600
      IF(RHS(I) .LT. 0.0) GOTO 9601
      GOTO 9600
9601 IF(BNDX(I) .LE. N) GOTO 9605
      IF(BNDX(I) .GT. NN) GOTO 9606
      GOTO 9600
9605 KROW=I
      KC=BNDX(I)+M2+N
      IF(A(KROW,KC) .EQ. 0.0) GOTO 9600
      GOTO 9991
9606 KROW=I
      KC=BNDX(I)-M2-N
      IF(A(KROW,KC) .EQ. 0.0) GOTO 9600
      GOTO 9991
9600 CONTINUE
      KROW=0
      KC=KC1
      ST=1000.0
      COUNT=0
      DO 965 I=1,N2
      IF(A(I,KC)) 965,965,963
963  Q=RHS(I)/A(I,KC)
      COUNT=COUNT+1
      IF(Q-ST) 964,965,965
964  IF(BNDX(I) .GT. NN2) GOTO 9651
      GOTO 9652
9651 IF(BNDX(I) .LE. KUM) GOTO 965
9652 ST=Q
      KROW=I
965  CONTINUE
      IF(COUNT .GT. 0) GOTO 9661
      ST=-10000.0
      KROW=0
      COUNT=0
}

```

```

DO 9771 I=1,N2
IF(A(I,KC)) 9772,9771,9771
9772 QQ=RHS(I)/A(I,KC)
COUNT=COUNT+1
IF(QQ-ST) 9771,9771,9773
9773 IF(BNDX(I) .GT. NN2) GOTO 9774
GOTO 9775
9774 IF(BNDX(I) .LE. KUM) GOTO 9771
9775 ST=QQ
KROW=I
9771 CONTINUE
9661 IF(BNDX(KROW) .LE. NN) GOTO 966
GOTO 971
966 DO 967 I=1,N2
RATIO(I)=-1.0
IF(A(I,KC) .EQ. 0.0) GOTO 967
IF(A(I,KC) .LT. 0.0) GOTO 967
RATIO(I)=RHS(I)/A(I,KC)
967 CONTINUE
DO 968 I=1,N2
IF(RATIO(I) .LT. 0.0) GOTO 968
IF(I .EQ. KROW) GOTO 968
IF(RATIO(I) .EQ. RATIO(KROW)) GOTO 969
GOTO 968
969 IF(BNDX(I) .GT. NN) KROW=I
968 CONTINUE
C
C CHECK FOR CONDITION 2 OF PHASE III
C
971 IF(KC .EQ. KMU) GOTO 9991
IF(KC .LE. NN) GOTO 970
IF(KC .GT. NN2) GOTO 985
970 IF(KC .GT. NN) GOTO 980
IF(KC .GT. N) GOTO 976
KJ=KC+NN
DO 975 I=1,N2
IF(BNDX(I) .EQ. KJ) D(KC)=10000.0
IF(BNDX(I) .EQ. KJ) GOTO 936
975 CONTINUE
GOTO 990
976 KJ=KC+N+MM
DO 977 I=1,N2
IF(BNDX(I) .EQ. KJ) D(KC)=10000.0
IF(BNDX(I) .EQ. KJ) GOTO 936
977 CONTINUE
GOTO 990
985 IF(KC .LE. KUM) GOTO 990
IF(KC .EQ. KMU) GOTO 990
KJ=KC-N-MM
DO 986 I=1,N2
IF(BNDX(I) .EQ. KJ) D(KC)=10000.0
IF(BNDX(I) .EQ. KJ) GOTO 936
986 CONTINUE
GOTO 990

```

```

980 KJ=KC-NN
    DO 995 I=1,N2
    IF(BNDX(I) .EQ. KJ) D(KC)=10000.0
    IF(BNDX(I) .EQ. KJ) GOTO 936
995 CONTINUE
C
990 IF(COUNT .EQ. 0) GOTO 992
    GOTO 996
992 WRITE(6,994)
994 FORMAT('MU IS UNBOUNDED')
    STOP
996 CONTINUE
    DO 998 J=1,KMU
    D(J)=SD(J)
998 CONTINUE
9991 DO 999 I=1,N2
    AS(I,KC)=A(I,KC)
999 CONTINUE
    DD(KC)=D(KC)
    PVT=A(KROW,KC)
    BNDX(KROW)=KC

```

C

C

C

TRANSFORM THE TABLEAU

C

C

```

RHS(KROW)=RHS(KROW)/PVT
DO 1205 I=1,N2
IF(I .EQ. KROW) GOTO 1205
RHS(I)=RHS(I)-A(I,KC)*RHS(KROW)
1205 CONTINUE
RMU=RMU-D(KC)*RHS(KROW)
DO 1210 J=1,KMU
A(KROW,J)=A(KROW,J)/PVT
1210 CONTINUE
DO 1215 J=1,KMU
D(J)=D(J)-DD(KC)*A(KROW,J)
IF(ABS(D(J)) .LE. TOL) D(J)=0.0
1215 CONTINUE
DO 1220 I=1,N2
IF(I .EQ. KROW) GOTO 1220
DO 1225 J=1,KMU
A(I,J)=A(I,J)-A(KROW,J)*AS(I,KC)
1225 CONTINUE
1220 CONTINUE

```

C

```

DO 1230 J=1,KMU
DO 1230 I=1,N2
XX=A(I,J)
IF(ABS(XX)-TOL) 1232,1232,1230
1232 A(I,J)=0.0
1230 CONTINUE

```

C

DO 1240 J=1,NN

```

DO 1245 I=1,N2
IF(J .EQ. BNDX(I)) GOTO 1248
GOTO 1245
1248 X(J)=RHS(I)
GOTO 1240
1245 CONTINUE
X(J)=0.0
1240 CONTINUE
RRMU(2)=RMU
DO 1250 J=1,NN
XT(2,J)=X(J)
1250 CONTINUE
IT3=IT3+1
GOTO 910
C
C      OBTAIN THE SOLUTION FOR MU=1.0
C
1500 RS1=(RRMU(2)-1)/(RRMU(2)-RRMU(1))
RS2=(1-RRMU(1))/(RRMU(2)-RRMU(1))
DO 1510 J=1,NN
X(J)=(RS1*XT(1,J))+(RS2*XT(2,J))
IF(J .NE. N+1) GOTO 1913
WRITE(6,1914)
1914 FORMAT(/, 'SLACK VARIABLES',/)
1913 WRITE(6,1511) KNC(J),X(J)
1510 CONTINUE
1511 FORMAT('X',I3,'=',F12.5)
GOTO 1700
1600 DO 1610 J=1,NN
X(J)=((XT(2,J)-XT(1,J))*(1-RRMU(2))
$/ (RRMU(2)-RRMU(1)))+XT(2,J)
IF(J .NE. N+1) GOTO 1915
WRITE(6,1916)
1916 FORMAT(/, 'SLACK VARIABLES',/)
1915 WRITE(6,1620) KNC(J),X(J)
1610 CONTINUE
1620 FORMAT('X',I3,'=',F12.5)
1700 DO 1710 I=1,NCB
CB(I)=C13(I)
DO 1720 J=1,N
IF(CO(I,J) .EQ. 0.0) GOTO 1720
CB(I)=CB(I)-CO(I,J)*X(J)
1720 CONTINUE
CB(I)=CB(I)**2
1710 CONTINUE
FUN=0.0
DO 1730 I=1,NCB
FUN=FUN+CB(I)
1730 CONTINUE
WRITE(6,1740) FUN
1740 FORMAT(/,F12.5,/)
RETURN
END

```

```

SUBROUTINE AROW(AO,BB,NDIM,N,M1,M2,M3,C)
C
C This subroutine rearranges, i.e interchanges the rows
C of the dependent variables matrix, C, such that no
C diagonal elements are zero.
C
C Description of variables
C
C AO : array containing coefficients of
C       the constraint matrix
C BB : right hand side vector for the constraints
C NDIM : declared dimension of constraint matrix
C N : total number of functional groups
C M1 : number of equality constraints
C M2 : number of inequality constraints of the
C       form less than or equal to
C M3 : number of inequality constraints of the
C       form greater than or equal to
C C : square matrix of the dependent variables
C SS,BS: arrays for temporary storing of AO and BB
C       respectively
C TT,TC,TD : arrays containing the count number of
C       non zero elements in rows, columns, and
C       diagonal of C
C
C
C INTEGER NDIM,N,M1,M2,M3
C REAL AO(NDIM,NDIM),BB(NDIM),C(NDIM,NDIM)
C REAL SS(50,50),BS(50),TT(50),TC(50),TD(50)
C
C
NN=N+M2+M3
MM=M1+M2+M3
NIN=N-M1
DO 405 I=1,MM
DO 406 J=1,MM
C(I,J)=AO(I,J+NIN)
406 CONTINUE
405 CONTINUE
DO 651 I=1,MM
TT(I)=0
DO 652 J=1,MM
IF(C(I,J) .EQ. 0) GOTO 652
TT(I)=TT(I)+1
652 CONTINUE
651 CONTINUE
C
DO 653 I=1,MM
IF(TT(I)-1) 653,654,653
654 DO 655 J=1,MM
IF(C(I,J) .EQ. 0) GOTO 655
KK=J
DO 656 JJ=1,MM
SS(KK,JJ)=C(KK,JJ)
C(KK,JJ)=C(I,JJ)
C(I,JJ)=SS(KK,JJ)

```

```

656 CONTINUE
DO 659 JJ=1,NIN
SS(KK,JJ)=AO(KK,JJ)
AO(KK,JJ)=AO(I,JJ)
AO(I,JJ)=SS(KK,JJ)
659 CONTINUE
BS(KK)=BB(KK)
BB(KK)=BB(I)
BB(I)=BS(KK)
655 CONTINUE
653 CONTINUE
DO 671 J=1,MM
TC(J)=0
DO 672 I=1,MM
IF(C(I,J) .EQ. 0) GOTO 672
TC(J)=TC(J)+1
672 CONTINUE
671 CONTINUE
C
DO 673 J=1,MM
IF(TC(J)-1) 673,674,673
674 KP=J
DO 675 I=1,MM
IF(C(I,J) .EQ. 0) GOTO 675
KK=I
DO 676 JJ=1,MM
SS(KK,JJ)=C(KK,JJ)
C(KK,JJ)=C(KP,JJ)
C(KP,JJ)=SS(KK,JJ)
676 CONTINUE
DO 679 JJ=1,NIN
SS(KK,JJ)=AO(KK,JJ)
AO(KK,JJ)=AO(KP,JJ)
AO(KP,JJ)=SS(KK,JJ)
679 CONTINUE
BS(KK)=BB(KK)
BB(KK)=BB(KP)
BB(KP)=BS(KK)
675 CONTINUE
673 CONTINUE
C
DO 681 I=1,MM
TD(I)=0
IF(C(I,I) .EQ. 0) GOTO 682
GOTO 681
682 TD(I)=1
681 CONTINUE
C
DO 683 II=1,MM
IF(TD(II)-1) 683,684,683
684 KK=II
DO 685 I=1,MM
IF(C(I,KK) .EQ. 0) GOTO 685
KP=I

```

```
IF(C(KK,KP) .EQ. 0) GOTO 685
DO 686 J=1,MM
SS(KP,J)=C(KP,J)
C(KP,J)=C(KK,J)
C(KK,J)=SS(KP,J)
686 CONTINUE
DO 689 J=1,NIN
SS(KP,J)=AO(KP,J)
AO(KP,J)=AO(KK,J)
AO(KK,J)=SS(KP,J)
689 CONTINUE
BS(KK)=BB(KK)
BB(KK)=BB(KP)
BB(KP)=BS(KK)
685 CONTINUE
683 CONTINUE
DO 691 I=1,MM
DO 691 J=1,MM
AO(I,J+NIN)=C(I,J)
691 CONTINUE
C
C      DO 5 I=1,MM
C      WRITE(6,3)(AO(I,J),J=1,NN)
C5' CONTINUE
C      DO 7 I=1,MM
C      WRITE(6,3)(C(I,J),J=1,MM)
C7' CONTINUE
C      DO 8 I=1,MM
C      WRITE(6,3) BB(I)
C8' CONTINUE
C3 FORMAT(8F7.3)
C
RETURN
END
```

```

SUBROUTINE DECOMP(NDIM,N,A,COND,IPVT,WORK)
C
C      INTEGER NDIM,N
C      REAL A(NDIM,N),COND,WORK(N)
C      INTEGER IPVT(N)
C
C      C DECOMPOSES A REAL MATRIX BY GAUSSIAN ELIMINATION
C      C AND ESTIMATES THE CONDITION OF THE MATRIX.
C      C USE SOLVE TO COMPUTE SOLUTIONS TO LINEAR SYSTEMS.
C
C      C INPUT:
C      C      NDIM =DECLARED ROW DIMENSION OF THE ARRAY CONTAINING A.
C      C      N     =ORDER OF THE MATRIX
C      C      A     =MATRIX TO BE TRIANGULARIZED.
C
C      C OUTPUT:
C      C      A CONTAINS AN UPPER TRIANGULAR MATRIX U AND A PERMUTED
C      C      VERSION OF A LOWER TRIANGULAR MATRIX L-SO THAT
C      C      (PERMUTATION MATRIX)*A=L*U
C
C      C      COND=AN ESTIMATE OF THE CONDITION OF A.
C      C      FOR THE LINEAR SYSTEM A*X=B, CHANGES IN A AND B
C      C      MAY CAUSE CHANGES COND TIMES AS LARGE IN X.
C      C      IF COND>1.0 .EQ. COND, A IS SINGULAR TO WORKING
C      C      PRECISION. COND IS SET TO 1.0E+32 IF EXACT
C      C      SINGULARITY IS DETECTED.
C
C      C      IPVT=THE PIVOT VECTOR.
C      C      IPVT(K)=THE INDEX OF THE K-TH PIVOT ROW.
C      C      IPVT(N)=(-1)**(NUMBER OF INTERCHANGES)
C
C      C      WORK SPACE: THE VECTOR MUST BE DECLARED AND INCLUDED
C      C      IN THE CALL. ITS INPUT CONTENTS ARE IGNORED.
C      C      ITS OUTPUT CONTENTS ARE USUALLY UNIMPORTANT.
C
C      C      THE DETERMINANT OF A CAN BE OBTAINED ON OUTPUT BY
C      C      DET(A)=IPVT(N)*A(1,1)*A(2,2)*...*A(N,N).
C
C      C      REAL EK,T,ANORM,YNORM,ZNORM
C      C      INTEGER NM1,I,J,K,KP1,KB,KM1,M
C
C      C      IPVT(N)=1
C      C      IF(N.EQ.1)GOTO 80
C      C      NM1=N-1
C
C      C      COMPUTE 1-NORM OF A
C
C      C      ANORM=0.0
C      DO 10 J=1,N
C          T=0.0
C          DO 5 I=1,N
C              T=T+ABS(A(I,J))
C 5      CONTINUE
C      IF(T.GT.ANORM)ANORM=T
C 10     CONTINUE

```

```

C
C GAUSSIAN ELIMINATION WITH PARTIAL PIVOTING
C
DO 35 K=1,NM1
  KP1=K+1
C
C FIND PIVOT
C
M=K
DO 15 I=KP1,N
  IF(ABS(A(I,K)).GT.ABS(A(M,K)))M=I
15  CONTINUE
  IPVT(K)=M
  IF(M.NE.K)IPVT(N)=-IPVT(N)
  T=A(M,K)
  A(M,K)=A(K,K)
  A(K,K)=T
C
C SKIP STEP IF PIVOT IS ZERO
C
IF(T.EQ.0.0)GOTO 35
C
C COMPUTE MULTIPLIERS
C
DO 20 I=KP1,N
  A(I,K)=-A(I,K)/T
20  CONTINUE
C
C INTERCHANGE AND ELIMINATE BY COLUMNS
C
DO 30 J=KP1,N
  T=A(M,J)
  A(M,J)=A(K,J)
  A(K,J)=T
  IF(T.EQ.0.0)GOTO 30
  DO 25 I=KP1,N
    A(I,J)=A(I,J)+A(I,K)*T
25  CONTINUE
30  CONTINUE
35 CONTINUE
C
C COND=(1-NORM OF A)*(AN ESTIMATE OF 1-NORM OF A-INVERSE)
C ESTIMATE OBTAINED BY ONE-STEP OF INVERSE ITERATION FOR THE
C SMALL SINGULAR VECTOR. THIS INVOLVES SOLVING TWO SYSTEMS
C OF EQUATIONS, (A-TRANSPOSE)*Y=E AND A*Z=Y WHERE E
C IS A VECTOR OF +1 OR -1 CHOSEN TO CAUSE GROWTH IN Y.
C ESTIMATE=(1-NORM OF Z)/(1-NORM OF Y)
C
C SOLVE (A-TRANSPOSE)*Y=E
C
DO 50 K=1,N
  T =0.0
  IF(K.EQ.1)GOTO 45
  KM1=K-1

```

```

DO 40 I=1,KM1
  T=T+A(I,K)*WORK(I)
40 CONTINUE
45 EK=1.0
  IF(T.LT.0.0)EK=-1.0
  IF(A(K,K).EQ.0.0)GOTO 90
  WORK(K)=-(EK+T)/A(K,K)
50 CONTINUE
  DO 60 KB=1,NM1
    K=N-KB
    T=0.0
    KP1=K+1
    DO 55 I=KP1,N
      T=T+A(I,K)*WORK(K)
55 CONTINUE
    WORK(K)=T
    M=IPVT(K)
    IF(M.EQ.K)GOTO 60
    T=WORK(M)
    WORK(M)=WORK(K)
    WORK(K)=T
60 CONTINUE
C
C   YNORM=0.0
  DO 65 I=1,N
    YNORM=YNORM+ABS(WORK(I))
65 CONTINUE
C
C   SOLVE A*Z=Y
C
C   CALL SOLVE(NDIM,N,A,WORK,IPVT)
C
C   ZNORM=0.0
  DO 70 I=1,N
    ZNORM=ZNORM+ABS(WORK(I))
70 CONTINUE
C
C   ESTIMATE CONDITION
C
C   COND=ANORM*ZNORM/YNORM
  IF(COND.LT.1.0)COND=1.0
  RETURN
C
C   1-BY-1
C
C   80 COND=1.0
  IF(A(1,1).NE.0.0)RETURN
C
C   EXACT SINGULARITY
C
C   90 COND=1.0E+32
  RETURN
END

```

```

SUBROUTINE SOLVE(NDIM,N,A,B,IPVT)
C
C      INTEGER NDIM,N,IPVT(N)
C      REAL A(NDIM,N),B(N)
C
C      SOLUTION OF LINEAR SYSTEM, A*X=B
C      DO NOT USE IF DECOMP HAS DETECTED SINGULARITY
C
C      INPUT:
C      NDIM =DECLARED ROW DIMENSION OF ARRAY CONTAINING A
C      N    =ORDER OF MATRIX
C      A    =TRIANGULARIZED MATRIX OBTAINED FROM DECOMP
C      B    =RIGHT HAND SIDE VECTOR
C      IPVT =PIVOT VECTOR OBTAINED FROM DECOMP
C
C      OUTPUT:
C
C      B    =SOLUTION VECTOR X.
C
C      INTEGER KB,KM1,NM1,KP1,I,K,M
C      REAL T
C
C      FORWARD ELIMINATION
C
C      IF(N.EQ.1)GOTO 50
C      NM1=N-1
C      DO 20 K=1,NM1
C          KP1=K+1
C          M=IPVT(K)
C          T=B(M)
C          B(M)=B(K)
C          B(K)=T
C          DO 10 I=KP1,N
C              B(I)=B(I)+A(I,K)*T
C 10      CONTINUE
C 20      CONTINUE
C
C      BACK SUBSTITUTE
C
C      DO 40 KB=1,NM1
C          KM1=N-KB
C          K=KM1+1
C          B(K)=B(K)/A(K,K)
C          T=-B(K)
C          DO 30 I=1,KM1
C              B(I)=B(I)+A(I,K)*T
C 30      CONTINUE
C 40      CONTINUE
C 50      B(1)=B(1)/A(1,1)
C      RETURN
C      END

```

B.3. Marquardt algorithm

The results from the direct search method are further tested by the Marquardt algorithm (subroutine MARQ) which is a least square parameter estimation algorithm where the direction of search is obtained by the Jacobian of the objective function matrix. Other subroutines used by the algorithm are:

1. JACG

This subroutine row-reduces the matrix of constraints, uses the row-reduced form to obtain each dependent variable as a linear combination of independent variables, then replaces the dependent variables in the objective function by the corresponding linear combination of the independent variables. The Jacobian matrix for the objective function is then obtained. Since each row in the objective function matrix represent a linear equation, the Jacobian matrix is constant. The Jacobian matrix is used in the Marquardt algorithm to obtain an improved solution at each iteration.

2. INV

This is a matrix inversion subroutine which is a required operation in the Marquardt algorithm.

3. SOLVE

This subroutine is called at each iteration to solve for dependent variables once the independent variables are determined.

Detailed description of the algorithm is given elsewhere (Marquardt, 1963). A brief discussion is presented here.

Marquardt algorithm can be applied to optimization problems where the objective function can be expressed as the sum of squares of s functions of the independent variables as is the case for the objective function formulated from ^{13}C -NMR data. Let the objective function be F . Then,

$$F = \sum_{k=1}^s \phi_k^2 \quad (14)$$

and

$$\phi_k = C_{13k} - \sum_{j=1}^t CO_{kj} X_j \quad (15)$$

where s is the number of bands in the ^{13}C -NMR spectra each with a corresponding concentration of C_{13k} , t is the number of independent variables, X_j are the functional group concentrations, and CO_{kj} are modified objective function coefficients such that all the dependent variables are expressed in terms of the independent variables.

The solution for the $(r+1)$ th iteration is then obtained by the following procedure:

$$\underline{\delta} = (J^T J + \lambda(r) I)^{-1} J^T \underline{\Phi}(r) \quad (16)$$

$$\underline{X}(r+1) = \underline{X}(r) + \underline{\delta} \quad (17)$$

where r indicates values from r th iteration, $\underline{\Phi}$ is the column vector containing ϕ_k , I is the identity matrix, J is the Jacobian of the objective function matrix, and λ is a positive parameter known as the Marquardt parameter. Once a suitable λ is obtained, one can proceed to determine $\underline{\delta}$, the radius of increment, and hence obtain the solution vector

for the next iteration. The initial solution vector is that obtained from the direct search method. The procedure to obtain λ at each iteration and the criteria for convergence is given by Marquardt (1963). Since the algorithm allows for negative values for each variable, each time a non-negativity constraint is violated, the solution is rejected.

```
SUBROUTINE JACC(AOO,X,CO,C13,RJ,BB,B3,MM,NIN,NCB)
```

C This subroutine consists of three parts.
C In part one the matrix of the dependent
C variables is reduced to the row-echelon
C form. The same operations are performed
C on the right hand side vector. In part two,
C the dependent variables are obtained as
C linear combination of the independent
C variables and in part three, the Jacobian
C for the objective function matrix is obtained.

C Description of variables

C AOO : constraint matrix
C A2 : dependent variable submatrix
C A3 : matrix containing coefficients for dependent
C variables as linear combination of the
C independent variables
C B3 : array containing the constant term for
C dependent variables as linear combination of
C independent variables
C BB,B : right hand vector of the constraint matrix
C CO : objective function matrix
C CO2 : objective function matrix rearranged such
C that the dependent variables are linear
C combination of the independent variables
C C13 : right hand side vector of the objective
C function matrix
C RJ : Jacobian of the objective function
C X : concentration of functional groups
C MM : total number of constraints
C NN : total number of variables
C NIN : number of independent variables

```
REAL AOO(120,120),A2(120,120),BB(120),CO2(120,120)
REAL A3(120,120),RJ(120,120),CO(120,120),C13(120)
REAL B(120),B3(120),X(120)
INTEGER MM,NIN,NCB
```

C PART ONE

```
NN=MM+NIN
DO 10 I=1,MM
DO 10 J=1,MM
A2(I,J)=AOO(I,J+NIN)
10 CONTINUE
MM1=MM-1
DO 100 I=1,MM1
I2=I+1
IF(A2(I,I)) 15,20,15
15 DO 25 J=I2,MM
20
```

```

      IF(J.EQ. I) GOTO 25
      IF(A2(J,I)) 30,25,30
30   JJ=J
      DO 35 K=1,MM
      SAVE=A2(I,K)
      A2(I,K)=A2(JJ,K)
      A2(JJ,K)=SAVE
35   CONTINUE
      SAVE=BB(I)
      BB(I)=BB(JJ)
      BB(JJ)=SAVE
      DO 40 K=1,NIN
      SAVE=AOO(I,K)
      AOO(I,K)=AOO(JJ,K)
      AOO(JJ,K)=SAVE
40   CONTINUE
      GOTO 15
25   CONTINUE
15   IF(A2(I,I)-1) 45,50,45
45   SAVE=A2(I,I)
      DO 55 J=1,MM
      A2(I,J)=A2(I,J)/SAVE
55   CONTINUE
      BB(I)=BB(I)/SAVE
      DO 60 J=1,NIN
      AOO(I,J)=AOO(I,J)/SAVE
60   CONTINUE
50   II=I+1
      DO 65 J=II,MM
      IF(A2(J,I)) 70,65,70
70   SAVE=A2(J,I)
      DO 75 K=1,MM
      A2(J,K)=A2(J,K)-SAVE*A2(I,K)
75   CONTINUE
      BB(J)=BB(J)-SAVE*BB(I)
      DO 80 K=1,NIN
      AOO(J,K)=AOO(J,K)-SAVE*AOO(I,K)
80   CONTINUE
65   CONTINUE
100  CONTINUE
      SAVE=A2(MM,MM)
      A2(MM,MM)=A2(MM,MM)/SAVE
      BB(MM)=BB(MM)/SAVE
      DO 105 I=1,MM
      DO 105 J=1,MM
      AOO(I,J+NIN)=A2(I,J)
105  CONTINUE
      DO 5000 I=1,MM
      B(I)=0.0
      DO 5010 J=1,NN
      B(I)=B(I)+AOO(I,J)*X(J)
5010 CONTINUE
C      WRITE(6,5020) B(I)
C5020 FORMAT(F12.3)

```

```

5000 CONTINUE
C      DO 5255 I=1,MM
C      WRITE(6,5556)(AOO(I,J),J=1,NN)
C5255 CONTINUE
C5556 FORMAT(13F10.3)
C      DO 6665 I=1,MM
C      WRITE(6,6666) BB(I)
C6665 CONTINUE
C6666 FORMAT(F10.5)
C
C      PART TWO
C
DO 110 I=1,NIN
DO 110 J=1,NIN
A3(I,J)=0.0
110  CONTINUE
MMK=MM+1
DO 115 I=1,MM
K=MMK-I
IF(K-MM) 120,125,120
125  DO 130 J=1,NIN
A3(K,J)=AOO(K,J)
130  CONTINUE
B3(K)=BB(K)
GOTO -115
120  K2=K+1
DO 135 J2=K2,MM
IF(A2(K,J2) .EQ. 0.0) GOTO 135
DO 140 J=1,NIN
AOO(K,J)=AOO(K,J)-A2(K,J2)*AOO(J2,J)
140  CONTINUE
BB(K)=BB(K)-A2(K,J2)*BB(J2)
135  CONTINUE
DO 145 J=1,NIN
A3(K,J)=AOO(K,J)
145  CONTINUE
B3(K)=BB(K)
115  CONTINUE
C      DO 7234 I=1,MM
C      WRITE(6,7235)(A3(I,J),J=1,NIN)
C7234 CONTINUE
C7235 FORMAT(8F12.3)
C      DO 7236 I=1,MM
C      WRITE(6,7237) B3(I)
C7236 CONTINUE
C7237 FORMAT(F12.5)
C
C      PART THREE
C
SS=0.0001
DO 210 I=1,NCB
DO 210 J=1,NIN
RJ(I,J)=(-1.0)*CO(I,J)
210  CONTINUE

```

```
      DO 215 I=1,NCB
      DO 215 J=1,MM
      CO2(I,J)=CO(I,J+NIN)
215   CONTINUE
      DO 220 I=1,NCB
      DO 225 J=1,MM
      IF(CO2(I,J) .EQ. 0.0) GOTO 225
      DO 230 K=1,NIN
      RJ(I,K)=RJ(I,K)+CO2(I,J)*A3(J,K)
230   CONTINUE
      C13(I)=C13(I)-CO2(I,J)*B3(J)
225   CONTINUE
220   CONTINUE
      DO 240 I=1,NCB
      DO 240 J=1,NIN
      IF(ABS(RJ(I,J)) .LT. SS) RJ(I,J)=0.0
240   CONTINUE
C      DO 8235 I=1,NCB
C      WRITE(6,8236)(RJ(I,J),J=1,NIN)
C8235 CONTINUE
C8236 FORMAT(5F12.5)
C      DO 8237 I=1,NCB
C      WRITE(6,8238) C13(I)
C8237 CONTINUE
C8238 FORMAT(F12.5)
      RETURN
      END
```

SUBROUTINE MARQ(X,C,C13,RJ,BBB,AO2,IPVT,NDIM,N,M1,
\$NCB,NIN,RF,M2,M3,KNC)

C This subroutine uses the Marquardt algorithm to
C obtain the optimum solution. Details of the
C algorithm, the convergence criteria, and the strategy
C for choosing the appropriate Marquardt parameter are
C given in the reference (Marquardt; 1963).

C Description of variables

C M1 : number of equality constraints
C M2 : number of inequality constraints (< or =)
C M3 : number of inequality constraints (> or =)
C MM : total number of constraints
C N : number of variables (functional groups)
C NIN : number of independent variables
C NCB : number of bands in the C13-NMR spectra
C RF : initial value of the objective function
C FUN : value of the objective function
C RM : array containing the Marquardt parameter at
C each iteration
C ITT : counter for the number of iterations
C ITMAX: maximum number of iterations
C ITERM: maximum number of iterations to improve on
C a solution
C AO2 : constraint matrix
C KNC : array containing the group numbers
C C : matrix of the dependent variables
C B,BBB: vectors containing the right hand side of
C the constraints
C C13 : vector containing the right hand side of
C the objective function matrix
C NDIM : declared dimension of the constraint matrix
C RJ : Jacobian matrix of the objective function
C RJT : transpose of RJ
C RJTJ : product matrix of (RJT * RJ)
C DJ : product matrix of (RJTJ + (RM * I)) where
C I is the identity matrix
C DJIN : inverse of DJ
C PHI : column vector containing the objective
C function equations with dependent variables as
C linear combination of independent variables
C DI : product matrix of (DJIN * (RJT * PHI))
C DEL : vector containing the radius of increment
C at each iteration
C EP,TAU: constants used to establish criteria for
C convergence
C TST : array used to test if the convergence
C criteria is achieved
C V : constant used in the strategy to determine
C the Marquardt parameter
C FF : array for storing values of the objective
C function at each iteration

```

C      F   : array for storing the value of the objective
C           function at each iteration in determining
C           the appropriate Marquardt parameter
C      SMAX : an arbitrary large real number assigned
C           to the objective function when a
C           non-negativity constraint is violated
C      XX   : array to store the functional group
C           concentrations at each iteration
C      X,XI,XS: functional group concentrations
C
C
REAL X(120),C(120,120),C13(120),RJ(120,120),BBB(120)
REAL RF
INTEGER IPVT(120),NIN,NN,MM,NCB,NDIM
INTEGER KNC(120)
REAL RJT(120,120),RJTJ(120,120),XI(120),FF(120)
REAL F(120,120),XX(120,120),B(120),PHI(120),TST(120)
REAL DI(120,120),DJIN(120,120),DEL(120),DJ(120,120)
REAL XS(120),RM(120),AO2(120,120)
C
C
NN=N+M2+M3
MM=M1+M2+M3
FF(1)=RF
FUN=RF
RM(1)=0.01
V=2.
EP=0.0000001
TAU=0.001
IFLAG=0
SMAX=1000.
ITMAX=500
ITERM=100
DO 10 I=1,NIN
DO 10 J=1,NCB
RJT(I,J)=RJ(J,I)
10 CONTINUE
DO 20 I=1,NIN
DO 20 J=1,NIN
RJTJ(I,J)=0.0
DO 30 K=1,NCB
RJTJ(I,J)=RJTJ(I,J)+(RJT(I,K)*RJ(K,J))
30 CONTINUE
20 CONTINUE
DO 25 J=1,NN
XI(J)=X(J)
XS(J)=X(J)
25 CONTINUE
C
C      ITERATIVE PROCEDURE STARTS HERE
C
DO 500 ITT=2,ITMAX
ITER=0
II=1
RM(ITT)=RM(ITT-1)/V

```

```

35 DO 38 J=1,NIN
      X(J)=XI(J)
38 CONTINUE
      DO 40 I=1,NIN
      DO 45 J=1,NIN
          IF(I .EQ. J) DJ(I,J)=RJTJ(I,J)+RM(ITT)
          IF(I .EQ. J) GOTO 45
          DJ(I,J)=RJTJ(I,J)
45 CONTINUE
40 CONTINUE
      CALL INV(DJ,NIN,DJIN)
      DO 50 I=1,NIN
      DO 50 J=1,NCB
          DI(I,J)=0.0
      DO 55 K=1,NIN
          DI(I,J)=DI(I,J)+(DJIN(I,K)*RJT(K,J))
55 CONTINUE
50 CONTINUE
      DO 60 I=1,NCB
          PHI(I)=C13(I)
      DO 65 J=1,NIN
          PHI(I)=PHI(I)+RJ(I,J)*X(J)
65 CONTINUE
60 CONTINUE
      DO 70 J=1,NIN
          DEL(J)=0.0
      DO 75 I=1,NCB
          DEL(J)=DEL(J)+(DI(I,J)*PHI(I))
75 CONTINUE
70 CONTINUE
      DO 80 J=1,NIN
          XX(J,II)=X(J)+DEL(J)
80 CONTINUE
      DO 90 I=1,MM
          B(I)=BBB(I)
      DO 95 J=1,NIN
          B(I)=B(I)-XX(J,II)*AO2(I,J)
95 CONTINUE
90 CONTINUE
      CALL SOLVE(NDIM,MM,C,B,IPVT)
      DO 100 J=1,MM
          XX(J+NIN,II)=B(J)
100 CONTINUE
      DO 110 J=1,NN
          IF(XX(J,II) .LT. 0.0) F(ITT,II)=SMAX
          IF(XX(J,II) .LT. 0.0) IFLAG=1
110 CONTINUE
          IF(IFLAG .EQ. 1) GOTO 118
          F(ITT,II)=0.0
          DO 115 I=1,NCB
              PHI(I)=C13(I)
          DO 120 J=1,NIN
              PHI(I)=PHI(I)+RJ(I,J)*XX(J,II)
120 CONTINUE

```

```

      F(ITT,II)=F(ITT,II)+(PHI(I)**2)
115  CONTINUE
      GOTO 125
118  F(ITT,II)=SMAX
125  CONTINUE
C     WRITE(6,119) F(ITT,II),RM(ITT),II,ITT,ITER
C119  FORMAT(/,F12.5,E12.5,3I3,/)

C     DO 1118 J=1,NIN
C     WRITE(6,1119) DEL(J)
C1118 CONTINUE
C1119 FORMAT(/,F12.8)
C     DO 121 J=1,NN
C     WRITE(6,122) XX(J,II)
C121  CONTINUE
C122  FORMAT(F12.5)
      RM(ITT)=RM(ITT-1)
      II=II+1
      IFLAG=0
      IF(II .EQ. 2) GOTO 35
      IF(F(ITT,1) .LE. FF(ITT-1)) GOTO 300
      IF(F(ITT,2) .LE. FF(ITT-1)) GOTO 400
      RM(ITT)=RM(ITT-1)*V
130  ITER=ITER+1
      DO 132 J=1,NN
      XI(J)=X(J)
132  CONTINUE
      DO 140 I=1,NIN
      DO 145 J=1,NIN
      IF(I .EQ. J) DJ(I,J)=RJTJ(I,J)+RM(ITT),
      IF(I .EQ. J) GOTO 145
      DJ(I,J)=RJTJ(I,J)
145  CONTINUE
140  CONTINUE
      CALL INV(DJ,NIN,DJIN)
      DO 150 I=1,NIN
      DO 150 J=1,NCB
      DI(I,J)=0.0
      DO 155 K=1,NIN
      DI(I,J)=DI(I,J)+(DJIN(I,K)*RJT(K,J))
155  CONTINUE
150  CONTINUE
      DO 160 I=1,NCB
      PHI(I)=C13(I)
      DO 165 J=1,NIN
      PHI(I)=PHI(I)+(RJ(I,J)*X(J))
165  CONTINUE
160  CONTINUE
      DO 170 J=1,NIN
      DEL(J)=0.0
      DO 175 I=1,NCB
      DEL(J)=DEL(J)+(DI(I,J)*PHI(I))
175  CONTINUE
170  CONTINUE
      DO 180 J=1,NIN

```

```

      XI(J)=X(J)+DEL(J)
180  CONTINUE
      DO 190 I=1,MM
      B(I)=BBB(I)
      DO 195 J=1,NIN
      B(I)=B(I)-(XI(J)*AO2(I,J))
195  CONTINUE
190  CONTINUE
      CALL SOLVE(NDIM,MM,C,B,IPVT)
      DO 200 J=1,MM
      XI(J+NIN)=B(J)
200  CONTINUE
      DO 210 J=1,NN
      IF(XI(J) .LT. 0.0) FF(ITT)=SMAX
      IF(XI(J) .LT. 0.0) IFLAG=1
210  CONTINUE
      IF(IFLAG .EQ. 1) GOTO 218
      FF(ITT)=0.0
      DO 215 I=1,NCB
      PHI(I)=C13(I)
      DO 220 J=1,NIN
      PHI(I)=PHI(I)+(RJ(I,J)*XI(J))
220  CONTINUE
      FF(ITT)=FF(ITT)+(PHI(I)**2)
215  CONTINUE
      GOTO 225
218  FF(ITT)=SMAX
225  IFLAG=0
C     WRITE(6,226) FF(ITT),RM(ITT),ITT,ITER
C226  FORMAT(/,F12.5,E12.5,2I3,/)

C     DO 2118 J=1,NIN
C     WRITE(6,2119) DEL(J)
C2118 CONTINUE
C2119 FORMAT(/,F12.8)
C     DO 227 J=1,NN
C     WRITE(6,228) XI(J)
C227  CONTINUE
C228  FORMAT(F12.5)
      IF(FF(ITT) .GT. FF(ITT-1)) RM(ITT)=RM(ITT)*V
      IF(ITER .GT. ITERM) GOTO 600
      IF(FF(ITT) .GT. FF(ITT-1)) GOTO 130
      FUN=FF(ITT)
      GOTO 450
300  RM(ITT)=RM(ITT-1)/V
      FF(ITT)=F(ITT,1)
      FUN=FF(ITT)
      DO 310 J=1,NN
      XI(J)=XX(J,1)
      XS(J)=XI(J)
310  CONTINUE
      GOTO 450
400  RM(ITT)=RM(ITT-1)
      FF(ITT)=F(ITT,2)
      FUN=FF(ITT)

```

```

DO 410 J=1,NN
XI(J)=XX(J,2)
XS(J)=XI(J)
410 CONTINUE
450 DO 460 J=1,NIN
TST(J)=DEL(J)/(TAU+ABS(X(J)))
460 CONTINUE
COUNT=0.0
DO 470 J=1,NIN
IF(TST(J) .LT. EP) GOTO 470
COUNT=COUNT+1.
470 CONTINUE
IF(COUNT .EQ. 0.0) GOTO 550
C WRITE(6,496) FUN,ITT
C496 FORMAT(/, 'FUNCTION VALUE', F12.5, /, 'ITERATION', I3)
C DO 494 J=1,NN
C WRITE(6,495) XI(J)
C494 CONTINUE
C495 FORMAT(F12.5)
500 CONTINUE
550 GOTO 650
600 WRITE(6,601)
601 FORMAT('NO FARTHER IMPROVEMENT')
DO 605 J=1,NN
X(J)=XS(J)
IF(J .NE. N+1) GOTO 1605
WRITE(6,1606)
1606 FORMAT(/, 'SLACK VARIABLES', /)
1605 WRITE(6,606) KNC(J),XS(J)
605 CONTINUE
606 FORMAT('X', I3, '=' ,F12.5)
WRITE(6,610) FUN
610 FORMAT(/, 'FUNCTION VALUE', F12.5)
STOP
650 DO 660 J=1,NN
X(J)=XS(J)
IF(J .NE. N+1) GOTO 1608
WRITE(6,1609)
1609 FORMAT(/, 'SLACK VARIABLES', /)
1608 WRITE(6,670) KNC(J),XS(J)
660 CONTINUE
670 FORMAT('X', I3, '=' ,F12.5)
WRITE(6,680) FUN
680 FORMAT(/, 'FUNCTION VALUE' ;F12.5)
RETURN
END

```

```

SUBROUTINE INV(A,N,AIN)
C
REAL A(120,120),AIN(120,120)
INTEGER N
C
THIS SUBROUTINE COMPUTES THE INVERSE OF A SQUARE
MATRIX BY REDUCING THE MATRIX TO THE IDENTITY
MATRIX WHILE PERFORMING THE SAME OPERATION ON AN
IDENTITY MATRIX TO OBTAIN THE INVERSE MATRIX.
C
INPUT :
C
A : SQUARE MATRIX TO BE INVERTED
N : SIZE OF MATRIX A
C
OUTPUT:
C
AIN : INVERSE OF A
C
DO 10 I=1,N
DO 10 J=1,N
IF(I .EQ. J) AIN(I,J)=1.0
IF(I .EQ. J) GOTO 10
AIN(I,J)=0.0
10 CONTINUE
N1=N-1
DO 100 I=1,N1
I2=I+1
IF(A(I,I)) 15,20,15
20 DO 25 J=I2,N
IF(J .EQ. I) GOTO 25
IF(A(J,I)) 30,25,30
30 JJ=J
DO 35 K=1,N
SAVE=A(I,K)
A(I,K)=A(JJ,K)
A(JJ,K)=SAVE
SAVE=AIN(I,K)
AIN(I,K)=AIN(JJ,K)
AIN(JJ,K)=SAVE
35 CONTINUE
GOTO 15
25 CONTINUE
15 IF(A(I,I)-1) 45,50,45
45 SAVE=A(I,I)
DO 55 J=1,N
A(I,J)=A(I,J)/SAVE
AIN(I,J)=AIN(I,J)/SAVE
55 CONTINUE
50 II=I+1
DO 65 J=II,N
IF(A(J,I)) 70,65,70
70 SAVE=A(J,I)
DO 75 K=1,N

```

```
A(J,K)=A(J,K)-SAVE*A(I,K)
AIN(J,K)=AIN(J,K)-SAVE*AIN(I,K)
75  CONTINUE
65  CONTINUE
100 CONTINUE
    SAVE=A(N,N)
    A(N,N)=A(N,N)/SAVE
    DO 105 J=1,N
    AIN(N,J)=AIN(N,J)/SAVE
105  CONTINUE
    DO 110 I=1,N1
    K=N-I+1
    K1=K-1
    DO 115 II=1,K1
    SAVE=A(II,K)
    DO 113 J=1,N
    A(II,J)=A(II,J)-SAVE*A(K,J)
    AIN(II,J)=AIN(II,J)-SAVE*AIN(K,J)
113  CONTINUE
115  CONTINUE
110  CONTINUE
    RETURN
    END
```